Improving the Foundation Layers for Concrete Pavements

TECHNICAL REPORT:

Jointed Concrete Pavement Rehabilitation with Injected High Density Polyurethane Foam and Dowel Bar Retrofitting – Pennsylvania US 422 Field Study

August 2015

Sponsored by
Federal Highway Administration (DTFH 61-06-H-00011 (Work Plan #18))
FHWA TPF-5(183): California, Iowa (lead state), Michigan, Pennsylvania, Wisconsin

National Concrete Pavement Technology Center

Tech Center

CENTER FOR CEER EARTHWORKS ENGINEERING RESEARCH

IOWA STATE UNIVERSITY
Institute for Transportation

About the National CP Tech Center

The mission of the National Concrete Pavement Technology (CP Tech) Center is to unite key transportation stakeholders around the central goal of advancing concrete pavement technology through research, tech transfer, and technology implementation.

About CEER

The mission of the Center for Earthworks Engineering Research (CEER) at Iowa State University is to be the nation's premier institution for developing fundamental knowledge of earth mechanics, and creating innovative technologies, sensors, and systems to enable rapid, high quality, environmentally friendly, and economical construction of roadways, aviation runways, railroad embankments, dams, structural foundations, fortifications constructed from earth materials, and related geotechnical applications.

Disclaimer Notice

The contents of this report reflect the views of the authors, who are responsible for the facts and the accuracy of the information presented herein. The opinions, findings and conclusions expressed in this publication are those of the authors and not necessarily those of the sponsors.

The sponsors assume no liability for the contents or use of the information contained in this document. This report does not constitute a standard, specification, or regulation.

The sponsors do not endorse products or manufacturers. Trademarks or manufacturers' names appear in this report only because they are considered essential to the objective of the document.

Iowa State University Non-Discrimination Statement

Iowa State University does not discriminate on the basis of race, color, age, ethnicity, religion, national origin, pregnancy, sexual orientation, gender identity, genetic information, sex, marital status, disability, or status as a U.S. veteran. Inquiries regarding non-discrimination policies may be directed to Office of Equal Opportunity, Title IX/ADA Coordinator, and Affirmative Action Officer, 3350 Beardshear Hall, Ames, Iowa 50011, 515-294-7612, email eooffice@iastate.edu.

Iowa Department of Transportation Statements

Federal and state laws prohibit employment and/or public accommodation discrimination on the basis of age, color, creed, disability, gender identity, national origin, pregnancy, race, religion, sex, sexual orientation or veteran's status. If you believe you have been discriminated against, please contact the Iowa Civil Rights Commission at 800-457-4416 or the Iowa Department of Transportation affirmative action officer. If you need accommodations because of a disability to access the Iowa Department of Transportation's services, contact the agency's affirmative action officer at 800-262-0003.

The preparation of this report was financed in part through funds provided by the Iowa Department of Transportation through its "Second Revised Agreement for the Management of Research Conducted by Iowa State University for the Iowa Department of Transportation" and its amendments.

The opinions, findings, and conclusions expressed in this publication are those of the authors and not necessarily those of the Iowa Department of Transportation or the U.S. Department of Transportation Federal Highway Administration.

Technical Report Documentation Page

1. Report No.	2. Government Accession No.	3. Recipient's Catalog No.
DTFH 61-06-H-00011 Work Plan 18		

4. Title and Subtitle	5. Report Date
Improving the Foundation Layers for Pavements: Jointed Concrete Pavement Rehabilitation with Injected High Density Polyurethane Foam and Dowel Bar Retrofitting – Pennsylvania US 422 Field Study	August 2015
	6. Performing Organization Code
7. Author(s)	**8. Performing Organization Report No.**
David J. White, Pavana Vennapusa, Yang Zhang, and Alexander J. Wolfe	InTrans Project 09-352
9. Performing Organization Name and Address	**10. Work Unit No. (TRAIS)**
National Concrete Pavement Technology Center and Center for Earthworks Engineering Research (CEER) Iowa State University 2711 South Loop Drive, Suite 4700 Ames, IA 50010-8664	**11. Contract or Grant No.**
12. Sponsoring Organization Name and Address	**13. Type of Report and Period Covered**
Federal Highway Administration U.S. Department of Transportation 1200 New Jersey Avenue SE Washington, DC 20590	Technical Report
	14. Sponsoring Agency Code TPF-5(183)

15. Supplementary Notes

Visit www.cptechcenter.org or www.ceer.iastate.edu for color PDF files of this and other research reports.

16. Abstract

This report is one of the field project reports developed as part of the TPF-5(183) and FHWA DTFH 61-06-H-00011:WO18 studies.

This report presents experimental test results and analysis from a field evaluation conducted on a 15-year-old jointed portland cement concrete pavement section on US 422 near Indiana, Pennsylvania. The pavement exhibited premature mid panel cracking and faulting. A 9.7 km section of the highway was rehabilitated by injecting light weight high density polyurethane foam into the underlying open-graded stone (OGS) layer to improve support conditions beneath the pavement and installing dowel bar retrofits at selected crack locations to improve load transfer efficiency. A 160 m long section of the project was stabilized with cementitious grout for comparison with areas that were stabilized with HDP foam. Laboratory testing was conducted on OGS and OGS+foam mixture samples to determine undrained shear strength and resilient modulus properties. Field testing was conducted in several test sections before and after HDP/cementitious grout stabilization, after dowel bar retrofitting, and six to nine months after stabilization for performance evaluation. Testing that was conducted in full-depth patching areas after HDP foam injection provided the opportunity to observe migration of the injected foam and directly test the stabilized support layers under the pavement. Field observations indicated that the foam did not fully penetrate the full width and depth of the OGS layer, thus creating non-uniform support conditions with variable stiffness, strength, and permeability characteristics. OGS+foam material showed lower permeability, lower elastic modulus, and high shear strength, than OGS material alone, in both lab and field testing. Pavement surface elevation monitoring results indicated that the slab movements were greater than the allowable 1.3 mm per specifications, and better process control measures are needed to control vertical movements, particularly with the HDP stabilization method. FWD test measurements showed improvements near cracks and joints in both cementitious and grout stabilized sections, although no statistically significant improvements were observed near mid-panel. The findings of this study improve the understanding of the benefits and limitations of using injected foam technology to rehabilitate concrete pavements.

17. Key Words	18. Distribution Statement
pavement foundation—polyurethane foam—portland cement concrete pavements—rehabilitation—retrofitting—stabilization	No restrictions.

19. Security Classification (of this report)	20. Security Classification (of this page)	21. No. of Pages	22. Price
Unclassified.	Unclassified.	121	NA

Form DOT F 1700.7 (8-72) **Reproduction of completed page authorized**

IMPROVING THE FOUNDATION LAYERS FOR CONCRETE PAVEMENTS: JOINTED CONCRETE PAVEMENT REHABILITATION WITH INJECTED HIGH DENSITY POLYURETHANE FOAM AND DOWEL BAR RETROFITTING – PENNSYLVANIA US 422 FIELD STUDY

Technical Report
August 2015

Research Team Members
Tom Cackler, David J. White, Jeffrey R. Roesler, Barry Christopher, Andrew Dawson, Heath Gieselman, and Pavana Vennapusa

Report Authors
David J. White, Pavana K. R. Vennapusa,
Yang Zhang, Alexander J. Wolfe
Iowa State University

Sponsored by
the Federal Highway Administration (FHWA)
DTFH61-06-H-00011 Work Plan 18
FHWA Pooled Fund Study TPF-5(183): California, Iowa (lead state), Michigan, Pennsylvania, Wisconsin

Preparation of this report was financed in part
through funds provided by the Iowa Department of Transportation
through its Research Management Agreement with the
Institute for Transportation
(InTrans Project 09-352)

National Concrete Pavement Technology Center and
Center for Earthworks Engineering Research (CEER)
Iowa State University
2711 South Loop Drive, Suite 4700
Ames, IA 50010-8664
Phone: 515-294-5768
www.cptechcenter.org and www.ceer.iastate.edu

TABLE OF CONTENTS

ACKNOWLEDGMENTS xi

LIST OF ACRONYMS AND SYMBOLS xiii

EXECUTIVE SUMMARY xv

Laboratory Testing xvi
Penn DOT's IRI Testing History (2005 to 2014) xvi
In Situ Testing in Patching Areas with and without HDP Foam Stabilization xvii
Pavement Surface Elevation Monitoring in HDP Foam Treated Sections xvii
Comparison between Cementitious Grout and HDP Foam Stabilization Sections xvii
Long-Term Performance of HDP Foam Stabilization Sections xviii
Recommendations for Future Work xviii

CHAPTER 1. INTRODUCTION 1

CHAPTER 2. BACKGROUND 3

Material Properties and Mix Design 7
Construction and Testing Procedures 7
Previous Performance Monitoring Studies 8
Cementitious Grout 8
HDP Foam 9

CHAPTER 3. EXPERIMENTAL TESTING METHODS 13

Laboratory Testing Methods 13
Particle Size Analysis and Fines Content Determination 13
Resilient Modulus and Shear Strength Testing 13
In Situ Testing Methods 18
Real-Time Kinematic Global Positioning System 19
Robotic Total Station 19
Zorn Light Weight Deflectometer 21
Dynamic Cone Penetrometer 21
Falling Weight Deflectometer (FWD) 21
Humboldt Nuclear Gauge 24
Rapid Air Permeameter Test (APT Device) 25
Crack and Fault Measurements 25
I-Buttons 26
International Roughness Index 27
Statistical Analysis Method 27

CHAPTER 4. US 422 REHABILITATION PROJECT OVERVIEW AND TESTING 29

Project Overview 29
Pre-Stabilization Penn DOT Field Test Results 29
Rehabilitation Process 35
Description of Test Sections and Test Measurements 38

CHAPTER 5. MATERIAL PROPERTIES 40

Particle Size Analysis 40
Resilient Modulus and Shear Strength....44

CHAPTER 6. FIELD PERFORMANCE TEST RESULTS 51

Penn DOT IRI Measurements....51
TS1/TS2: Evaluation of Spatial Propagation of Injected Foam and Properties of Stabilized and Unstabilized Subbase Layer in Patching Areas 51
TS6/TS7: Pavement Surface Elevation Changes Due to Foam Injection....58
TS6 US422 EB....58
TS7 US422 WB 59
TS5/TS8: Comparison between Cementitious Grout Stabilized and HDP Foam Stabilized Sections....61
TS3/TS4: Effects of HDP Foam Stabilization Shortly Before and Shortly After Stabilization near Mid-Panel....71
TS7: Effects of Initial and Secondary Foam Injection on FWD Measurements 80
TS8: Performance Assessment of HDP Foam Injected Test Section 82
TS9: Temperature Monitoring in Stabilized and Unstabilized Sections 88

CHAPTER 7. SUMMARY AND CONCLUSIONS....91

Laboratory Testing....91
Penn DOT's IRI Testing History (2005 to 2014) 91
In Situ Testing in Patching Areas with and without HDP Foam Stabilization....91
Pavement Surface Elevation Monitoring in HDP Foam Treated Sections....92
Comparison between Cementitious Grout and HDP Foam Stabilization Sections 92
Long-Term Performance of HDP Foam Stabilization Sections 93
Recommendations for Future Work....93

REFERENCES 95

APPENDIX A: SLAB STABLIZATION (SECTION 679, PENNDOT 2011) 99

APPENDIX B: INTERNATIONAL ROUGHNESS INDEX RATING....103

LIST OF FIGURES

Figure 1. Triaxial chamber and load frame (left) and computer setup (right) 14
Figure 2. Graphical representation of one load cycle in M_r testing 15
Figure 3. Preparation of an OGS sample for laboratory M_r and UU testing 16
Figure 4. Preparation of OGS+Foam samples for laboratory M_r and UU testing 17
Figure 5. Top view of HDP foam (top) and OGS+Foam mixture (bottom) samples 18
Figure 6. In situ test devices: Trimble SPS-881 hand-held receiver; Trimble SP-851 base station and RTS hand-held laser receiver (top row left to right); Kuab falling weight deflectometer and Zorn light weight deflectometer (middle row left to right); dynamic cone penetrometer, nuclear gauge, and gas permeameter device (bottom row left to right) 20
Figure 7. Void detection using load-deflection data from FWD tests 22
Figure 8. FWD deflection sensor setup used for this study and sample deflection basin data illustrating SCI, BDI, and BCI calculations 23
Figure 9. Crack width (left) and fault (right) measurements 26
Figure 10. I-button installation 27
Figure 11. Map showing approximate locations of segments 134 to 184 on US 422EB and segments 135 to 185 on US 422WB and locations of ISU test sections 30
Figure 12. IRI measurements in EB (top) and WB (bottom) lanes from 2005 to 2009 (data represents average values for each segment) 31
Figure 13. Box plots of IRI measurements on US 422 EB (top) and WB (bottom) lanes from 2005 to 2010 32
Figure 14. Pre-stabilization Penn DOT FWD LTE measurements at joints on US 422 EB (top) and WB lanes (bottom) 33
Figure 15. Pre-stabilization PennDOT FWD I measurements at joints on US 422 EB (top) and WB (bottom). 34
Figure 16. Histogram of pre-stabilization FWD test results: joint LTE (top left), D_0 under loading plate at 40 kN applied load (top right), and I (bottom left) 35
Figure 17. Equipment used to drill holes for foam injection (a); foam injection process (b); truck carrying the liquids (c); dial gauges used to monitor slab movement (d); dowel bar retrofitting performed at cracks (e); and a concrete patching area (f) 37
Figure 18. Foam+aggregate mixture (left) and HDP foam ejected through a hole drilled in the pavement (right) 38
Figure 19. Particle size distribution curves for OGS material from TS1/TS2 40
Figure 20. Particle size distribution curves for 2A material from TS1/TS2 41
Figure 21. Histograms of particle size distribution for OGS and Class 2A materials 42
Figure 22. Histograms of gradation parameters c_u and c_c for OGS and Class 2A materials 43
Figure 23. Histogram of fines content for OGS samples from TS2-3 and TS2-4 43
Figure 24. TS1: Aggregate particle breakdown observed in OGS layer 44
Figure 25. Particle size distribution curves of OGS material before and after scalp and replace procedure (for material retained on 19 mm (3/4 in.) sieve) 45
Figure 26. Cyclic stress-strain curves from M_r test for foam sample 46
Figure 27. Cyclic stress-strain curves from M_r tests for OGS sample 47
Figure 28. Cyclic stress-strain curves from M_r test for OGS+Foam sample 48

Figure 29. Bulk stress versus resilient modulus (top) and stress-strain curves from UU tests (bottom) for OGS, OGS+Foam, and foam samples....49
Figure 30. M_r and UU test results of foam, OGS, and OGS+Foam samples....50
Figure 31. Box plots of IRI measurements on US 422 EB (top) and WB (bottom) lanes from 2005 to 2010....52
Figure 32. TS1: Crane lifting the PCC surface layer of a patch area....53
Figure 33. TS1: Bottom of the PCC surface layer in the patch area with treated subbase layer....53
Figure 34. TS1: Picture of patch no. 2 showing OGS+Foam mixture boundary (left), close-up view of OGS+Foam mixture sample extracted from patch no. 2 (right)....54
Figure 35. TS1/TS2: Location of cracks, OGS+Foam mixture boundaries, foam injection locations, and in-situ test locations on four patching areas overlaid with spatial contours of $E_{LWD\text{-}Z2}$....55
Figure 36. TS1/TS2: Location of cracks, OGS+Foam mixture boundaries, foam injection locations, and in-situ test locations on four patching areas overlaid with spatial contours of K_{Sat}....56
Figure 37. DCP-CBR profiles from patches areas 2, 3, and 4....57
Figure 39. TS6: Results of elevation monitoring near joints and cracks on nine panels along A-A, B-B, and C-C lines....59
Figure 40. TS7: Plan layout showing cracks, initial and secondary foam injection locations, and elevation survey profile lines....60
Figure 41. TS7: ΔElevation profiles from RTS measurements....60
Figure 42. TS5: Plan view showing FWD test and crack locations, and fault measurements on cracked panels....61
Figure 43. TS8: Plan view showing FWD test and crack locations, and fault measurements on cracked panels....62
Figure 44. TS5/TS8: Box plots of (a) crack faulting and (b) shoulder faulting, before and after HDP/grout stabilization and dowel bar retrofitting at cracks....64
Figure 45. TS5/TS8: Box plots of (a) D_0 at joints; (b) D_0 at cracks; (c) D_0 at midway between joint and crack; (d) intercept at joints; (e) intercept at cracks; (f) intercept at midway of joint and crack, before and after HDP/grout stabilization and dowel bar retrofitting at cracks....65
Figure 46. TS5/TS8: Box plots of (a) BDI at joints; (b) BDI at cracks; (c) BDI at midway between joint and crack; (d) BCI at joints; (e) BCI at cracks; (f) BCI at midway of joint and crack, before and after HDP/grout stabilization and dowel bar retrofitting at cracks....66
Figure 47. TS5/TS8: Box plots of (a) SCI at joints; (b) SCI at cracks; (c) SCI at midway between joint and crack; (d) area factor at joints; (e) area factor at cracks; (f) area factor at midway of joint and crack, before and after HDP/grout stabilization and dowel bar retrofitting at cracks....67
Figure 48. TS5/TS8: Box plots of (a) LTE at joints and (b) LTE at cracks, before and after HDP/grout stabilization and dowel bar retrofitting at cracks....68
Figure 49. TS3/TS4: Plan layout of FWD test locations (left) and photograph of TS3/TS4 (right)....72
Figure 50. TS3/TS4: Pre- and post-stabilization $E_{FWD\text{-}K3}$ and D_0 deflection measurements....73
Figure 51. TS3/TS4: Pre- and post-stabilization SCI measurements....74

Figure 52. TS3/TS4: Pre- and post-stabilization BDI measurements 75
Figure 53. TS3/TS4: Pre- and post-stabilization BCI measurements 76
Figure 54. TS3/TS4: Pre- and post-stabilization FWD area factor measurements 77
Figure 55. TS3-3, TS3-7 and TS3-10: Pre-stabilization DCP-CBR profiles 78
Figure 56. TS3/TS4: Pre- and post-stabilization FWD zero load intercept (I) measurements 78
Figure 57. TS3/TS4: Pre- and post-stabilization D_0, E_{LWD-K3}, SCI, BDI, BCI, Area Factor, and I measurements with 1 x σ error bars 79
Figure 58. TS7: Photograph showing FWD testing along the center lane 80
Figure 59. TS8: Plan view showing FWD test locations 83
Figure 60. TS8: Photograph showing test locations on driving and passing lanes 83
Figure 61. TS8: Results from FWD testing (at 40 kN applied load) shortly before and after stabilization, and 6 months and 9 months after stabilization: (a) D_0 values at joints, cracks, and mid-panel; (b) I-values at joints, cracks, and mid-panel; and (b) LTE values at joints and cracks 85
Figure 62. TS8: Results for $k_{dynamic}$ values from FWD testing (at 40 kN applied load) at mid-panel shortly before and after stabilization, and 6 months and 9 months after stabilization 86
Figure 63. TS9: Temperatures in ambient air and at six depths below the pavement surface in control, foam, and grout sections 89
Figure 64. TS9: Temperature measurements with depth in control and foam sections during the freezing period (top two figures) and during the thawing period (bottom two figures) 90

LIST OF TABLES

Table 1. Summary of state DOT specifications for cementitious grout 4
Table 2. Summary of HDP in state DOT specifications.....6
Table 3. Summary of field case studies documented in the literature 10
Table 4. Summary of field case studies documented in the literature (continued).....11
Table 5. Summary of field case studies documented in the literature (continued).....12
Table 6. M_r testing sequences for base/subbase materials (AASHTO 1999).....15
Table 7. Summary of test sections and in situ testing.....39
Table 8. M_r and UU test results of Foam, OGS, and OGS+Foam.....45
Table 9. TS1/TS2: Summary statistics of in situ measurements from test patches 2, 3, and 4 56
Table 10. TS5/TS8: Results of statistical analysis comparing before and after stabilization test results.....69
Table 11. TS5/TS8: Results of statistical analysis comparing HDP and grout stabilization methods.....70
Table 12. TS7: Summary statistics of FWD test measurements and t-test results 81
Table 13. TS8: Summary statistics of FWD test measurements and results of t-tests.....86

ACKNOWLEDGMENTS

This study was sponsored by the Federal Highway Administration under agreement No. DTFH61-06-H-00011 and Pennsylvania Department of Transportation (PennDOT) under Transportation Pooled Fund Program TPF-5(183). Terry Kerr, Marc Gardner, Paul Majoris, Joshua Freeman, Lydia Peddicord, and several others from PennDOT provided assistance in identifying the project, providing access to the project site, and traffic control during testing. We greatly appreciate their help.

We also thank Brian Zimmerman, Heath Gieselman, Wenjuan Li, Stephen Quist, Nathan Meisgeier, and Micah Loesch of the Center for Earthworks Engineering Research (CEER) at Iowa State University for their help with laboratory and field testing.

LIST OF ACRONYMS AND SYMBOLS

BCI	Base curvature index
BDI	Base damage index
CBR	California bearing ratio
CF	Faulting measured at the crack (maximum)
COV	Coefficient of variation
CW	Crack width (maximum)
DCP	Dynamic cone penetrometer
DPI	Dynamic cone penetration index
D_0	Deflection measured under the plate
D_1 to D_7	Deflections measured away from the plate at various set distances
D_{10}	Grain size diameter corresponding to 10% passing by mass
D_{60}	Grain size diameter corresponding to 60% passing by mass
E	Elastic modulus
$E_{LWD\text{-}Z2}$	Elastic modulus determined from a 200 mm diameter plate light weight deflectometer
$E_{FWD\text{-}K3}$	Surface modulus determined from a 300 mm diameter plate Kuab falling weight deflectometer
F	Shape factor
FWD	Falling weight deflectometer
GPS	Global positioning system
GPT	Gas permeameter test
HDP	High density polyurethane
IRI	International roughness index
K_{sat}	Saturated hydraulic conductivity determined using rapid gas permeameter test device
k_1, k_2, k_3	Regression coefficients in “universal” model
LTE	Load transfer efficiency
LWD	Light weight deflectometer
M_r	Resilient modulus
NG	Nuclear density gauge
OGS	Open graded stone
PCC	Portland cement concrete
P_a	Atmospheric pressure
r	Plate radius
RTK	Real time kinematic
RTS	Robotic total station
s_u	Undrained shear strength determined from unconsolidated-undrained triaxial test
SCI	Surface curvature index
SF	Faulting measured at the shoulder (maximum)
UU	Unconsolidated undrained test
ε	Axial strain
ε_p	Permanent strain
γ_d	Dry unit weight determined from Humboldt nuclear gauge

μ	Statistical mean or average
η	Poisson's ratio
σ	Statistical standard deviation
σ_B	Bulk stress
σ_d	Deviator stress
σ_d	Applied stress
$\sigma_1, \sigma_2, \sigma_3$	Principal stresses
τ_{oct}	Octahedral shear stress
w	Gravimetric moisture content

EXECUTIVE SUMMARY

Quality foundation layers (the natural subgrade, subbase, and embankment) are essential to achieving excellent pavement performance. Unfortunately, many pavements in the United States still fail due to inadequate foundation layers. To address this problem, a research project, Improving the Foundation Layers for Pavements (FHWA DTFH 61-06-H-00011 WO #18; FHWA TPF-5(183)), was undertaken by Iowa State University to identify, and provide guidance for implementing, best practices regarding foundation layer construction methods, material selection, in situ testing and evaluation, and performance-related designs and specifications. As part of the project, field studies were conducted of several in-service concrete pavements across the country that represented either premature failures or successful long-term pavements. A key aspect of each field study was to tie performance of the foundation layers to key engineering properties and pavement performance. In-situ foundation layer performance data, as well as original construction data and maintenance/rehabilitation history data, were collected and geospatially and statistically analyzed to determine the effects of site-specific foundation layer construction methods, site evaluation, materials selection, design, treatments, and maintenance procedures on the performance of the foundation layers and of the related pavements. A technical report was prepared for each field study.

This report presents laboratory and in situ test results and analysis from an experimental field study conducted on jointed PCC pavement on US 422 near Indiana, Pennsylvania. The 9.7 km (6 mile) highway section was built in 1995 with 280 mm (11 in.) thick portland cement concrete (PCC) layer over a nominal 100 mm (4 in.) thick open-graded stone (OGS) base layer; a nominal 100 mm (4 in.) thick well-graded subbase layer; and variable subgrade with mixed clay/shale/sandstone rock. The PCC slabs are about 3.7 m (12 ft) wide by 6.1 m (20 ft) long and are jointed using dowel bars. The slabs showed significant distresses with mid-panel cracking and faulting. Based on preliminary International Roughness Index (IRI) and falling weight deflectometer (FWD) testing, Pennsylvania Department of Transportation (PennDOT) personnel surmised that the observed surface distresses were linked to the support conditions provided by the OGS base layer. The Pennsylvania Department of Transportation (Penn DOT) initiated a rehabilitation strategy that primarily involved injecting HDP foam. A 160 m (500 ft) long control was stabilized using cementitious grout for performance comparison. The purpose of the stabilization was to: (1) stabilize the open-graded subbase layer, (2) reduce deflections under loading, and (3) improve load transfer efficiency (LTE) near joints and cracks. At selected locations, full-depth patching and dowel bar retrofitting was performed after the stabilization.

The Iowa State University (ISU) research team was present at the project site during HDP foam injection operations from October 1 to October 2, October 13 to October 15, and November 3–4, 2009, to conduct field testing before and after stabilization, and on April 28 and July 21, 2010, to conduct performance monitoring tests. Field testing involved: obtaining pavement surface profiles using high accuracy robotic total station (RTS) surveying to monitor slab movements related to HDP foam injection; mapping cracks on the pavement surface using RTS and real-time kinematic global positioning system (GPS) surveying; and obtaining falling weight deflectometer (FWD) tests on pavements before and after stabilization. Light weight deflectometer (LWD), nuclear moisture-density gauge (NG), dynamic cone penetrometer (DCP), and rapid in situ air permeameter tests (APTs) were conducted in the full-depth patching areas after stabilization to

observe migration of the injected foam and directly test the treated support layers under the pavement. Temperature sensors (I-buttons) were installed in three locations to monitor seasonal temperature variations in the pavement foundation layers. Laboratory testing was conducted on foundation layer materials obtained from field to determine index properties, moisture-dry unit weight relationships from compaction tests, resilient modulus (Mr), and undrained shear strength.

Key findings from the laboratory and field testing conducted in this study are summarized as follows:

Laboratory Testing

- Particle size distribution curves of OGS materials indicate that 6 of the 11 samples collected were outside the specification limits for material passing the 38.1 mm (3/8 in.), No. 20, No. 40, No. 100, and No. 200 sieves. Percent fines content tests conducted on OGS materials indicated that 31 of the 41 samples contained percent fines content greater than the maximum 5% specification limit.
- Particle size distribution curves of 2A materials indicate that four of the 11 samples collected were outside the specification limits for material passing the 38.1 mm (3/8 in.), No. 4, and No. 100 sieves. Six of the 11 samples contained percent fines content greater than the maximum 10% specification limit.
- Compared to the OGS and OGS+Foam samples, the foam sample produced much higher permanent strain (ε_p), produced much lower M_r, and underwent much higher elastic deformation. The OGS+Foam sample showed a lower (about 0.75 times on average) M_r value than the OGS sample. However, it should be noted that the OGS sample had considerably higher γ_d than the OGS+Foam sample (OGS γ_d = 18.54 kN/m^3, OGS+Foam γ_d = 14.92 kN/m^3).
- The UU stress-strain curve for the foam sample showed a near linear increase in deviator stress up to 6% axial strain. The OGS+Foam sample resulted in about 3.4 time higher shear strength at failure than the OGS sample.

Penn DOT's IRI Testing History (2005 to 2014)

- The results from annual IRI testing from 2005 to 2010 indicate that the pavement sections were mostly within "fair" to "good" rating range. On average, the IRI increased slightly from 2005 (1.6 m/km or 99 in./mile) to 2009 (1.7 m/km or 106 in./mile).
- In 2010, after HDP foam stabilization and dowel bar retrofitting, the average IRI further increased to about 1.9 m/km (122 in./mile), which suggest poor ability to control variations in the pavement surface elevation to minimize IRI. On average, the IRI measurements remained at about 1.9 m/km in 2014.

In Situ Testing in Patching Areas with and without HDP Foam Stabilization

- Field observations indicate that the foam did not fully penetrate the full width and depth of the OGS layer, thus creating non-uniform support conditions.
- $E_{LWD\text{-}Z2}$ and K_{sat} values are higher at test locations with untreated subbase than at locations with OGS+Foam mixture. The average $E_{LWD\text{-}Z2}$ was about two times greater and the average K_{sat} was about two orders of magnitude greater at locations with untreated subbase than at locations with OGS+Foam mixture. Further, the average DCP-CBR_{OGS} value was higher at locations with OGS+Foam mixture than at locations with untreated subbase. Two of the three DCP tests (on the OGS+Foam material indicated refusal near the surface (with < 1 mm per blow penetration). The K_{sat} contour maps highlighted the spatially concentrated low permeability zones in areas with OGS+Foam material.
- Low permeability of the OGS+Foam material was expected as the foam has a closed cell structure and is virtually impermeable. Low modulus but high shear strength (i.e., DCP-CBROGS) in the OGS+Foam mixture is an important determination in terms of selecting pavement design input values for this material. The field results are confirmed by resilient modulus laboratory test results =, which showed that the OGS+Foam sample had a 3.4 times higher undrained shear strength and 1.5 times lower resilient modulus, when compared to an unstabilized OGS sample.

Pavement Surface Elevation Monitoring in HDP Foam Treated Sections

- Pavement surface elevation monitoring on one test section (TS6) indicated that the panels were raised by an average of about 6 mm during the injection process. The upward movement in all panels was greater than the 1.3 mm maximum limit per the project specification. However, this process minimized the faulting at the cracks.
- Results on another test section (TS7) indicated that the pavement slabs were raised by an average of about 13 mm with a standard deviation of about 8 mm across the test section after initial injection, and by about 21 mm with a standard deviation of about 8 mm across slabs 2 and 3 after secondary injection. Similar to the results in TS6, the upward movement measured at all locations was greater than the 1.3 mm maximum limit per the project specification.

Comparison between Cementitious Grout and HDP Foam Stabilization Sections

- LTE showed statistically significant improvement near cracks and joints in both cementitious grout and HDP foam stabilized sections. LTE measurements at cracks, although improved after HDP stabilization, did not meet the targeted criteria (> 65%) until after dowel bar retrofitting.
- D_0 and I values showed statistically significant improvement only near cracks (and not near joints) in the HDP foam section and only near joints (and not near cracks) in the cementitious grout section.

- No statistically significant improvement was determined in any of the FWD measurements obtained at the mid-panel, for both stabilization methods.
- Faulting reduced by about 2.5 mm near cracks and by about 4.6 mm near shoulder after HDP foam injection. On cementitious grout section, faulting was reduced on average by about 0.5 mm near cracks and by about 2.2 mm near shoulder.
- These measurements indicate that slab movements were sometimes greater than the allowable 1.3 mm (per project specifications) and better process control measures are needed to control vertical movements, particularly with the HDP stabilization method.

Long-Term Performance of HDP Foam Stabilization Sections

- Statistical analysis of D_0 measurements indicated that improvement at joints and at mid-panel (i.e., a reduction in D_0) was not statistically significant after stabilization. However, the improvement at cracks was statistically significant after stabilization. The D_0 values decreased further during testing after 9 months, due to dowel bar retrofitting performed at 5 out of 7 crack locations and patching performed at 2 crack locations.
- I-values at crack locations were higher than at joint or mid-panel locations before stabilization. These values decreased after stabilization with a statistically significant difference. However, the measurements at all locations and at all testing times were lower than the critical value (0.076 mm).
- LTE measurements at cracks showed statistically significant improvement after stabilization. LTE at joints, however, did not show any statistically significant improvement. But, the values obtained 6 months and 9 months after stabilization showed statistically significant improvement.
- No statistically significant difference was noted in the $k_{dynamic}$ measurements obtained before and at all times after stabilization.

Recommendations for Future Work

The findings of this paper improve the understanding of the benefits and limitations of using injected foam technology to rehabilitate concrete pavements. Additional field studies that characterize the long-term durability of foam treated materials and life-cycle cost analysis of the rehabilitation method are needed to fully evaluate the use of this technology. Based on the lack of control for setting the final panel elevation, improved control systems may be needed to garner the full potential of injected foam technology.

The findings from the field studies under the Improving the Foundation Layers for Pavements research project will be of significant interest to researchers, practitioners, and agencies dealing with design, construction, and maintenance of PCC pavements. The technical reports are included in Volume II (Appendices) of the *Final Report: Improving the Foundation Layers for Pavements*. Data from the field studies are used in analyses of performance parameters for pavement foundation layers in the *Mechanistic-Empirical Pavement Design Guide* (M-E PDG) program. New knowledge gained from this project will be incorporated into the follow-up *Manual of Professional Practice for Design, Construction, Testing and Evaluation of Concrete Pavement Foundations*, to be published in 2015.

CHAPTER 1. INTRODUCTION

Aging highway infrastructure and increasing traffic volumes have caused premature failures in many pavements, resulting in significant maintenance, repair, and rehabilitation costs to the transportation industry (Tayabji et al. 2000). Development of new technologies that rehabilitate in-service pavements suffering from premature distress is a challenge facing the transportation industry. Many highway agencies are now evaluating different rehabilitation techniques that can potentially provide cost-effective and rapid solutions. Slab stabilization, also referred to as undersealing, is a commonly used rehabilitation procedure for portland cement concrete (PCC) pavements that suffer from faulting and transverse cracking. The purpose of slab stabilization is to fill voids beneath the slab thus minimizing deflections under loading. By controlling deflection, deflection-related distresses are reduced (FHWA 2005). Cementitious grout is the most common material used for slab stabilization (ACPA 1994). The use of injected expanding polyurethane foam is increasingly being used as an alternative to grout, primarily because of the shortened construction time, reduced materials/equipment requirements, and less labor (Abu al-Eis and LaBarca 2007, Barron 2004, Chen et al. 2008, Gaspard and Zhang 2010, Priddy et al. 2010).

Currently, a few state agencies (Missouri and New Jersey) have included high density polyurethane (HDP) foam technology as part of their standard specifications for slab stabilization (MoDOT 2009a; NJDOT 2007a). However, concerns over the long-term performance and mixed conclusions with respect to improvements in ride quality have been reported in the literature (Chen et al. 2009; Gaspard and Zhang, 2010). Further, to the authors' knowledge, field performance comparisons between cementitious grout and injected foam stabilization methods have not been well documented.

This report presents laboratory and in situ test results and analysis from an experimental field study conducted on jointed PCC pavement on US 422 near Indiana, Pennsylvania. The 9.7 km (6 mile) highway section was built in 1995 with 280 mm (11 in.) thick portland cement concrete (PCC) layer over a nominal 100 mm (4 in.) thick open-graded stone (OGS) base layer; a nominal 100 mm (4 in.) thick well-graded subbase layer; and variable subgrade with mixed clay/shale/sandstone rock. The PCC slabs are about 3.7 m (12 ft) wide by 6.1 m (20 ft) long and are jointed using dowel bars. The slabs showed significant distresses with mid-panel cracking and faulting. Based on preliminary International Roughness Index (IRI) and falling weight deflectometer (FWD) testing, Pennsylvania Department of Transportation (Penn DOT) personnel surmised that the observed surface distresses were linked to the support conditions provided by the OGS base layer. Similar surface distresses were documented on JPCP sections on Interstate 80 in Pennsylvania that are supported by an OGS base layer (Beckemeyer et al. 2002). Penn DOT initiated a rehabilitation strategy that primarily involved injecting HDP foam. A 160 m (500 ft) long control was stabilized using cementitious grout for performance comparison.

The purposes of the stabilization were to: (1) stabilize the open-graded subbase layer, (2) reduce deflections under loading, and (3) improve load transfer efficiency (LTE) near joints and cracks. At selected locations, full-depth patching and dowel bar retrofitting was performed after the stabilization.

The Iowa State University (ISU) research team was present at the project site during HDP foam injection operations from October 1 to October 2, October 13 to October 15, and November 3–4, 2009, to conduct field testing before and after stabilization, and on April 28 and July 21, 2010, to conduct performance monitoring tests. Field testing involved: obtaining pavement surface profiles using high accuracy robotic total station (RTS) surveying to monitor slab movements related to HDP foam injection; mapping cracks on the pavement surface using RTS and real-time kinematic global positioning system (GPS) surveying; and obtaining falling weight deflectometer (FWD) tests on pavements before and after stabilization. Light weight deflectometer (LWD), nuclear moisture-density gauge (NG), dynamic cone penetrometer (DCP), and rapid in situ air permeameter tests (APTs) were conducted in the full-depth patching areas after stabilization to observe migration of the injected foam and directly test the treated support layers under the pavement. Temperature sensors (I-buttons) were installed in three locations to monitor seasonal temperature variations in the pavement foundation layers.

Field tests were conducted on nine test sections. The objectives of this testing are categorized as follows:

- Evaluate the pavement foundation layer (i.e., OGS base, subbase, and subgrade) support conditions in full-depth patching areas following HDP foam stabilization.
- Evaluate the PCC surface and foundation layers before and after HDP foam stabilization and their performance over time.
- Compare the performance of PCC surface and foundation layers in the HDP foam treated sections with the cementitious grout treated section.
- Compare temperature profiles in the foundation layers between HDP foam treated, cementitious grout treated, and control (no stabilization) sections.

This report contains seven chapters. Chapter 2 provides background information on HDP and cementitious grout stabilization methods and documented case histories on field performance. Chapter 3 presents descriptions of experimental test methods and procedures followed in the laboratory and field testing, and the statistical data analysis methods. Chapter 4 provides an overview of the project, results of Penn DOT's pre-stabilization testing, and a summary of the rehabilitation process. Chapter 5 presents results and findings obtained from detailed laboratory testing including gradation test results of OGS materials and resilient modulus and shear strength tests on OGS, and OGS material mixed with foam, and foam materials. Chapter 6 presents results and findings from field testing conducted by PennDOT and ISU. Chapter 7 provides a summary of key findings and conclusions from this project.

The findings from this report should be of significant interest to researchers, practitioners, and agencies who deal with design, construction, and maintenance aspects of PCC pavements. Results from this project provide one of several field project reports being developed as part of the TPF-5(183) and FHWA DTFH 61-06-H-00011:WO18 studies.

CHAPTER 2. BACKGROUND

Voids beneath concrete pavement slabs cause loss of support and lead to distresses such as transverse cracking, faulting, and corner breaks. These distresses lead to poor ride quality. Slab stabilization involves injecting durable materials into the voids. The main purpose of slab stabilization process is to reduce deflections under loading and not to lift pavements (FHWA 2005). Slab jacking is another similar rehabilitation process used to vertically lift faulted slabs (Del Val 1981; Taha et al. 1994). Slab jacking is a common technique used to fill voids beneath faulted bridge approach pavement slabs (see White et al. 2007).

Cementitious grout is the most common material used for slab stabilization (ACPA 1994). The use of injected expanding polyurethane foam is increasingly being used as an alternative to grout, primarily because of the shortened construction time, reduced materials/equipment requirements, and less labor (Abu al-Eis and LaBarca 2007, Barron 2004, Chen et al. 2008, Gaspard and Zhang 2010, Priddy et al. 2010). Currently, a few state agencies (Missouri and New Jersey) have included HDP foam technology as part of their standard specifications for slab stabilization (MoDOT 2009b; NJDOT 2007a). Concerns over the benefits to long-term pavement performance and ride quality, however (Chen et al. 2009, Gaspard and Zhang 2010), have slowed use of slab stabilization technologies.

A summary of the current state highway agency specifications for slab stabilization and slab jacking using cementitious grout is provided in Table 1 and Table 2 provides specifications for HDP. Many agencies use cementitious grouts as they are readily available within reasonable distance for most projects (ACPA 1994). Of the 7 state agency specifications reviewed, only 2 agencies currently allow HDP foam for slab stabilization, but all 7 allow HDP foam for slab jacking applications. The foam injection method has been gaining popularity for slab stabilization applications because of its advantages with faster setting times and strength gains compared to cementitious grouts (Abu al-Eis and LaBarca 2007; Barron 2004; Chen et al. 2008; Gaspard and Zhang 2010). Appendix A is a pdf of “Slab stabilization (Section 679)” (PennDOT 2011), the PennDOT specifications for stabilization.

When cementitious grouts are used, traffic delay times typically vary from several hours to three days depending on how fast the grout achieves its strength (Table 1). The traffic delay time is typically < 1 hr when injected foam is used (Table 2).

The following sections of this chapter describe material properties and mix design of cementitious grouts and HDP foam, discuss the construction quality control and testing, and review previous studies documenting the field performance of the two materials.

Table 1. Summary of state DOT specifications for cementitious grout

State	Reference	Application	Materials	Mix Design	Requirements	Slab Movement	Testing	Traffic Delay
AL	ALDOT (2012a)	Slab jacking	Type I or III PC, $CaCl_2$, FA, air entraining additives or chemical admixtures, LD, FS.	The following mix design proportions (by volume) are specified: 80% FA + 20% PC; 50% LD + 30% FA + 20% PC; 80% LD + 20% PC; 20% FS + 50% FA + 20% PC; 50% FS + 30% FA + 20% PC; 50% FS + 30% LD + 20% PC.	PP: ≤ 1.5 MPa ET: 18–25 s	± 6 mm of the final grade	4.5m long straight edge is used to verify that the final grade is within ± 6 mm.	Minimum of 3 hrs. For Type III cement, delay should be greater than the initial set time.
	ALDOT (2012b)	Slab stabilization			PP: ≤ 1.5 MPa ET: 14–22 s	≤ 1 mm	A rubber-tired 90 kN single axle load is used to check if slab movement under loading < 0.8 mm. Increase in IRI values after stabilization should be < 10 mm/km.	
CA	Caltrans (2010a)	Slab stabilization	PC, class C/F FA, chemical admixtures and $CaCl_2$ (optional).	2.4–2.7 parts FA to 1 part PC by weight.	7-day CS: ≥ 5.2 MPa ET: 10–16 s PP: ≤ 1.0 MPa	≤ 1.3 mm	Not specified	
	Caltrans (2010b)	Slab jacking			ET: 16–26 s PP: ≤ 1.4 MPa	± 3 mm of the final grade		
IA	Iowa DOT (2012)	Slab stabilization	Type I PC, class C FA.	1 part by volume of Type I PC and 3 parts by volume of class C FA.	ET: 10–16 s Initial PP: ≤ 0.15 MPa PP: ≤ 0.05 MPa	≤ 2.5 mm	Not specified	Delay time should be greater than the initial set time (6 hours at 4°C and 4 hours at 10°C).
KS	KDOT (2015)	Slab stabilization	Type I or II PC, FA, air entraining or chemical admixtures (optional).	≥ 25% by volume of PC and ≥ 50% by volume of FA.	ET: 9–15 s 7-day CS: ≥ 4.1 MPa PP: sustained 1.0 MPa	≤ 3.2 mm	FWD test is used to determine the effectiveness of the undersealing operation through voids under the slabs.	Not Specified
LA	Louisiana DOTD (2006)	Slab stabilization and slab jacking	Type I PC, FA, Powdered ammonium sulphonate.	1 part PC and 3 parts FA by volume and powdered ammonium lignin sulphonate at 0.5 to 1.5% by weight of PC.	ET: 12–18 s for undersealing and 15–26 s for slab jacking PP: ≤ 1.4 MPa.	± 3 mm of the final grade	Not specified	At least 1 hour after pumping operations.
MO	MoDOT (2009b)	Slab stabilization	Type I, II or III PC, FA.	≥ 1 part PC by volume to 3 parts FA.	7-day CS: ≥ 4.1 MPa ET: 10–16 s Initial PP: 1.380 MPa PP: ≤ 0.69 MPa (0.205 to 0.345 MPa)	≤ 3 mm	FWD test is used for void detection and undersealing verification. Requires $\Delta_L \leq 0.38$ mm or $(\Delta_A - \Delta_L) \leq 0.25$ mm.	Three hours after the end of pumping operations, and after all drill holes are plugged.

State	Reference	Application	Materials	Mix Design	Requirements	Slab Movement	Testing	Traffic Delay
NJ	NJDOT (2007a; 2007b)	Slab stabilization	Type I, II, III PC, FA chemical admixtures.	1 part PC to 3 parts FA. Use admixtures if needed.	7-day CS: ≥ 4.1 MPa ET: 9–16 s PP: ≤ 0.4 MPa	≤ 2.5 mm	Deflection test is needed to verify if the deflection value is less than 0.25 mm.	At least one hour after initial set.
OK	OKDOT (2009)	Slab stabilization	PC, FA, air/chemical/corrosion-inhibiting/latex emulsion admixtures.	A mix design showing the CS, ET, VC, and initial set time needs to be reviewed and approval by the Engineer.	7-day CS: ≥ 5.5 MPa ET: 10–16 s Pumping head: 1.54 m^3/hr	0.825 mm–0.925 mm	A standard Benkelman Beam is used to monitor excessive lifting of pavement or rising of the adjacent shoulders.	3 calendar days or directed by the Resident Engineer.
PA	Penn DOT (2011)	Slab stabilization	PC, pozzolan (class C/ F/FA, ground granulated blast furnace slag, silica fume)	1 part PC to 3 parts of pozzolan by volume and admixtures if required.	7-day CS: ≥ 4.8 MPa ET: 10–15 s PP: ≤ 1.4 MPa VC: -2.5–10% Initial set time: 1–6 hr	≤ 1.3 mm	A vehicle having a dual-tire single axle with an 80 kN single axle load is used to detect if slab corner deflection ≤ 0.5 mm and joint efficiency ≥ 65%.	At least 12 hours after completing grouting operations.
SD	SDDOT (2004a)	Slab stabilization	Type I or II PC, class C FA.	1 part PC to 3 parts FA.	7-day CS: ≥ 4.1 MPa ET: 9–15 s PP: ≤ 0.4 MPa	≤ 3 mm	FWD test or a single axle truck needs to be used to determine if the deflection is in excess of 0.25 mm. A laser leveling unit is used to ensure if the concrete is raised to an even plane and to the required elevation.	Not specified
	SDDOT (2004b)	Slab jacking			7-day CS: ≥ 4.1 MPa Initial ET: 9–15 s ET: 16–36 s PP: ≤ 1.4 MPa	± 6 mm of the final grade		
UT	UDOT (2012)	Slab jacking	Hydraulic cement, fine aggregate, other ingredients.	Packaged dry, hydraulic-cement grout (non-shrink) by manufacturer.	7-day CS: ≥ 24 MPa 28-day CS: ≥ 34 MPa Early age VC: ≤ 4% Hardened VC: ≤ 0.3%	± 3.2 mm of the final grade	Not specified	

Note: PC–portland cement, FA–fly ash, LD– limestone dust, FS–fine sand, PP–pumping pressure, ET–efflux time, CS–compressive strength, Δ_L–the average of three normalized deflections on leave side, Δ_A–the average of three normalized deflections on approach side

Table 2. Summary of HDP in state DOT specifications

State	Reference	Application	Requirements	Slab Movement	Testing	Traffic Delay
MO	MoDOT (2009a) MoDOT (2009b)	Slab stabilization Slab jacking	Density: ≥ 64 ± 8 kg/m3 CS: ≥ 0.55 MPa TS: ≥ 0.62 MPa VC: ≤ 5% CR: ≤ 15 min. for 90% CS	≤ 3 mm ≤ 3 mm of the final grade	FWD test is used for void detection and undersealing verification. ΔL ≤ 0.38 mm or (ΔA-ΔL) ≤ 0.25 mm.	At least 30 min after ceasing pumping operations. Three hours after the end of pumping operations, and after all drill holes are plugged.
NJ	NJDOT (2007a; 2007b)	Slab stabilization and slab jacking	Density: 90.5–94.5 kg/m3 CS: 0.45- 0.66 MPa TS:0.48–0.69 MPa VC: 5% to 11% for humid 28-day, -0.1% to -0.9% for 5-day freezing SS: 0.28–0.59 MPa Close cell %: 85%–95% CR: ≤ 15 min. for 90% CS	≤ 2.5 mm for undersealing and ± 6.4 mm of the final grade for slab jacking	Deflection test is needed to verify if the deflection value is less than 0.25 mm.	At least one hour after initial set.
NC	NCDOT (2008)	Slab jacking	Density: 48–67.3 kg/m3 CS: ≥ 0.28 MPa	± 6.4 mm of the final grade	A tight string line is used to monitor and verify elevations for slab lengths of 15.24 m or less.	Not specified
OH	Ohio DOT (2007)	Slab jacking	Density: ≥ 48 kg/m3 TS: ≥ 0.28 MPa CS: ≥ 0.28 MPa VC: -0.6%–4% Water absorption: ≤ 2.0%	± 5 mm of the final grade.	Use a tight string or laser level to monitor and verify elevations.	Not specified
PA	Penn DOT (2010)	Slab jacking	Density: ≥ 64 kg/m3 CS: ≥ 0.41 MPa TS: ≥ 0.48 MPa SS: ≥ 0.28 MPa Close cell content: ≥ 85%	± 1.3 mm of the final grade	Deflection test is performed to check if slab corner deflection ≤ 0.5 mm and joint efficiency ≥ 80% at least 24 hours after injection.	At least 30 min after injection.
SD	SDDOT (2004b)	Slab jacking	Free rise density: 48–51 kg/m3 CS: ≥ 0.28 MPa CR: ≤ 15 min. for 90% CS	± 6 mm of the final grade	A laser leveling unit is used to ensure if the concrete is raised to an even plane and to the required elevation.	Not specified
UT	UDOT (2012)	Slab jacking	Density: 60.9–68.9 kg/m3 TS: ≥ 0.55 MPa Elongation: ≤ 5.1% CS: ≥ 0.41 MPa CR: ≤ 15 min. for 100% CS	± 3.2 mm of the final grade	Not specified	

Note: CS–compressive strength, TS–tensile strength, VC–volume change, SS–shear strength, CR–curing rate, Δ_L–the average of three normalized deflections on leave side, Δ_A–the average of three normalized deflections on approach side

Material Properties and Mix Design

The materials and mix designs used in cementitious grouts vary between agencies. Most commonly used materials in the mixture are portland cement (type I or II or III) and pozzalonic material such as fly ash (class C or F). Pozzalonic materials have spherical shape fine particles which enhances the flow properties of the mixture. Other materials also considered in the mix design for cementitious grouts are CaCl, lime dust, silica fume, ammonium sulphonate, and blast furnace slag. The maximum pumping pressure (PP), efflux time (ET) range, and minimum compressive strength required are typically included in the specifications, as summarized in Table 1.

The HDP foam used for pavement rehabilitation is a closed cell rigid hydrophobic foam with nominal densities ranging from about 56 to 240 kg/m^3 (Priddy et al. 2010; Priddy and Newman 2010; Yu et al. 2013). These types of foams are referred to as HDP foams, while low density polyurethane foams comprise of densities less than 56 kg/m^3 (Priddy and Newman 2010). The HDP foam is primarily made of two liquid chemicals: (a) a blend of polyol comprising polyether-polyol and catalysts, and (b) water and isocyanate desmador (Brewer et al. 1994). These chemicals combine under heat to form a strong lightweight foam-like substance. When the two chemicals are injected together under pressure, a rapid chemical reaction occurs and causes the polyurethane foam to rapidly expand and fill the voids. The various material properties that are included in the specifications for HDP foam are summarized in Table 2. They have low viscosity, high expansion rate, low water content, high tensile and compressive strength, resistance to deterioration from freeze/thaw cycles, reaction times ranging from about 30 sec to 1 min, and curing times < 15 min, and low thermal conductivity (about 100 times lower than unfrozen coarse grained soil). Reaction time refers to the time to react and cause the material to expand, while curing time refers to the time for the foam to achieve its ultimate density and strength (Gaspard and Zhang, 2010).

Construction and Testing Procedures

As part of testing prior to construction, FHWA (2005) recommends conducting field deflection testing using a FWD or a loaded truck or ground penetrating radar (GPR) scanning to detect areas of voids that need stabilization.

Once the stabilization areas are determined, the construction process involves drilling holes, injecting foam/grout, and conducting QC/QA testing to control slab movements. A pattern of one to three holes, that are placed close enough to achieve flow of grout from one hole to the other, is typically used (FHWA 2005). An optimum hole pattern can be determined based on field trials. The holes are drilled to the bottom of the concrete slab or to the bottom of the subbase layer if the subbase layer needs stabilization (FHWA 2005).

Monitoring pavement slab movement is a critical part of QC during the injection process. For slab stabilization applications, slab movement is restricted to a specified maximum value, which varies between DOT agencies from 1 to 3 mm (see Tables 1 and 2). For slab jacking applications, slab movement is controlled by raising slabs to a uniform or original grade within a

minimum specified tolerance, which varied between ±2.5 and ±6.4 mm. Verification of slab movement is accomplished using a string level or a laser level or a straight edge. Deflection testing after stabilization is specified by some agencies using FWD or Benkelman beam and a loaded truck to verify a reduction in pavement deflections, voids have been filled, and LTE across joints or stabilized cracks has been improved. International roughness index (IRI) testing is specified in ALDOT (2012a; 2012b) with a requirement of <10 mm/km after slab stabilization.

Previous Performance Monitoring Studies

Cementitious Grout

Although cementitious grouting has been widely used for pavement rehabilitation applications, to the authors' knowledge, very limited performance monitoring data has been reported in the literature.

Taha et al. (1994) reported performance results from two slab stabilization projects (to fill voids beneath slabs) using cementitious grout on undoweled jointed PCC pavements (originally constructed in 1971) in comparison with nearby unstabilized sections. The grout used was a mixture one part cement to three parts fly ash by volume with a minimum 4.1 MPa (600 psi) 7-day compressive strength. On one project, slab stabilization was performed in 1987. A field survey conducted six years after stabilization indicated an average joint faulting of 2.5 mm in stabilized sections as compared to 4.8 mm average faulting unstabilized sections. FWD test results showed average corner deflections of 0.53 mm and LTE of 79% in stabilized sections, while average corner deflections were 0.64 mm and LTE was 45% in unstabilized sections. On the other project, stabilization was performed in 1989. No significant faulting was observed about five years after stabilization, but an average faulting of about 3.2 mm was observed in the unstabilized sections. FWD tests showed an average corner deflection of 0.69 mm and LTE of 39% in stabilized sections and an average corner deflection of 1.07 mm and LTE of 23% in unstabilized sections. Taha et al. (1994) concluded that while cementitious grout for slab stabilization is an effective method for void filling beneath the slabs and short-term improvement in performance, it does not fully prevent future faulting or significantly improve long-term performance. They also indicated that injecting cementitious grout is effective if joint faulting is < 5.1 mm (0.2 in.).

Ni and Cheng (2011) reported FWD and GPR test results before and after stabilization using cementitious grout on an airport runway pavement consisting of jointed PCC pavement. The grout consisted of 7% portland cement by weight with 0.8 water-cement ratio. Their GPR results indicated that the number of voids and the area voids present reduced after grouting, although the voids were not completely filled. The calculated zero load deflections (deflection intercept) and peak deflections from FWD testing also reduced after stabilization.

HDP Foam

Case studies have been conducted in the United States since 1993 at sites where HDP was used for slab jacking and slab stabilization applications. Key observations and findings from some of those case studies along with cost and time involved in using HDP foam stabilization technology are summarized in Table 3. Some of these case studies reported field performance results on HDP foam stabilized concrete pavements with mixed conclusions in terms of the observed improvements (Chen and Scullion 2007; Chen et al. 2009; Chen et al. 2008; Crawley et al. 1996; Gaspard and Morvant 2004; Gaspard and Zhang 2010; Opland and Barnhart 1995).

Opland and Barnhart (1995) conducted IRI and FWD tests before and after slab stabilization using HDP foam on concrete pavements supported on open-graded drainage course layers. They found that ride quality, LTE at joints and cracks, and peak deflections under FWD loads were improved shortly after stabilization, particularly in sites with previous severe cracks. However, , they reported differential frost heave in sections relative to the adjacent lane that were not stabilized and attributed this to the lower thermal conductivity of the foam. They also reported that the performance of the test sections within the one-year trial period varied significantly and in some cases had returned to pre-stabilization conditions.

Crawley et al. (1996) reported field observations and test results from a jointed PCC slab stabilization project using HDP foam to repair faulted joints and transverse cracks. Their observations indicated that, after stabilization, the joint LTE increased and maximum deflections under loading decreased. They also found that the injection process produced new voids under the panels, but re-injection mitigated the problem.

Gaspart and Morvant (2004) and Gaspard and Zhang (2010) reported FWD and ride quality tests on continuously reinforced PCC and jointed PCC pavements, before and after injecting HDP foam for filling slab voids and levelling slabs. Their results indicated that foam injection successfully filled voids beneath the pavements, but did not improve ride quality. They also found that LTE at joints was not improved after stabilization.

Chen and Won (2008) and Chen et al. (2009) documented field observations from projects in Texas where PCC pavement faulting was repaired using HDP foam injection. They reported that the foam injection process raised panels and reduce faulting during stabilization, but did not provide long-term improvement. Chen and Scullion (2007) conducted a GPR survey on a five year old HDP stabilized pavement section in Texas and found voids beneath the pavement that contributed to further cracks and faulting.

Table 3. Summary of field case studies documented in the literature

Reference	Project Location	Date	Project Size	Problem	Key Findings/Observations	Unit Cost	Time (Days)
Brewer et al. (1994); 10 sites in OK	I-35—SH 66 Interchange, Edmond, OK	Nov. 1993	2 slabs	Slab stabilization	The pavement slabs were raised by injecting foam to reduce faulting. About 204 kg (450 lb) of HDP material was used.	$11/kg ($5/lb)	1.25
	I-35, 0.2 miles south of SH 66, Edmond, OK	Nov. 1993	15 slabs	Slab jacking	The bridge approach slabs and pavement slabs were raised by injecting foam to reduce faulting and curling. About 680 kg (1500 lb) of HDP material was used.	$11/kg ($5/lb)	2.25
	OK SH 7, 1 mile east of I-44, OK	Nov. 1993	17 slabs	Slab stabilization and jacking	The bridge approach slabs and pavement slabs were raised by injecting foam to reduce faulting and curling. Few hairline cracks appeared during the stabilization process. About 1504 kg (3315 lb) of HDP material was used.	$11/kg ($5/lb)	1.75
	US 81, 0.8 mile south of OK SH 17	Nov. 1993	17 cracks	Slab stabilization	Most of the cracks on the pavement were repaired by injecting foam. Injection at one crack showed a large bulge and had to be repaired with conventional patching. About 508 kg (1120 lb) of HDP material was used.	$11/kg ($5/lb)	3.25
	I-44, Tulsa County, OK	Nov. 1993	3 slabs	Slab jacking	The bridge approach slabs were raised by injecting HDP foam. Cracks that developed in the slabs during stabilization resulted in curling and, in some cases, breaking of the slabs. About 1451 kg (2300 lb) of HDP material was used.	$11/kg ($5/lb)	1.50
	US 412, about 1 mile east of OK SH 66	Nov. 1993	8 slabs	Slab stabilization	The pavement slabs were raised by injecting foam to reduce faulting. Some slabs cracked during the stabilization process. About 481 kg (1060 lb) of HDP material was used.	$11/kg ($5/lb)	1.00
	US 62, Muskogee County, OK	Dec. 1993	4 slabs	Slab jacking	The bridge approach slabs were raised by injecting HDP foam. Shoulders next to the parapet wall were also raised to level with the bridge deck. About 1061 kg (2340 lb) of HDP material was used for stabilization.	$11/kg ($5/lb)	2.00
	US 64, Muskogee, OK	Dec. 1993	1 box culvert slab	Stabilization of a sinking box culvert	The pavement slab over the culvert was raised to level with the adjacent pavement slabs. About 227 kg (500 lb) of HDP material was used for stabilization.	$11/kg ($5/lb)	0.50
	SH 3, Ada, OK	Dec. 1993	4 slabs	Slab jacking	The bridge approach slabs were raised by injecting the foam. No cracks were observed in the slabs during stabilization. About 676 kg (1490 lb) of HDP material was used.	$11/kg ($5/lb)	1.50
	SH 1 south of OK SH 19	Dec. 1993	6 slabs	Slab stabilization	The pavement slabs were raised by injecting the foam to reduce curling and faulting. One slab with severe curling cracked during the stabilization. A total of about 383 kg (845 lb) of HDP material was used for stabilization.	$11/kg ($5/lb)	0.75

Table 4. Summary of field case studies documented in the literature (continued)

Reference	Project Location	Date	Project Size	Problem	Key Findings/Observations	Unit Cost	Time (Days)
Crawley et al. (1996); 2 sites in MS	I-55, Tate County, MS	May 1994, Jan. 1995,	13 slabs	Slab stabilization	The pavements were underlain by cement treated base. After stabilization, deflections under the FWD plate at the joints reduced by 40 to 70%, increased the joint LTE by 370 to 850%. However, increased deflections at the mid slab were noticed which indicates void under the slab. Secondary stabilization at those locations mitigated the problem. The average IRI reduced after stabilization by about 8 to 13%. A total of about 774 kg (1706 lb) of HDP material was used for stabilization.	*	2.00
	US 78, Marshall County, MS	May 1994	50 slabs	Slab stabilization	The pavements were underlain by cement treated base. After stabilization, deflections under the FWD plate at mid-slabs increased by an average of 43% for 25 slabs, and decreased by an average of 31% for 25 slabs. Joint deflections increased by an average of 106% at 18 joints and decreased by an average of 29% at 32 slabs. The LTE increased by an average of 70% at 40 joints and decreased by an average of 8% at 9 joints. A total of about 747 kg (1647 lb) of HDP material was used for stabilization.	*	1.00
Oplan and Barnhart (1995)	I-75, Monroe County, MI	Oct. 1993	3 test sections (90 ft, 400 ft, and 812 ft long)	Slab stabilization	The pavements were underlain by open-graded aggregate base and sand subbase. The stabilization process improved the base support significantly where the pavement was severely cracked, but showed limited improvement where the pavement had hairline cracks. The base support, LTE and ride quality improved shortly after stabilization, but decreased to the same level as before within a year. The depth of penetration of HDP into base was dependent on the gradation (porosity) of the base material. Differential frost heave between slabs was noticed due to insulating effect from the HDP material, where adjacent slabs were not treated. A total of about 2394 kg (5278 lb) of HDP was used.	$11/kg ($5/lb)	*
Barron (2004)	US 50, KS	Apr. 2004	50 lane miles	Slab stabilization	The pavements were underlain by drainable base and lime treated clay subgrade. No structural failures were noticed two years after stabilization. A 10-year material integrity guarantee was provided by the HDP manufacturer.	*	50.00

* Not provided.

Table 5. Summary of field case studies documented in the literature (continued)

Reference	Project Location	Date	Project Size	Problem	Key Findings/Observations	Unit Cost	Time (Days)
Gaspart and Morvant (2004)	I-10, St. James Parish, LA	Sep. 2003	90 ft long CRCP	Slab stabilization	The pavements were underlain by asphaltic concrete base and sand-shell subbase. The pavement was raised by an average of 50 mm at maximum depressions and IRI was reduced by about 30 to 70%. FWD deflections increased after injection process and the reason for increase was unknown. Structural number determined from Dynaflect did not change much after injection process.	*	2.00
		Oct. 2003	45 JCP slabs	Slab stabilization	The pavements were underlain by cement-treated silty clay subgrade. Voids underneath the pavement were filled as verified in core samples. Varying layers and densities of polyurethane foam were observed in the voids. FWD deflections at mid slab did not show much difference after stabilization. LTE at joints generally increased after stabilization. Structural number determined from Dynaflect did not change much after injection process. Field observations showed that the stabilization did not waterproof the pavement well. A total of about 1050 lb of HDP was used.	*	1.00
Abu and Labarca (2007)	I-39—US 78 Interchange, WI	Jun. 2001	4 slabs	Slab jacking	Four hairline cracks were observed in one slab six months after stabilization, and one crack was observed 5.5 years after stabilization. A slight dip developed at the end of the approach slab, but it was better than prior to stabilization. The treated pavement generally performed well. A total of about 1470 kg (3241 lb) of HDP was used.	$290/m^2 $13/kg ($6/lb)	0.75
	US 12, Dane County, WI	Jun. 2001	2 slabs	Slab jacking	No new cracks developed in the approach slabs. The ride quality remained adequate two years after stabilization. A total of about 473 kg (1043 lb) of HDP was used.	$139/m^2 $13/kg ($6/lb)	0.50
Tartabini (2008)	I-287, NJ	Apr. 2001	6.4 km (4 miles)	Slab stabilization	The pavements were underlain by open graded aggregate base. FWD tests showed lower joint deflections and intercepts at HDP treated sections compared to concrete grout treated sections. Deflections under the FWD plate at joints decreased by about 60 to 80%, and intercepts decreased by about 90 to 100%.	*	*
This Report	US 422, Indiana, PA	2009-2010	9.7 km (6 miles)	Slab stabilization	A total of about 286,530 kg (631,690 lb) of HDP was used.	$9.47/kg ($4.30/lb)	42

* Not provided.

CHAPTER 3. EXPERIMENTAL TESTING METHODS

Experimental testing in this research study involved laboratory testing of foundation layer materials and HDP foam samples, in situ testing to evaluate the properties of the pavement surface and underlying foundation layers, and in-ground instrumentation to monitor temperatures.

This chapter presents a summary of the laboratory and in situ testing methods, and the statistical analysis methods used in this study.

Laboratory Testing Methods

Particle Size Analysis and Fines Content Determination

Particle size analysis tests were conducted in accordance with ASTM C136-06 *Standard Test Method for Sieve Analysis of Fine and Coarse Aggregates*. Samples were collected from the field and were carefully sealed and transported to the laboratory for testing. The samples were properly mixed and separated using an aggregate splitter to collect approximately 2000 gm of air-dried sample for particle size analysis. The wet sieving method was used. The samples were washed through the No. 200 (75 μm) sieve following ASTM C117-04 *Standard Test Method for Materials Finer than 75μm (No. 200) Sieve in Mineral Aggregates by Washing.* The material retained on the No. 200 sieve was oven-dried for about 24 hours, and the oven-dried material was sieved through the 50.8 mm (2 in.), 25.4 mm (1 in.), 38.1 mm (3/8 in.), 19.1 mm (3/4 in.), 9.5 mm (1/2 in.), No. 4, No. 10, No. 20, No. 40, No. 100, and No. 200 sieves. Material retained on each sieve was recorded to determine particle size distributions.

Fines content tests were performed on bag samples obtained from the field. About 200–300 gm of sample were obtained at each test location. The fines content was determined by washing the sample through the No. 200 sieve following ASTM C117-04.

Samples were classified in accordance with the unified soil classification system (USCS) following ASTM D2487-10 *Standard Practice for Classification of Soils for Engineering Purposes (Unified Soil Classification System)* and the American Association of State Highway and Transportation Officials (AASHTO) classification system following the ASTM D3282-09 *Standard Practice for Classification of Soils and Soil-Aggregate Mixtures for Highway Construction Purposes.*

Resilient Modulus and Shear Strength Testing

Resilient modulus (M_r) tests were performed in accordance with AASHTO T-307 *Standard Method of Test for Determining Resilient Modulus of Soils and Aggregate Materials* (AASHTO 1999). The Geocomp automated M_r test setup (Figure 1) was utilized in this study. The setup consists of a Load Trac-II load frame, electrically controlled servo valve, an external signal

conditioning unit, and a computer with a network card for data acquisition. The system uses a real-time adjustment of proportional-integral-derivative (PID) controller to adjust the system control parameters as the stiffness of the sample changes to apply the target loads during the test.

Figure 1. Triaxial chamber and load frame (left) and computer setup (right)

Figure 1 shows the triaxial test chamber used in this study. The chamber is setup to perform 71 mm (2.8 in.) or 101.6 mm (4 in.) diameter samples. Two linear voltage displacement transducers (LVDTs) are mounted to the piston rod to measurement resilient strains in the sample during the test.

M_r tests were performed on 101.6 mm (4 in.) diameter by 203.2 mm (8 in.) height samples following the AASHTO T-307 conditioning and loading sequences (Table 4) suggested for base materials. Each load cycle consisted of a 0.1 second haversine load pulse followed by a 0.9 second rest period. Resilient modulus is calculated as the ratio of the applied cyclic deviator stress (σ_d) and resilient strain (ε_r). σ_d and ε_r values from a typical stress-strain cycle during the test are shown in Figure 2.

Table 6. M_r testing sequences for base/subbase materials (AASHTO 1999)

	Confining Pressure		Maximum Axial Stress		
Sequence	**kPa**	**psi**	**kPa**	**psi**	**Cycles**
0	103.4	15	103.4	15	500–1000
1	20.7	3	20.7	3	100
2	20.7	3	41.4	6	100
3	20.7	3	62.1	9	100
4	34.5	5	34.5	5	100
5	34.5	5	68.9	10	100
6	34.5	5	103.4	15	100
7	68.9	10	68.9	10	100
8	68.9	10	137.9	20	100
9	68.9	10	206.8	30	100
10	103.4	15	68.9	10	100
11	103.4	15	103.4	15	100
12	103.4	15	206.8	30	100
13	137.9	20	103.4	15	100
14	137.9	20	137.9	20	100
15	137.9	20	275.8	40	100

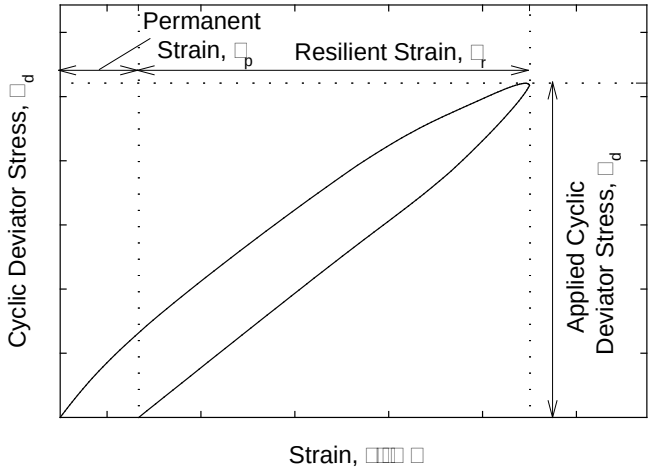

Figure 2. Graphical representation of one load cycle in M_r testing

The average σ_d and ε_r of the last five cycles of a loading sequence are used in M_r calculations. Following the M_r testing, unconsolidated undrained (UU) strength testing, also known as the quick-shear testing, was performed on each sample by applying a confining pressure of 27.6 kPa (5 psi) to the sample.

AASHTO T-307 requires that the maximum particle size of the material should be 1/5 of the sample diameter, which is approximately 20.3 mm (0.8 in.) for a101.6 mm (4 in.) diameter sample. The OGS material tested in this study contained a maximum particle size of 25.4 mm

(1 in.). To meet the AASHTO T-307 specifications, the particle size distribution of the OGS material was modified by scalping off particles retained on the 19.1 mm (¾ in.) sieve and replacing them with the same percentage by weight of the material that was retained on the No. 4 sieve and passing the 19.1 mm (¾ in.) sieve. Before separating the material, it was first oven-dried so that the weight of moisture did not affect the percentage removed and replaced.

OGS, OGS mixed with HDP foam (OGS+Foam), and HDP foam samples were tested in this research study. The OGS samples were compacted using a vibratory method. Vibratory compaction was achieved in five lifts of equal amount of material and thickness using an electric rotary drill hammer with a circular steel platen against the material (Figure 3).

Figure 3. Preparation of an OGS sample for laboratory M_r and UU testing

The OGS sample was compacted in the field in a steel split mold as shown in Figure 3. The OGS+Foam sample was compacted in the field similar in a plastic mold in the same procedure followed for the OGS sample (Figure 4). Following compaction, the plastic mold was capped and HDP foam was injected into the mold. After injecting a sufficient quantity of foam, pressure was applied on top of the sample cap for some time (until the foam hardened) to simulate the confinement effect under the pavement.

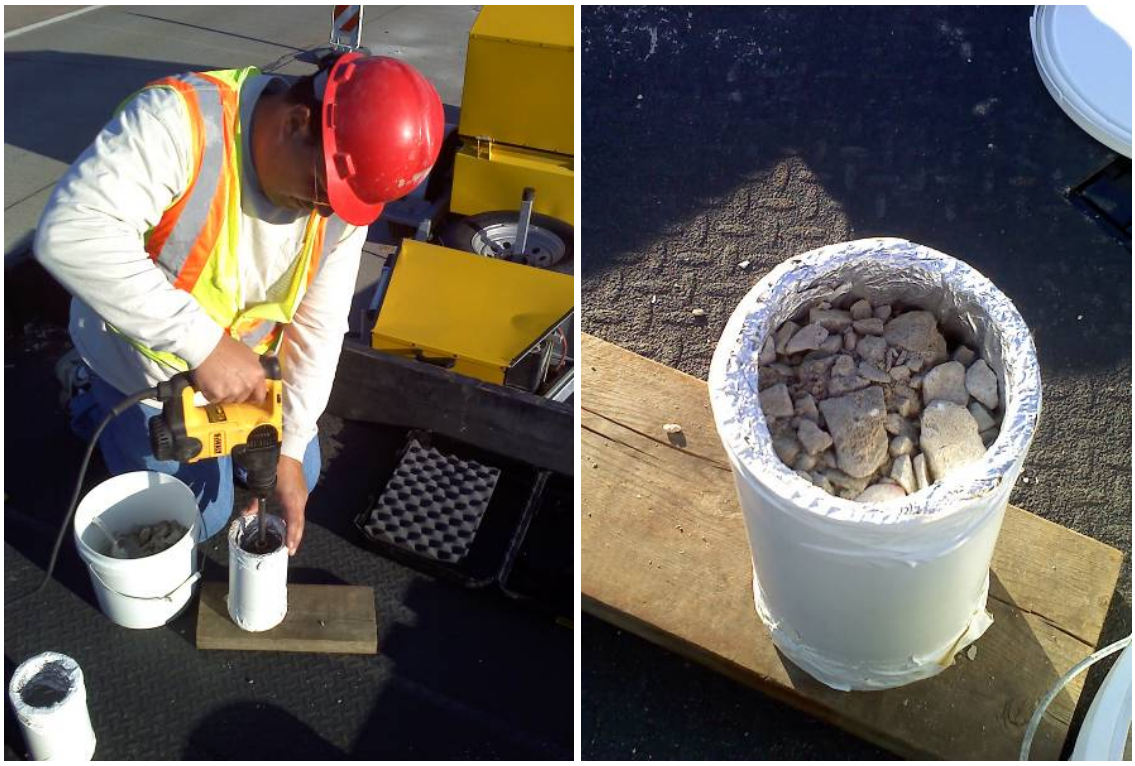

Figure 4. Preparation of OGS+Foam samples for laboratory M_r and UU testing

HDP foam samples were prepared in an empty plastic mold. The plastic molds were sealed and transported to the laboratory for further testing. These molds were cut at the ends to remove irregular edge surfaces and to achieve a height of 203.2 mm (8 in.). Trimmed foam and OGS+Foam samples are shown in Figure 5. M_r and UU tests were performed on OGS+Foam and foam samples.

M_r values are used in pavement design as a measure of stiffness of unbound materials in the pavement structure. The M_r parameter is highly stress dependent. Many non-linear constitutive models have been proposed that incorporate the effects of stress levels and predict M_r values. Most soils exhibit the effects of increasing stiffness with increasing confinement and decreasing stiffness with increasing shear stress (Andrei et al. 2004). Witczak and Uzan (1988) provided a "universal" model that combines both of these effects into a single constitutive model (Eq. 1):

$$M_r = k_1 P_a \left(\frac{\sigma_B}{P_a}\right)^{k_2} \left(\frac{\tau_{oct}}{P_a} + 1\right)^{k_3} \quad (1)$$

where P_a = atmospheric pressure (MPa); σ_B = bulk stress (MPa) = $\sigma_1 + \sigma_2 + \sigma_3$; τ_{oct} = octahedral shear stress (MPa) = $\{[(\sigma_1-\sigma_2)^2+(\sigma 2-\sigma_3)^2+(\sigma_3-\sigma_1)^2]^{1/2}\} / 3$; σ_1, σ_2 , σ_3 = principal stresses; and k_1, k_2, k_3 = regression coefficients.

The k_1 coefficient is proportional to M_r and therefore is always > 0. The k_2 coefficient explains the behavior of the material with changes in the volumetric stresses. Increasing volumetric stresses increase the M_r value and therefore the k_2 coefficient should be ≥ 0. The k_3 coefficient explains the behavior of the material with changes in shear stresses. Increasing shear stress softens the material and yields a lower M_r value. Therefore the k_3 coefficient should be ≤ 0.

Figure 5. Top view of HDP foam (top) and OGS+Foam mixture (bottom) samples

In Situ Testing Methods

The in situ test methods selected for this project included: (a) a real-time kinematic global positioning system (RTK-GPS) to locate test points; (b) robotic total station to monitor elevation

changes at the pavement surface, (c) light weight deflectometer to determine elastic modulus of the subbase layer, (d) dynamic cone penetrometer to determine the California bearing ratio (CBR) of the foundation layers; (e) air permeameter test device to determine saturated hydraulic conductivity (Ksat) of the subbase layer, (f) falling weight deflectometer to determine peak deflection under the loading plate (D_0), load transfer efficiency (LTE) at joints and cracks, voids at joints and cracks, foundation composite modulus of subgrade reaction, and deflection basin parameters; (g) calibrated Humboldt nuclear gauge to measure in situ moisture and dry density; (h) crack and fault measurements; (i) I-buttons for temperature measurements; and (g) international roughness index (IRI) index to characterize ride quality. Brief descriptions of these test procedures are provided below, and equipment used to conduct tests is shown in composite as Figure 6.

Real-Time Kinematic Global Positioning System

An RTK-GPS system was used to obtain the spatial coordinates (x, y, and z) of pavement slabs and test locations. A Trimble SPS881 receiver was used with base station correction provided from a Trimble SPS851 established on site (Figure 6, top left). This survey system is capable of horizontal accuracies of < 10 mm and vertical accuracies < 20 mm.

Robotic Total Station

A Trimble SPS930 universal robotic total station (RTS) system (Figure 6 top center shows the base station, and the top right photo shows the robotic total station hand-held laser receiver) integrated with servos and angle sensors was used to monitor changes in pavement surface elevations or surface elevation profiling (Trimble Navigation Ltd. 2013). An auto-lock prism was used as a tracking target and was mounted on a moving hand-held wheel or hand-held rover. Prior to taking measurements, local control points spaced across the area of interest were established for calibration. This system is capable of vertical accuracies of < 3 mm within 0 to 100 m distance from the total station base, and vertical accuracies of < 4 mm within 100 to 300 m distance from the total station base.

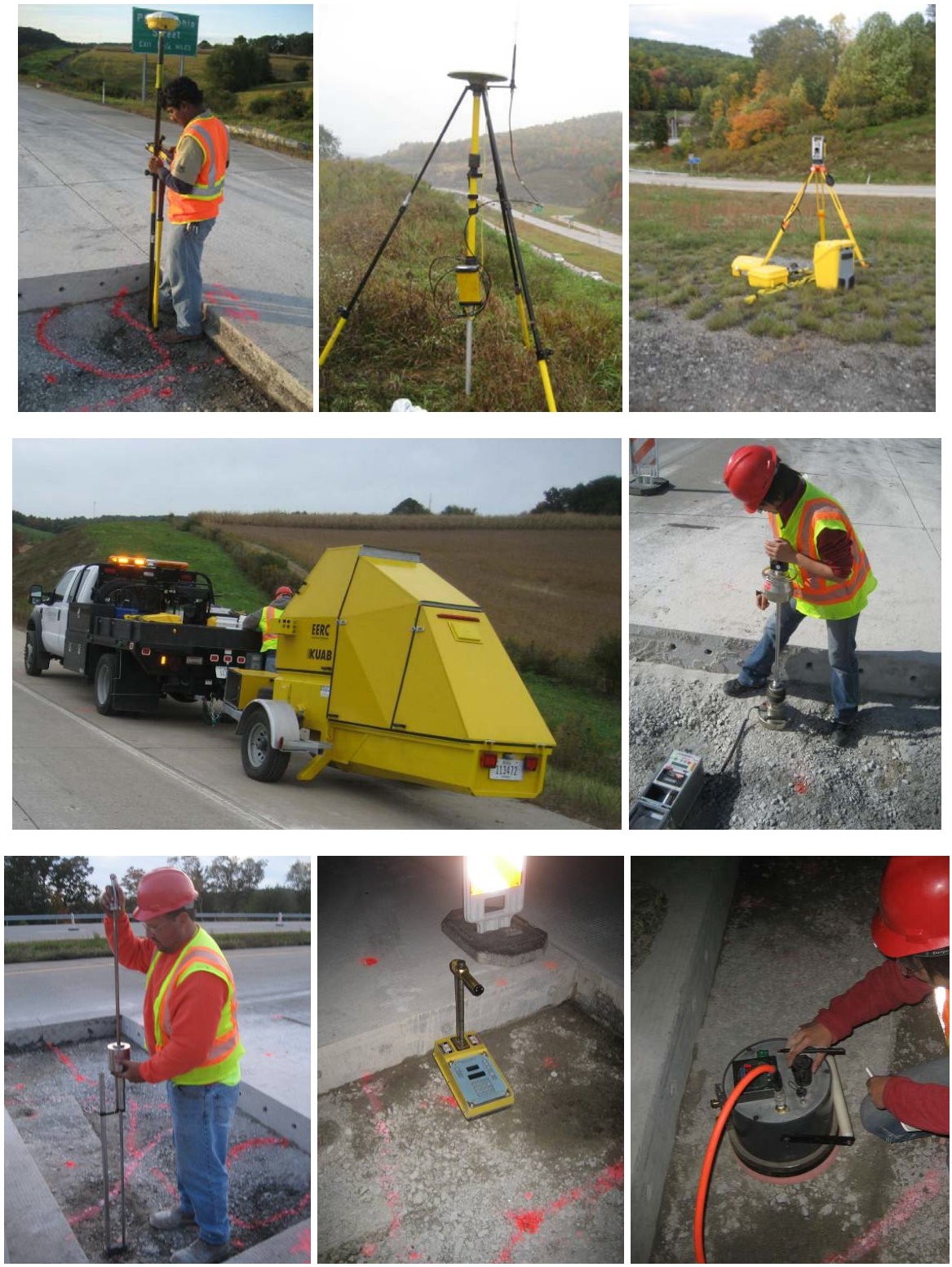

Figure 6. In situ test devices: Trimble SPS-881 hand-held receiver; Trimble SP-851 base station and RTS hand-held laser receiver (top row left to right); Kuab falling weight deflectometer and Zorn light weight deflectometer (middle row left to right); dynamic cone penetrometer, nuclear gauge, and gas permeameter device (bottom row left to right)

Zorn Light Weight Deflectometer

Zorn LWD tests were performed in patching areas where untreated base and HDP foam treated base layers were exposed. The LWD was set up with a 200 mm diameter plate and 50 cm drop height. The tests were performed following manufacturer recommendations (Zorn 2003), and the elastic modulus values were determined using Eq. 2:

$$E = \frac{(1-\eta^2)\sigma_0 r}{D_0} \times F \tag{2}$$

where E = elastic modulus (MPa); D_0 = measured deflection under the plate (mm); η = Poisson's ratio (0.4); σ_0 = applied stress (MPa); r = radius of the plate (mm); and F = shape factor depending on stress distribution (assumed as 8/3) (see Vennapusa and White 2009).

The results are reported as $E_{LWD\text{-}Z2}$ (Z represents Zorn LWD and 2 represents 200 mm diameter plate).

Dynamic Cone Penetrometer

DCP (Figure 6) tests were performed in accordance with ASTM D6951-03 *Standard Test Method for Use of the Dynamic Cone Penetrometer in Shallow Pavement Applications* to determine dynamic penetration index (DPI) and calculate California bearing ratio (CBR) using Eq. 8. The DCP test results are presented in this report as CBR with depth profiles at each test location. The CBR values were calculation using Eq. (3):

$$CBR = \frac{292}{DPI^{1.12}} \tag{3}$$

CBR of the OGS subbase layer (CBR_{OGS}) was determined in this study by measuring the number of blows required to penetrate the DCP down to the bottom of the OGS layer (about 100 mm) and calculating the DPI value.

Falling Weight Deflectometer (FWD)

FWD tests were conducted independently by Penn DOT and ISU research team using different devices. Penn DOT personnel conducted testing at joints prior to stabilization in 2009 to select the extent of injection stabilization. The authors conducted tests in selected test sections shortly before stabilization and at several times up to 9 months after stabilization. Procedures followed by Penn DOT and authors for conducting FWD tests and interpreting the results are described below.

Penn DOT FWD Testing

FWD tests were conducted at all joint locations to determine the type of repair needed, i.e., foam injection or full-depth patching. FWD tests were conducted by dropping a target dynamic load of about 40 kN to measure D_0. The actual applied load was measured and was varied from about 37.6 to 43.6 kN, with an average of about 40.3 kN. LTE values were determined by obtaining deflections under the 300 mm plate on the loaded panel (D_0) and deflections of the unloaded panel (D_1) using a sensor positioned about 305 mm away from the center of the plate. The LTE was calculated using Eq. 4.

$$LTE(\%) = \frac{D_1}{D_0} \times 100 \tag{4}$$

Criteria for predicting voids under the pavement were based on the zero-load intercept (I) value calculation using three applied loads varying from 40 to 71 kN and measuring the corresponding deflections. The intercept value of the linear regression relationship between applied load (x-axis) and deflection plot (y-axis) is determined as the I-value, which corresponds to deflection at zero-load, as illustrated in Figure 7.

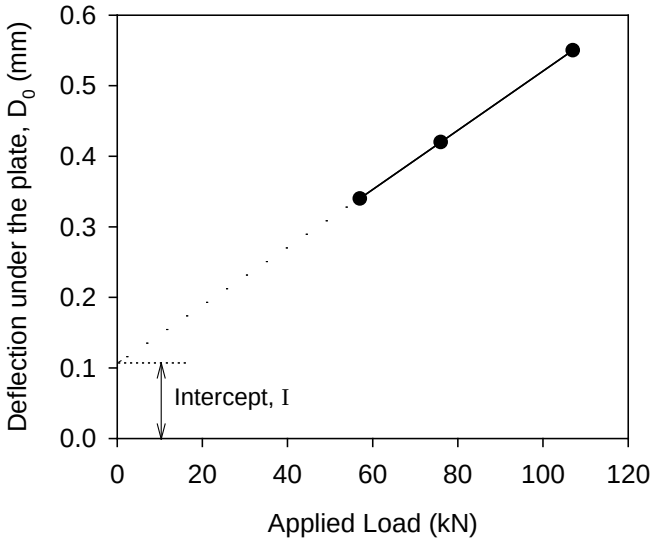

Figure 7. Void detection using load-deflection data from FWD tests

ISU FWD Testing

FWD tests were conducted in accordance with ASTM D4694 *Standard Test Method for Deflections with a Falling-Weight-Type Impulse Load Device*, using a segmented 300 mm diameter loading plate by applying one seating drop and four loading drops. A Kuab FWD device was used in this study (Figure 6). The applied loads varied from 22 to 75 kN. The deflection values at each test location were normalized to 40 kN. FWD tests were conducted near mid-panel (i.e., between the two joints or between the joint and the crack on a panel), joints, and transverse cracks.

The FWD deflection basin data was analyzed to determine peak deflections under the loading plate (D_0), surface curvature index (SCI), base damage index (BDI), base curvature index (BCI), area factor (AF), LTE near joints and cracks (using Eq. 4), and I values. An example deflection basin is shown in Figure 8.

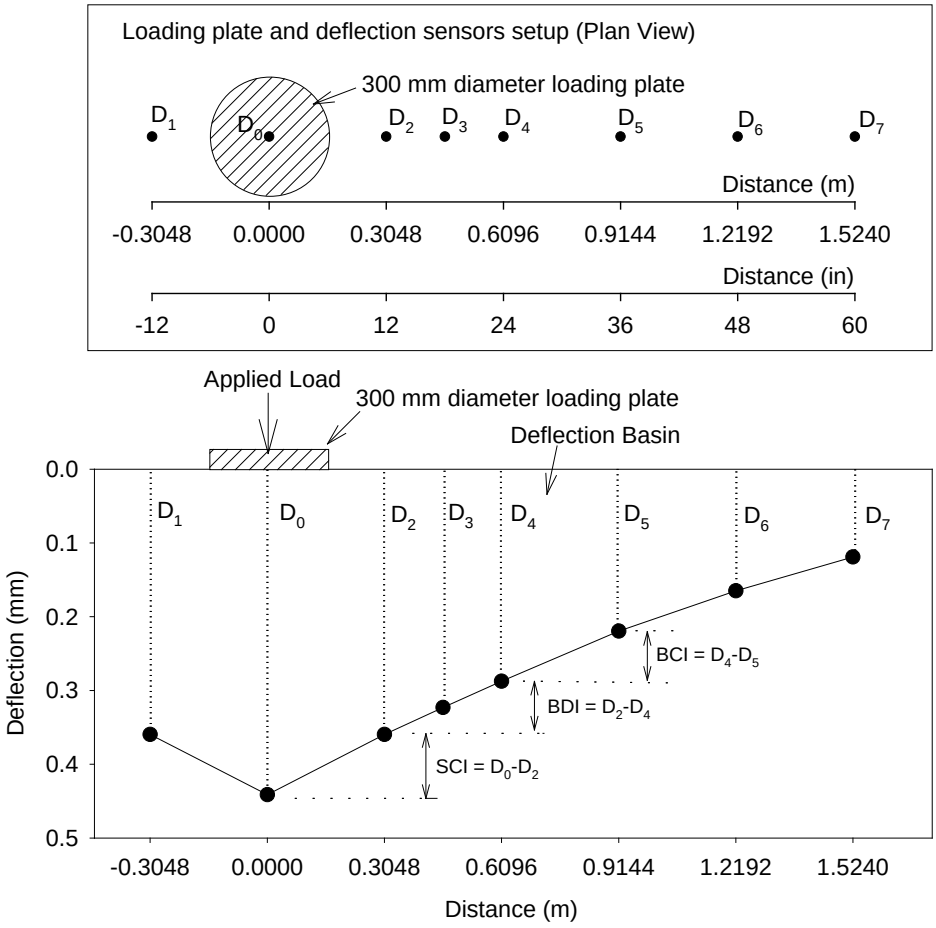

Figure 8. FWD deflection sensor setup used for this study and sample deflection basin data illustrating SCI, BDI, and BCI calculations

The SCI, BDI, BCI, and AF measurements are referred to as deflection basin parameters and are determined using the following equations:

$$SCI\ (mm) = D_0 - D_2 \quad (5)$$

$$BDI\ (mm) = D_2 - D_4 \quad (6)$$

$$BCI\ (mm) = D4 - D5 \quad (7)$$

$$\text{AF (mm)} = \frac{152.4 \times (D_0 + 2D_2 + 2D_4 + D_5)}{D_0} \quad (8)$$

where, D_0 = peak deflection measured directly beneath the plate, D_2 = peak deflection measured at 305 mm away from the plate center, D_4 = peak deflection measured at 510 mm away from the plate centre, and D_5 = peak deflection measured at 914 mm away from the plate centre.

According to Horak (1987), the SCI parameter provides a measure of the strength/ stiffness of the upper portion (base layers) of the pavement foundation layers (Horak 1987). Similarly, BDI represents layers between 300 mm and 600 mm depth (base and subbase layers) and BCI represents layers between 600 mm and 900 mm depth (subgrade layers) from the surface (Kilareski and Anani 1982). The AF is primarily the normalized (with D_0) area under the deflection basin curve up to sensor D_5 (AASHTO 1993). AF has been used to characterize variations in the foundation layer material properties by some researchers (e.g., Stubstad 2002). Comparatively, lower SCI or BDI or BCI or AF values indicate better support conditions (Horak 1987).

A composite modulus value ($E_{FWD\text{-}K3}$) was calculated using the D_0 corresponding to an applied contact force, and Eq. 2. Shape factor F = 2 was used in the calculations assuming a uniform stress distribution (see Vennapusa and White 2009). According to the FWD manufacturer, the segmented plate used results in a uniform stress distribution.

Tests conducted at mid-panel were also used to determine the dynamic modulus of subgrade reaction ($k_{dynamic}$) values. The $k_{dynamic}$ values were determined using deflection basin parameters and the area method described in AASHTO (1993), using Engineering and Research International (ERI) data analysis software. The deflection basin parameters included D_0, D_2, D_4, and D_5.

Pavement layer temperatures at different depths were obtained during FWD testing, in accordance with the guidelines from Schmalzer (2006). The temperature measurements were used to determine equivalent linear temperature gradients (TL) following the temperature-moment concept suggested by Jannsen and Snyder (2000). According to Vandenbossche (2005), the I-values are sensitive to temperature induced curling and warping affects. Large positive temperature gradients (i.e., when surface is warmer than bottom) that cause the panel corners to curl down result in false negative I-values. Conversely, large negative gradients (i.e., when surface is cooler than bottom) that cause the panel corners to curl upward result in false positive I-values. Interpretation of I-values therefore should consider the temperature gradient. Concerning LTE measurements for doweled joints, the temperature gradient is reportedly not a critical factor (Vandenbossche, 2005).

Humboldt Nuclear Gauge

A calibrated nuclear moisture-density gauge (NG) device (Figure 6) was used to provide rapid measurements of soil dry unit weight (γ_d) and moisture content (w) in the base materials. Tests

were performed following ASTM D6938-10 *Standard Test Method for In-Place Density and Water Content of Soil and Soil-Aggregate by Nuclear Methods (Shallow Depth)*. Back-scattering procedure was used in obtaining the measurements. Two measurements of moisture and dry unit weight were obtained at a particular location and the average value is reported.

Rapid Air Permeameter Test (APT Device)

APT device is a recently developed rapid in situ permeability testing device (White et al. 2014) that uses air as a permeating fluid to determine the saturated hydraulic conductivity (K_{sat}). The APT consists of a self-contained pressurized gas system with a self-sealing base plate and uses a theoretical algorithm to determine the K_{sat}. The test involves measuring air pressure on the inlet and outlet sides of a precision orifice, calculating gas flow rate, and assuming material properties (i.e., degree of saturation of the material, residual saturation of the material, and pore-size distribution properties of the material), to determine K_{sat}. The K_{sat} was calculated using Eq. 9 (White et al. 2014):

$$K_{sat} = \left[\frac{2\mu_{air} Q P_1}{r G_0 \left(P_1^2 - P_2^2\right)}\right] \cdot \frac{\rho g}{\mu_{water} (1 - S_e)^2 (1 - S_e^{((2+\lambda)/\lambda)})} \quad (9)$$

where K_{sat} = saturated hydraulic conductivity (cm/s); μ_{air} = dynamic viscosity of air (P_as); Q = volumetric flow rate (cm^3/s); P_1 = absolute gas pressure on the soil surface, $P_{o(g)}$ x 9.81 + 101325, (P_a); $P_{o(g)}$ = gauge pressure at the orifice outlet (mm of H_20); P_2 = atmospheric pressure (P_a); r = radius at the outlet (4.45 cm), G_o= Geometric factor ($4.16e^{(-0.1798 \cdot \delta)} + 4.74e^{(-0.0003 \cdot \delta)}$); δ = depth to impervious layer (assumed as 100 mm); S_e = effective water saturation [$S_e = (S - S_r)/(1-S_r)$]; λ = Brooks-Corey pore size distribution index; S_r = residual water saturation; S = water saturation; ρ = density of water (g/cm^3); g = acceleration due to gravity (cm/s^2); and μ_{water} = absolute viscosity of water (g/cm-s).

S values of the subbase layer material were determined based on field density and moisture content measurements (varied between 15% and 16%), and S_r = 0% and λ = 5.0 were assumed based on a database of typical properties provided in White et al. (2014).

Crack and Fault Measurements

Faulting was observed near mid-panel cracks and near shoulder/panel interface (due to panel settlement). Faulting was measured using a ruler at 8 to 10 locations along the width of the panel and along the crack to determine average crack faulting (CF). Similarly, faulting was measured at the shoulder at 8 to 10 locations along the length of the panel to determine average shoulder faulting (SF). The procedure to obtain these measurements is illustrated in Figure 9.

I-Buttons

I-buttons were installed at three locations on the project to monitor temperature profiles in the pavement foundation layers. I-buttons were installed by coring the pavement and drilling a 150 mm (6 in.) diameter bore hole into the pavement base, subbase, and subgrade layers down to approximately 1.5 m (5 ft) below the pavement surface. A plastic pipe was installed in the hole and then the hole was backfilled around the pipe using soil cuttings from the auger. I-buttons were taped to a thin wooden stick that was placed inside the plastic pipe. Photographs illustrating the installation procedure are provided in Figure 10.

The I-buttons were taped at marked locations on the wooden stick so that the sensors would be located at approximately 0.25 m (10 in.); 0.31 m (12 in.); 0.45 m (18 in.); 0.61 m (24 in.); 0.91 m (36 in.);, and 1.52 m (60 in.) beneath the pavement surface. A silty soil and silica sand slurry was mixed and poured into the plastic pipe, then the concrete core hole was patched and sealed with cement grout.

Figure 9. Crack width (left) and fault (right) measurements

Figure 10. I-button installation

International Roughness Index

To determine the pavement ride quality, IRI measurements were obtained by Penn DOT using a high-speed profiler (Penn DOT, 2015). Penn DOT uses the following criteria on non-interstate national highways (illustrated in Appendix B) to provide pavement ride quality ratings based on IRI measurements:

- Excellent: IRI ≤ 1.2 m/km
- Good: IRI > 1.2 m/km and ≤ 1.9 m/km
- Fair: IRI > 1.9 m/km and ≤ 2.7 m/km
- Poor: IRI > 2.7 m/km

Statistical Analysis Method

The results in this study from before and after stabilization were analyzed to statistically assess the differences between the measurements. Student t-test analysis (Ott and Longnecker, 2001) was conducted on the FWD test measurements to assess statistical significance in the difference in measurements obtained before and after stabilization. The t-values were determined using:

$$t = \frac{\mu_0 - \mu_1}{s_p \sqrt{\frac{1}{n_0} + \frac{1}{n_1}}} \quad (10)$$

$$s_p = \sqrt{\frac{(n_0 - 1) \times s_0^2 + (n_1 - 1) \times s_1^2}{n_0 + n_1 - 2}} \quad (11)$$

where, n_0 and n_1 = number of measurements obtained before and after stabilization, respectively; s_p = pooled standard deviation, and s_0 and s_1 = standard deviation of measurements obtained before and after stabilization, respectively.

The observed t-values were compared with the minimum t-value for a one-tailed test with degree of freedom (df) = $n_0 + n_1 - 2$, for 95% confidence level (i.e., $\alpha = 0.05$) If the t-values were greater than the minimum *t*-value, then it was concluded that there is sufficient evidence that the measurements after stabilization were different when compared to the measurements before stabilization.

CHAPTER 4. US 422 REHABILITATION PROJECT OVERVIEW AND TESTING

Project Overview

The test area is located on US Highway 422 in Indiana, Pennsylvania. It is about 9.7 km long with four-lanes and a dividing median. The jointed PCC pavement was originally built in 1995 with a nominal 280 mm thick PCC over 100 mm thick OGS subbase layer consisting of crushed limestone, 100 mm thick well-graded subbase also consisting of crushed limestone, and variable subgrade consisting of residual clay, shale, and sandstone rock. The material index properties of the foundation materials are presented in Chapter 4.

The PCC panels were approximately 3.7 m wide x 6.1 m long. The PCC layer started showing distresses in early 2000s with mid-panel cracking that progressively increased. Penn DOT conducted IRI testing yearly from 2005 to 2009, and FWD testing shortly prior to stabilization to determine locations for stabilization. Results from Penn DOT's IRI and FWD testing and details about the rehabilitation process that began in October 2009 are provided below.

Penn DOT used the following criteria based on FWD testing to determine the type of repair (Penn DOT 2011):

- Joints with $D_0 > 0.05$ mm under a 40 kN applied load, joint LTE < 65%, and I > 0.076 mm requires stabilization with foam injection and patching.
- Joints with I > 0.076 mm and that do not meet the LTE and D_0 criteria above, requires stabilization with foam injection only.

Pre-Stabilization Penn DOT Field Test Results

IRI measurements were obtained from 2005 to 2009 and the results were collected as average values over 12 segments with lengths varying from about 500 m to 1100 m on east bound (EB) and west bound (WB) lanes. The segments are identified in Figure 11. Average IRI values per segment from 2005 to 2009 are presented in Figure 12. The results are presented as box plots in Figure 13. Results indicated that the pavement sections were mostly within the "fair" to "good" IRI rating range. On average, the IRI values increased from 2005 (1.6 m/km) to 2009 (1.7 m/km) indicating a decrease in ride quality.

LTE and I measurements from over 1500 test locations obtained before stabilization in May 2009 are presented in Figure 14 and Figure 15, respectively. Histograms of D_0, LTE, and I-values are shown in Figure 16. Summary statistics of the measurements, i.e., mean (μ), standard deviation (σ), and coefficient of variation (COV), are provided in Figure 16. Based on these test results and the criteria outlined above per Penn DOT (2011), 40 locations qualified for both foam injection and patching, and 271 locations qualified for foam stabilization only.

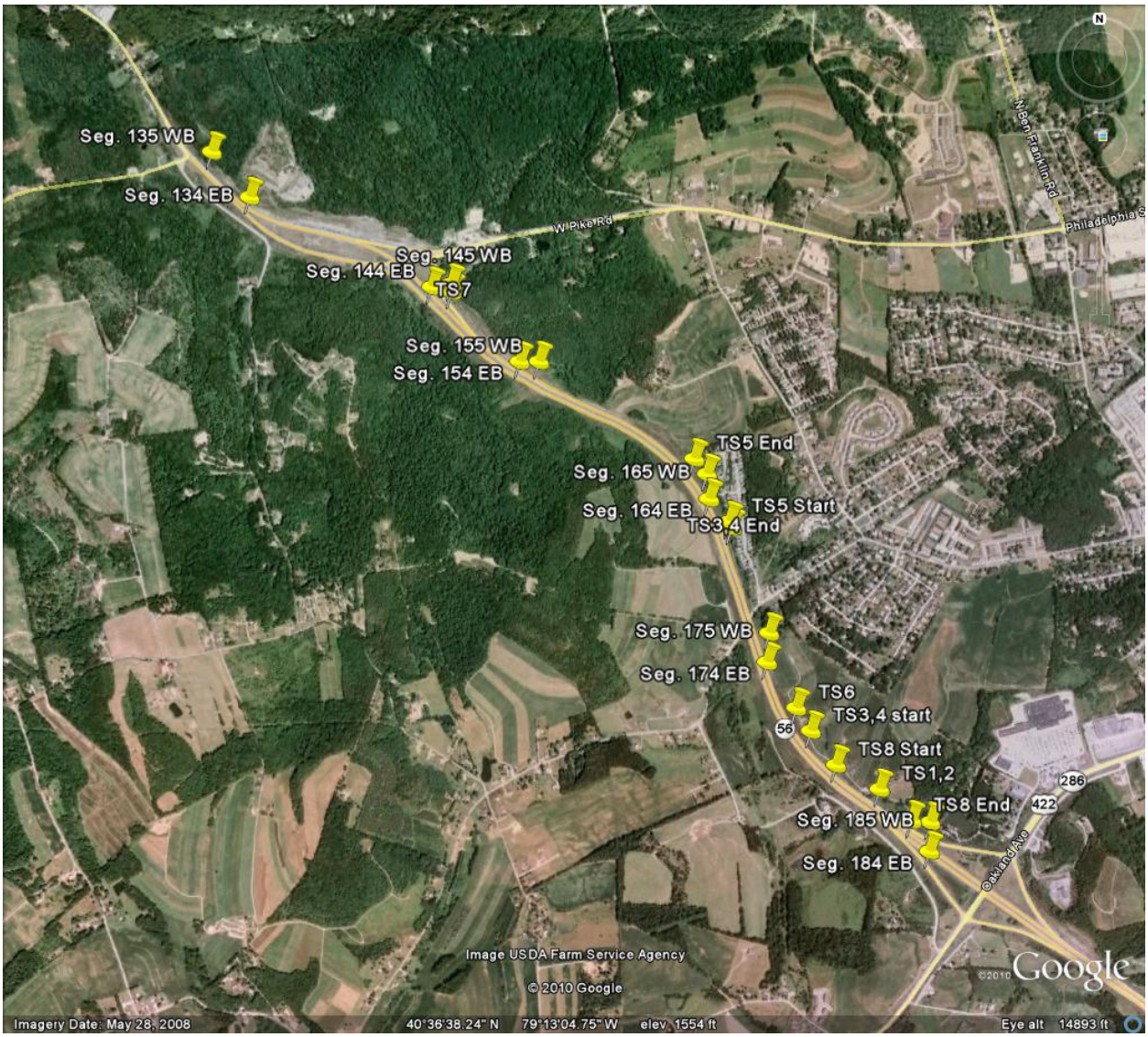

Figure 11. Map showing approximate locations of segments 134 to 184 on US 422EB and segments 135 to 185 on US 422WB and locations of ISU test sections

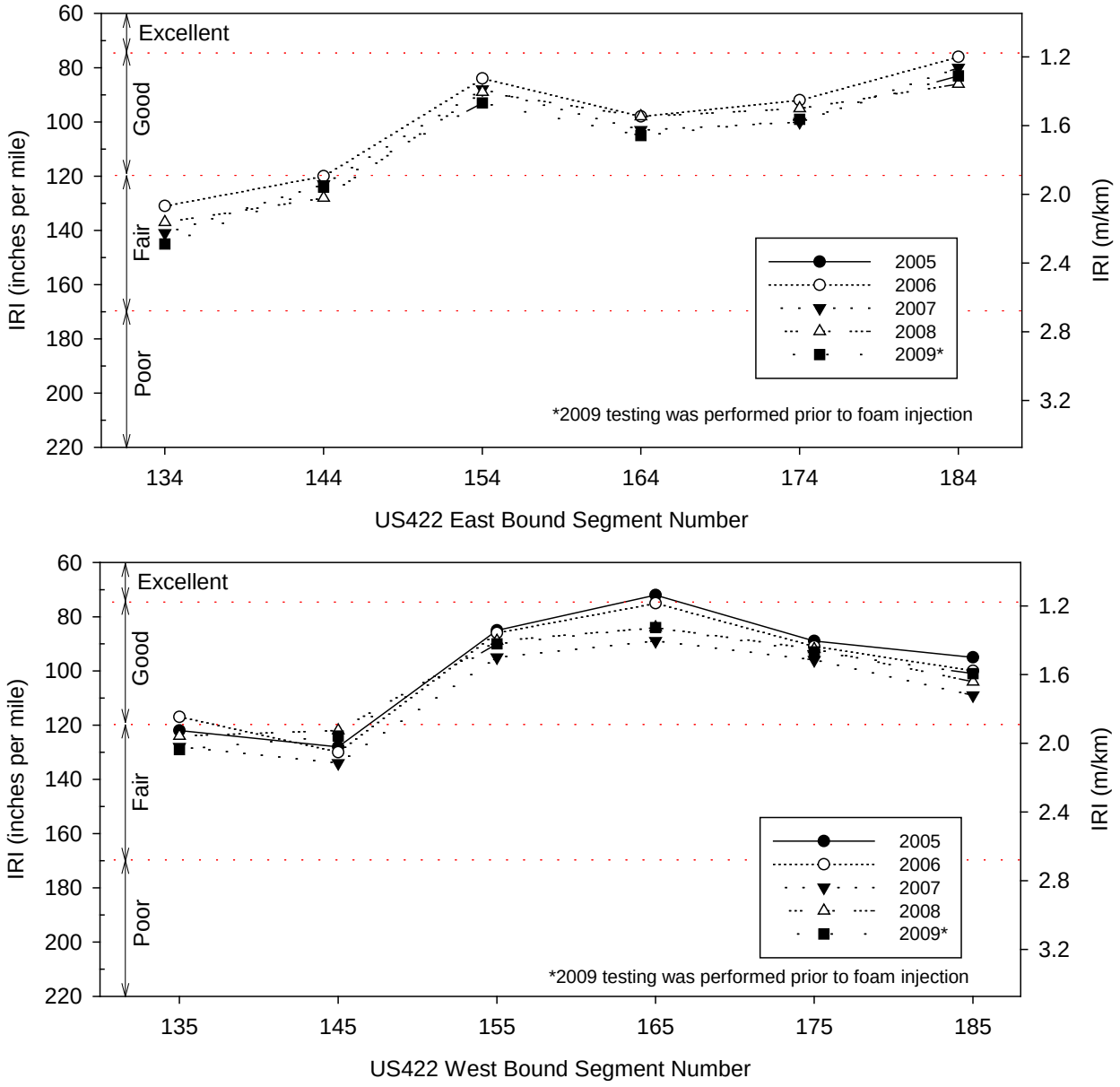

Figure 12. IRI measurements in EB (top) and WB (bottom) lanes from 2005 to 2009 (data represents average values for each segment)

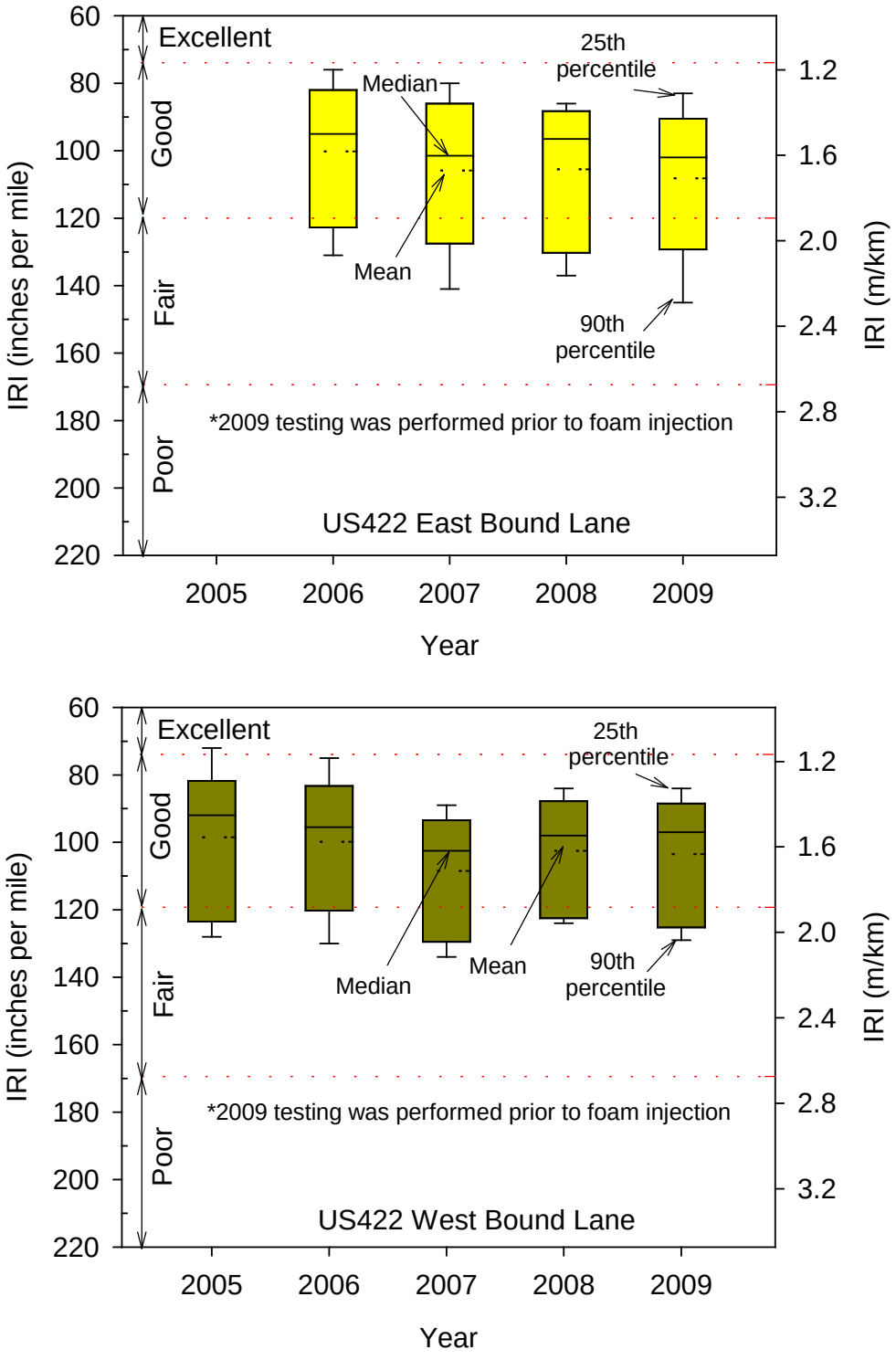

Figure 13. Box plots of IRI measurements on US 422 EB (top) and WB (bottom) lanes from 2005 to 2010

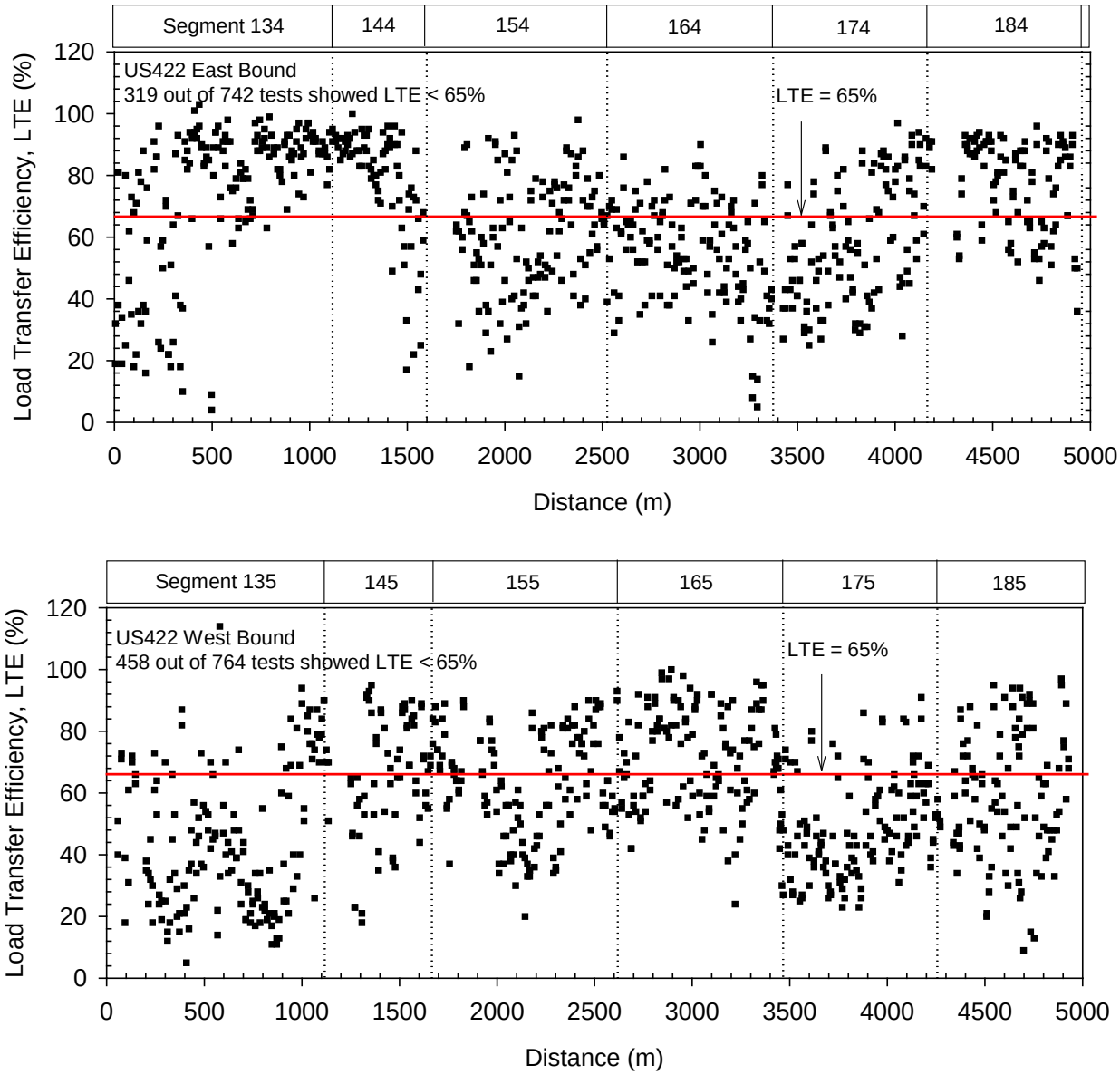

Figure 14. Pre-stabilization Penn DOT FWD LTE measurements at joints on US 422 EB (top) and WB lanes (bottom)

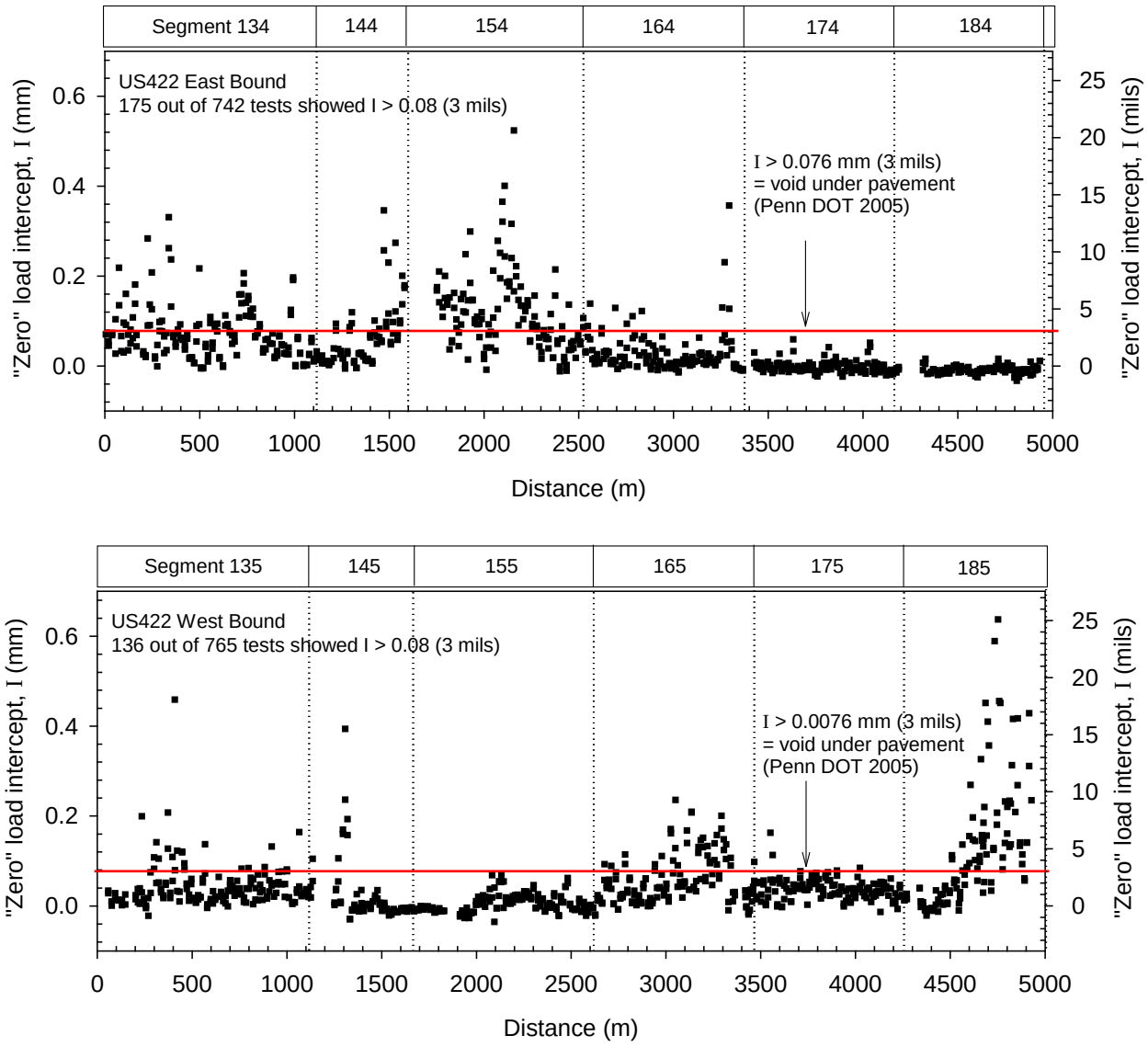

Figure 15. Pre-stabilization PennDOT FWD I measurements at joints on US 422 EB (top) and WB (bottom).

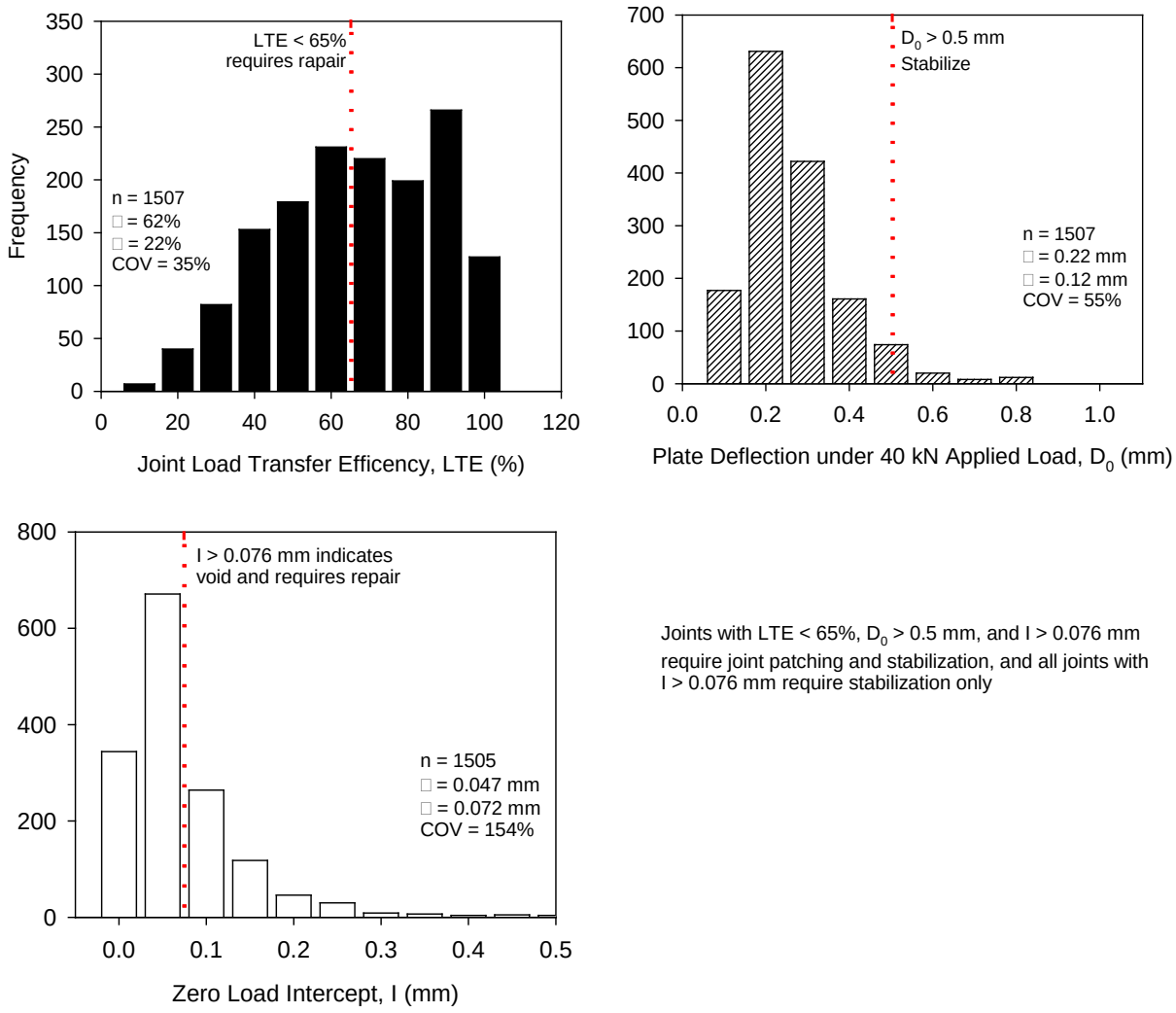

Figure 16. Histogram of pre-stabilization FWD test results: joint LTE (top left), D_0 under loading plate at 40 kN applied load (top right), and I (bottom left)

Rehabilitation Process

Penn DOT designed the rehabilitation process to include injected HDP foam under the pavement surface and dowel bar retrofitting or patching at selected crack locations. The foam injection process involved four steps: (1) drilling a series of 9.5 mm diameter holes in the PCC layer extending to the underlying base layer (Figure 17a) in a triangular spatial pattern on each panel (at 8 to 9 locations), (2) inserting a plastic sleeve in each hole to mate with the injection nozzle, and (3) injecting the HDP foam under pressure into the hole (Figure 17b). Mechanical deflection measurement gauges were used to monitor the panel lifting process by using the adjacent treated pavement panels or the shoulder as a reference (Figure 17d).

Based on the information provided by the manufacturer, the foam was injected at a maximum flow rate of about 272 kg/min and a maximum pressure of about 378 kPa. The density of the

HDP ranged between 80 kg/m^3 and 128 kg/m^3, and the shear strength ranged between 682 and 876 kPa. The material had a reaction time of < 1 min and a curing time of < 15 min.

The foam injection process was carried out between September 29, 2009 and November 10, 2009. Dowel bar retrofitting and concrete patching was carried out between March 31, 2010 and July 20, 2010. A picture of a dowel bar retrofitted cracked panel is shown in Figure 17e. Some sections were selected for patching as shown in Figure 17f.

Figure 18 shows photographs of foam+aggregate mixture sample obtained from patching areas and a foam sample that ejected through a hole in the slab. Approximately 286,530 kg (631,690 lb) of foam was used for stabilization on this project. Unit cost (including material and labor) of the foam material was about $9.47/kg ($4.30/lb) (volume and cost information provided by Marc Gardner, Project Engineer, PennDOT).

Cementitious grout stabilization was performed in a short test section (150 m long) in accordance with Pennsylvania standard specification for Slab Stabilization (Penn DOT 2011). Per specification, one part cement to two parts fly ash pozzolan by volume was used in preparing the grout. Slab movement was monitored during the injection process by the contractor as part of their QC program. The procedure involved: (1) drilling eight grout injection holes with diameters no larger than 38 mm (1.5 in.) in the PCC layer penetrating into the OGS layer; (2) mixing the grout; and (3) void filling by pumping the grout into the hole until maximum pressure is built up or material is observed flowing from hole to hole. The maximum allowable pressure was 1.4 MPa (200 psi). Two holes were drilled on either side of a joint or crack. These two holes were spaced about 0.6 m (25 in.) away from the slab edges in transverse direction (i.e., perpendicular to travel).

About 25 bags of cement, each weighing about 22.6 kg (50 lb), were used to treat the 152 m (500 ft) long test section. The unit cost of the stabilization was about $2.86/kg ($1.30/lb); volume and cost information was provided by Marc Gardner, Project Engineer, Penn DOT. After injecting the cementitious grout, all the cracks in that test section were retrofitted with dowel bars.

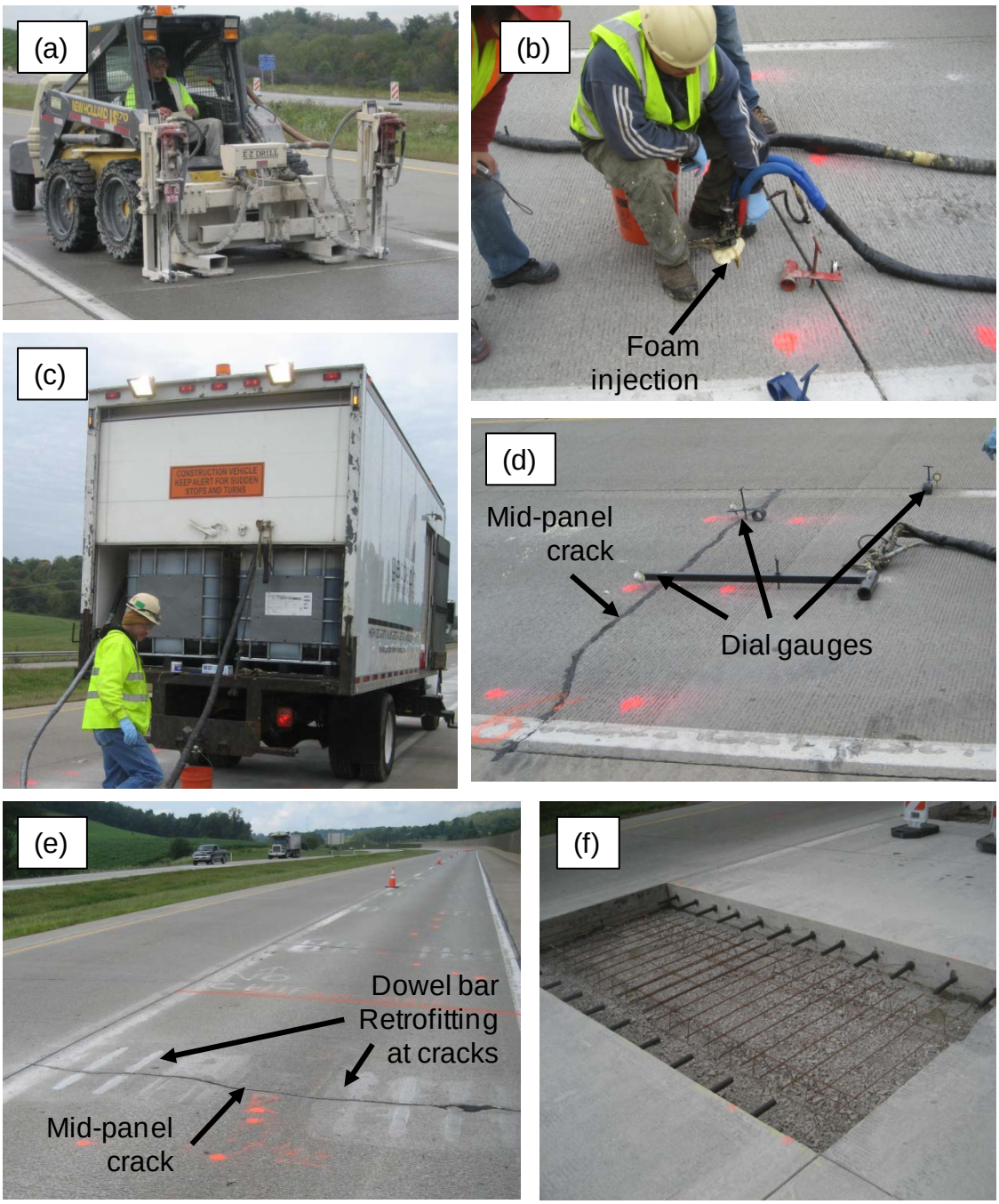

Figure 17. Equipment used to drill holes for foam injection (a); foam injection process (b); truck carrying the liquids (c); dial gauges used to monitor slab movement (d); dowel bar retrofitting performed at cracks (e); and a concrete patching area (f)

Figure 18. Foam+aggregate mixture (left) and HDP foam ejected through a hole drilled in the pavement (right)

Description of Test Sections and Test Measurements

Iowa State University researchers conducted field testing on nine test sections shortly before and at several times after stabilization for performance monitoring. The approximate locations for each test section (TS); the material tested; and the in situ tests performed are summarized in Table 5. TS locations are identified in Figure 11. TS1 and TS2 consisted of patching areas where the pavement panels were cut and removed, and the underlying HDP foam treated and untreated OGS base layers were tested. TS3, TS4, TS6, TS7, and TS8 involved testing on the PCC surface layer before and after HDP foam stabilization. TS5 involved testing on the PCC surface layer before and after cementitious grout stabilization. TS9 consisted of temperature sensor measurements in control, foam, and grout locations.

Table 7. Summary of test sections and in situ testing

TS	Date(s)	Location	Material	In situ Test Measurements	Comments
1	10/1/09	US 422 WB (west of Oakland Ave. exit ramp and near Sta. 8523+50)	HDP foam treated aggregate base	w, γ_d, DCP-CBR, $E_{LWD\text{-}Z2}$, K_{sat}	Two patching areas with aggregate base layer treated with foam
2	10/1/09	US 422 WB (west of Oakland Ave. exit ramp near sta. 8524+00)	Untreated aggregate base	w, γ_d, DCP-CBR, $E_{LWD\text{-}Z2}$, K_{sat}	Two patching areas with no stabilization
3	10/1/09	US 422 WB (Sta. 8507+15 to 8496+00)	Existing PCC surface (base treated using HDP foam)	$E_{FWD\text{-}K3}$, DCP-CBR, visual crack survey	Measurements before stabilization
4	10/13/09			$E_{FWD\text{-}K3}$, visual crack survey	Measurements after stabilization
5	10/02/09 10/13/09 07/21/10	US 422 WB (Sta. 8496+00 to 8501+00)	Existing PCC surface (base treated using cement grout)	$E_{FWD\text{-}K3}$, LTE, DCP-CBR, visual crack survey	Measurements (cracks and joints) before and after stabilization
6	10/02/09	US 422 EB (near Sta. 8506+00)	Existing PCC surface (base treated using HDP foam)	Elevation profiles	Measurements before and after stabilization
7	10/13/09, 11/03/09	US 422 WB (west of Pennsylvania Ave. exit ramp)	Existing PCC surface (base treated using HDP foam)	Elevation profiles, $E_{FWD\text{-}K3}$, LTE, visual crack survey	Measurements before and after stabilization including corner of slabs
8	10/13/09, 10/14/09, 11/03/09, 04/28/10, 07/21/10	US 422 EB (west of Oakland Ave. exit ramp)	Existing PCC surface (base treated using HDP foam)	$E_{FWD\text{-}K3}$, LTE, visual crack survey	Measurements before and after stabilization, after dowel-bar retrofitting/ patching, and after several months
9	Installation Date: 10/14/09	US 422 WB (TS9-1: on WB Oakland Ave. exit ramp; TS9-2: near Sta. 8525; TS9-3: 8497+00)*	Base, subbase, and subgrade	Temperature profile	Temperature profiles using I-buttons installed in three locations

Note: w – moisture content; γ_d – dry unit weight; CBR – California bearing ratio determined from dynamic cone penetrometer (DCP) test; $E_{LWD\text{-}Z2}$ – elastic modulus determined using Zorn model light weight deflectometer (LWD) with a 200 millimeter plate; APT K_{sat} – saturated hydraulic conductivity determined using air permeameter test (APT) device; $E_{FWD\text{-}K3}$ – elastic modulus determined using Kuab falling weight deflectometer (FWD); RTS – robotic total station; TS – test section; *location 1 = no stabilization; location 2 = base treated using HDP foam; location 3 = base treated using cement grout

CHAPTER 5. MATERIAL PROPERTIES

Particle Size Analysis

Untreated OGS base and class 2A subbase materials were obtained from two test sections (TS), TS1 and TS2, at various depths and test locations. The test sections consisted of an OGS layer to a depth of about 100 mm (4 in.), underlain by a 2A subbase layer to a depth of about 200 mm (8 in.) from the top of the OGS layer. TS1-1 and TS1-2 are located in TS1, and TS2-3 and TS2-4 are located in TS2. Samples were obtained from one test location in TS1-1 and from two locations each in TS1-2, TS2-3, and TS2-4. In addition, samples were also obtained from 15 test locations from TS2-3 and 2-4 each from the top 50 mm of the OGS for conducting fines content (% passing the No. 200 sieve) tests.

Particle size distribution curves of OGS and 2A materials obtained from different depths from each section are provided in Figure 19 and Figure 20, respectively. The gradation specification limits are also provided in these figures for reference.

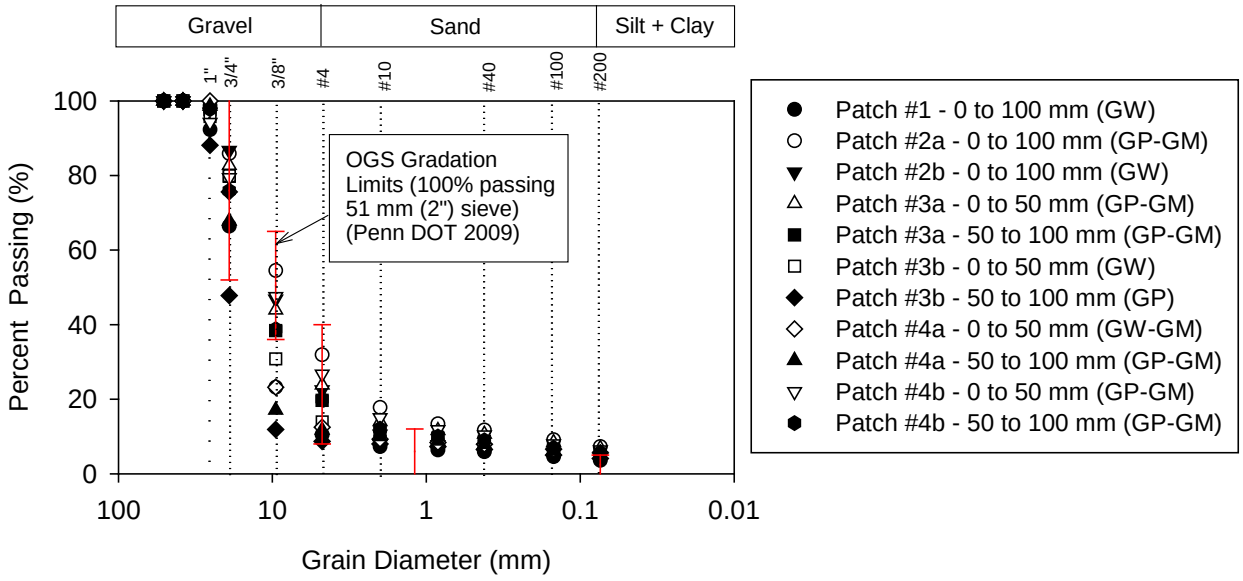

Figure 19. Particle size distribution curves for OGS material from TS1/TS2

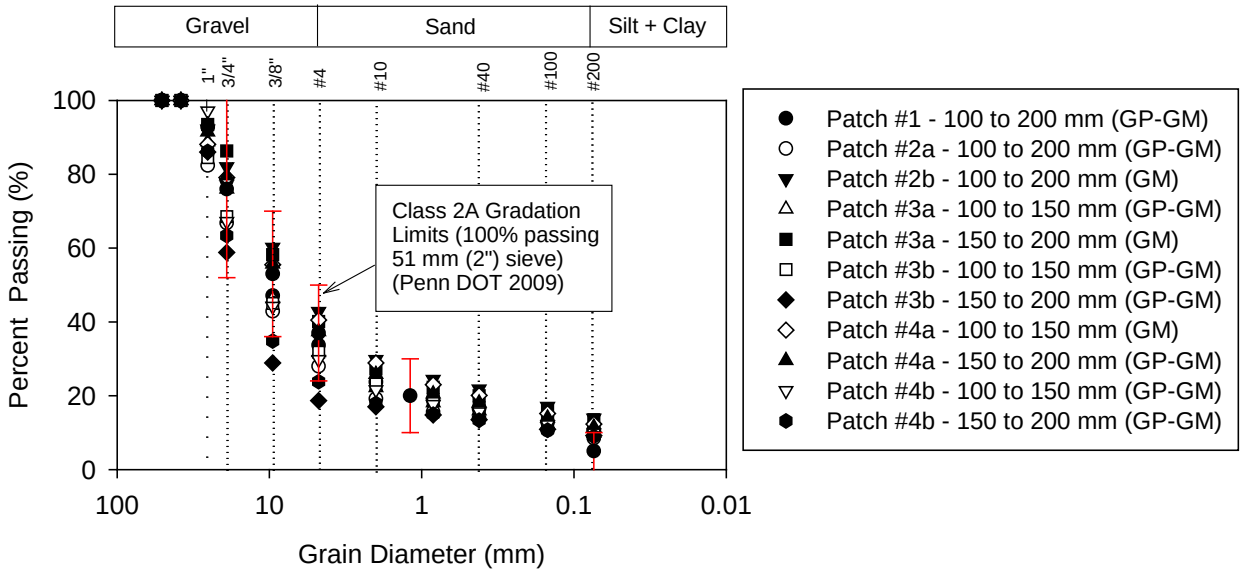

Figure 20. Particle size distribution curves for 2A material from TS1/TS2

Histogram plots of fines content, effective particle size (D_{10}, grain size diameter corresponding to 10% passing by mass); and D_{60} (grain size diameter corresponding to 60% passing by mass) calculated from the particle size analysis results are presented in Figure 21.

Histogram plots of aggregate particle coefficient of uniformity (c_u) and coefficient of curvature (c_c) are presented in Figure 22. Histogram plots of fines content samples from patches 3 and 4 OGS layer are presented in Figure 23.

Particle size distribution curves of OGS materials (Figure 19) indicate that 6 of the 11 samples collected were outside the gradation specification limits. Thirty-one of the 41 samples contained percent fines content greater than the maximum 5% specification limit (Figure 19 and Figure 23). D_{10} values of 1 of the 11 samples collected were outside the specification limits. D_{60} of all 11 samples were within the specification limits. The gradation parameters c_u of 3 and c_c of 8 out of 11 samples collected were outside the specification limits. The classification of the OGS materials varied from GP to GP-GM to GW to GW-GM according to the USCS and A-1-a according to the AASHTO classification system.

Particle size distribution curves of 2A materials (Figure 20) indicate that 4 out of the 11 samples collected were outside the gradation specification limits; 6 out of the 11 samples contained percent fines content greater than the maximum 10% specification limit for (Figure 23); D_{10} of the samples collected were less than the minimum 0.07 mm for 5 out of the 11 samples collected, while D_{60} were within the specification limits for all the samples collected. All the samples collected were outside the specification limits for c_u and c_c. The classification of the 2A materials varied from GM to GP-GM according to the USCS and was A-1-a according to the AASHTO classification system.

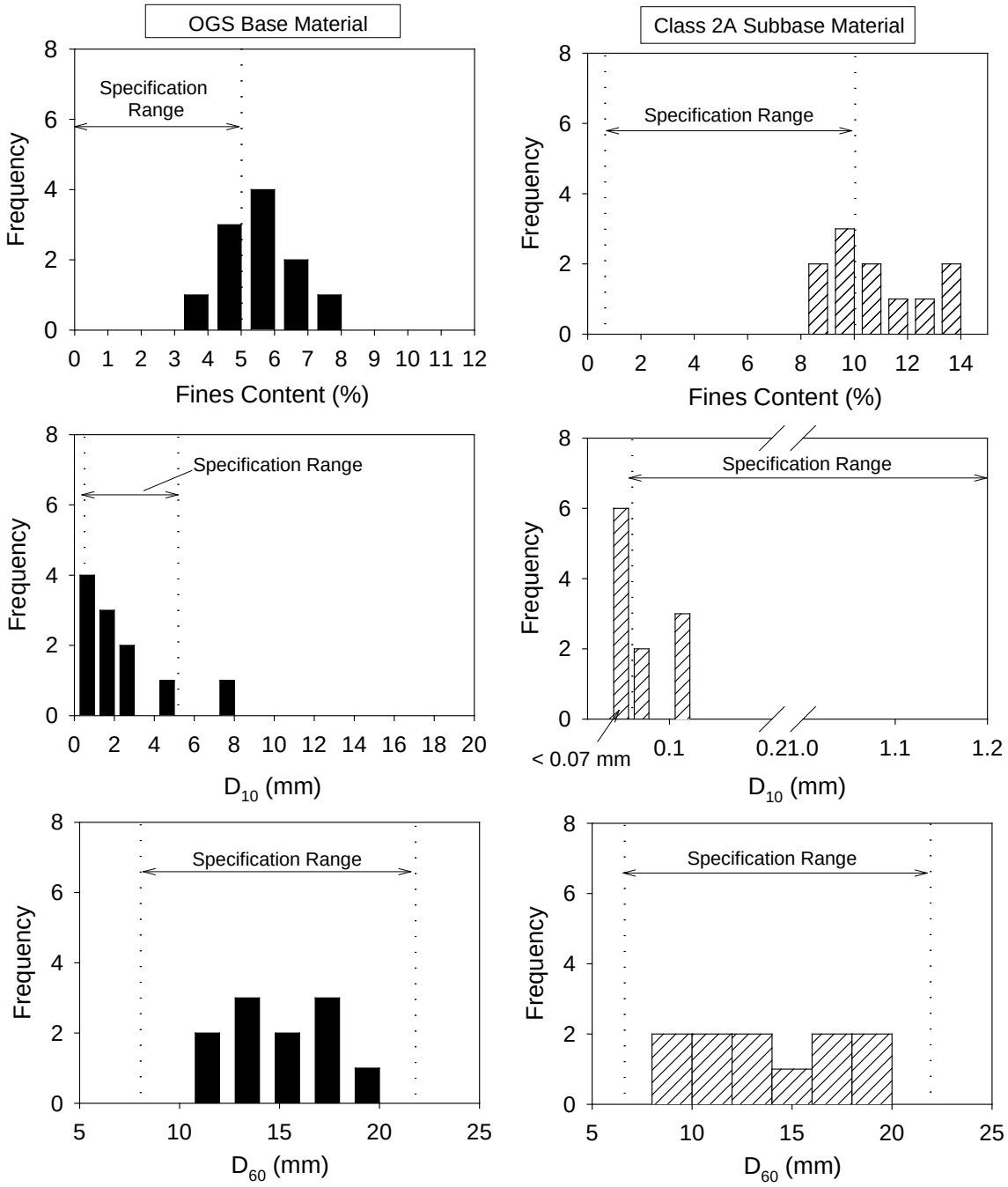

Figure 21. Histograms of particle size distribution for OGS and Class 2A materials

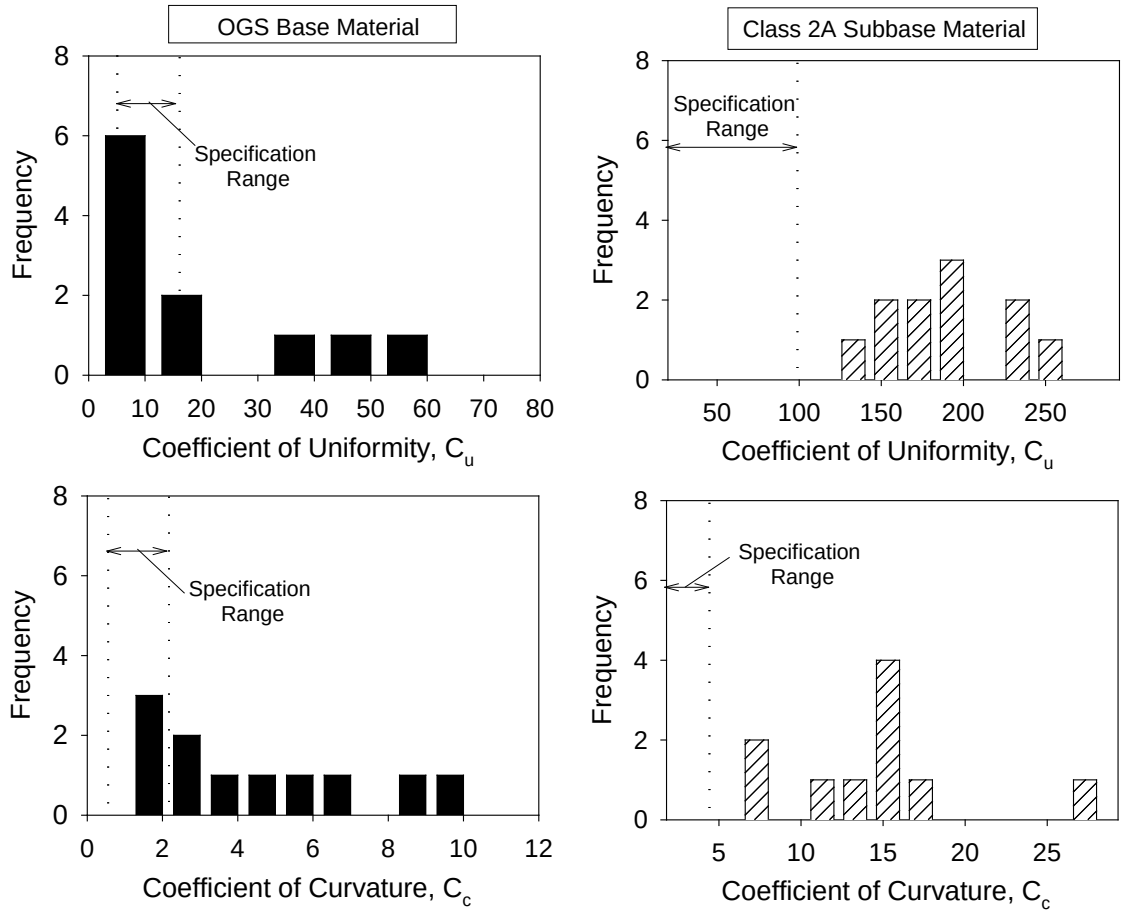

Figure 22. Histograms of gradation parameters c_u and c_c for OGS and Class 2A materials

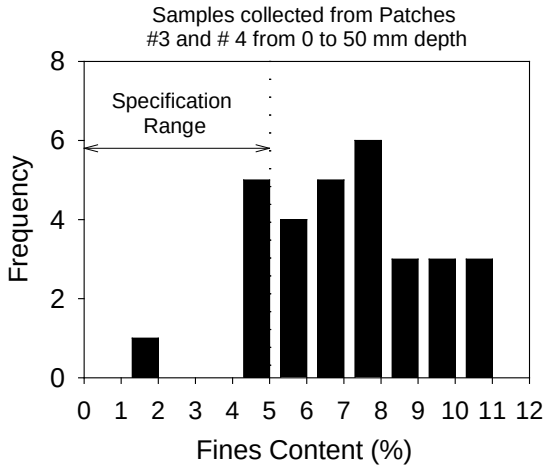

Figure 23. Histogram of fines content for OGS samples from TS2-3 and TS2-4

Percent fines contents in the OGS and 2A samples that exceed the maximum specification limit are likely a result of at least one of the following: particle segregation during construction of the

base and subbase layers; movement of the fine particles over time due to ground water fluctuations or infiltrated surface water in the base layers; and particle breakdown under pavement loads. Particle segregation during construction is a common problem and has been documented in several field case studies (e.g., White et al. 2004, 2010). Particle breakdown was observed in the OGS materials (Figure 24).

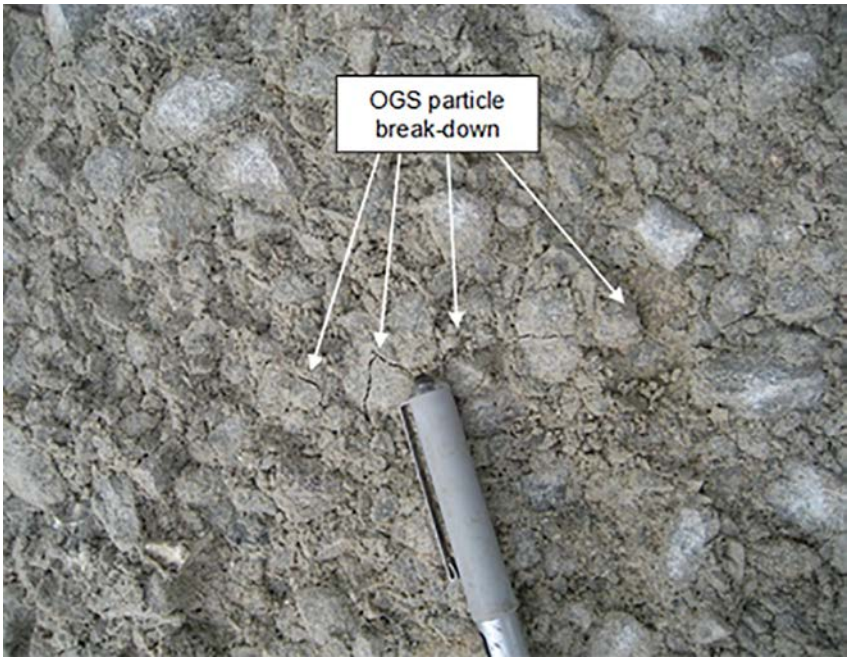

Figure 24. TS1: Aggregate particle breakdown observed in OGS layer

Resilient Modulus and Shear Strength

The gradation of the OGS samples used for M_r and UU tests was modified to meet the AASHTO T-307 standard procedure following a scalp and replace procedure (of material retained on 19 mm (¾ in.) sieve). The particle size distribution curves of the OGS material before and after the scalp and replace procedure is shown in Figure 25.

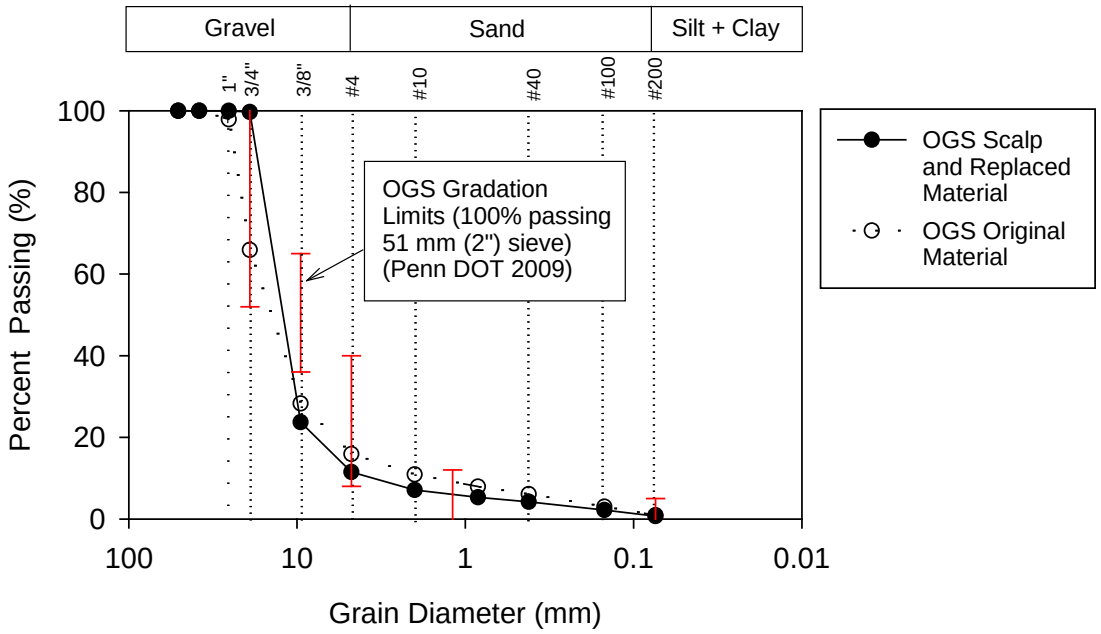

Figure 25. Particle size distribution curves of OGS material before and after scalp and replace procedure (for material retained on 19 mm (3/4 in.) sieve)

Cyclic stress strain curves from M_r test for the foam, OGS, and OGS+Foam samples are provided in Figure 26, Figure 27, and Figure 28, respectively. The M_r and UU test results for the three samples showing the γ_d; average M_r of the 15 AASHTO T-307 loading sequences; permanent strain (ε_p) at the end of the M_r test; "universal model" coefficients, undrained shear strength (s_u) at failure or at 5% axial strain, and s_u at 1% strain are presented in Table 8.

Table 8. M_r and UU test results of Foam, OGS, and OGS+Foam

			M_r Test						UU Test	
Sample	**γ_d (kN/m^3)**	**w (%)**	**Average M_r (MPa)**	**ε_p (%)**	**k_1**	**k_2**	**k_3**	**R^2**	**s_u (kPa)§**	**s_u @ ε = 1% (kPa)**
Foam	1.44	—*	32.8	1.3	287.1	0.20	-0.21	0.81	503	73
OGS	18.54	0.2	219.1	0.3	968.4	0.84	-0.35	0.93	202	157
OGS+Foam	14.92	—*	162.8	0.3	780.6	0.68	-0.10	0.95	685	282

*Not measured; §at axial strain ε = 5% or at failure

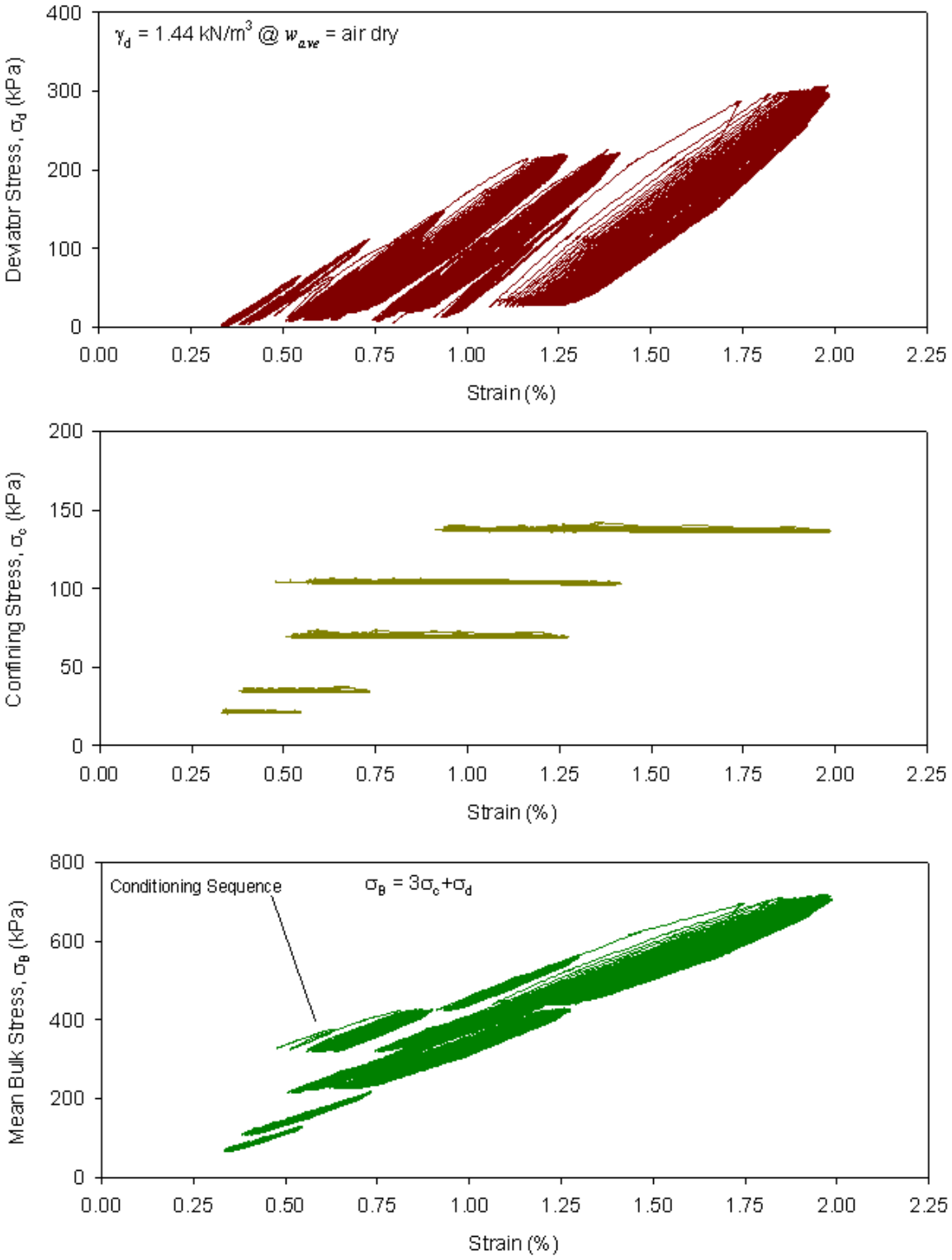

Figure 26. Cyclic stress-strain curves from M_r test for foam sample

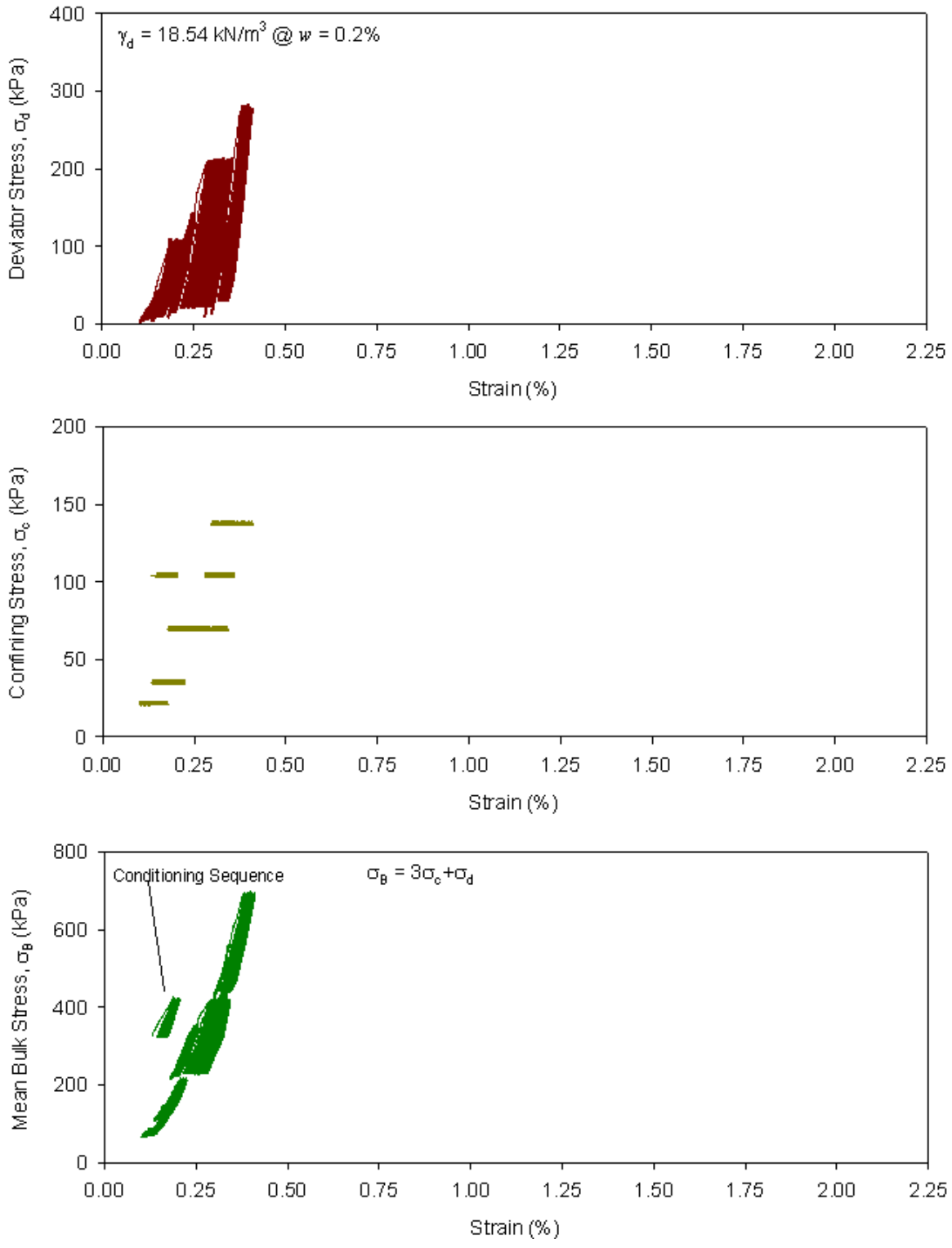

Figure 27. Cyclic stress-strain curves from M_r tests for OGS sample

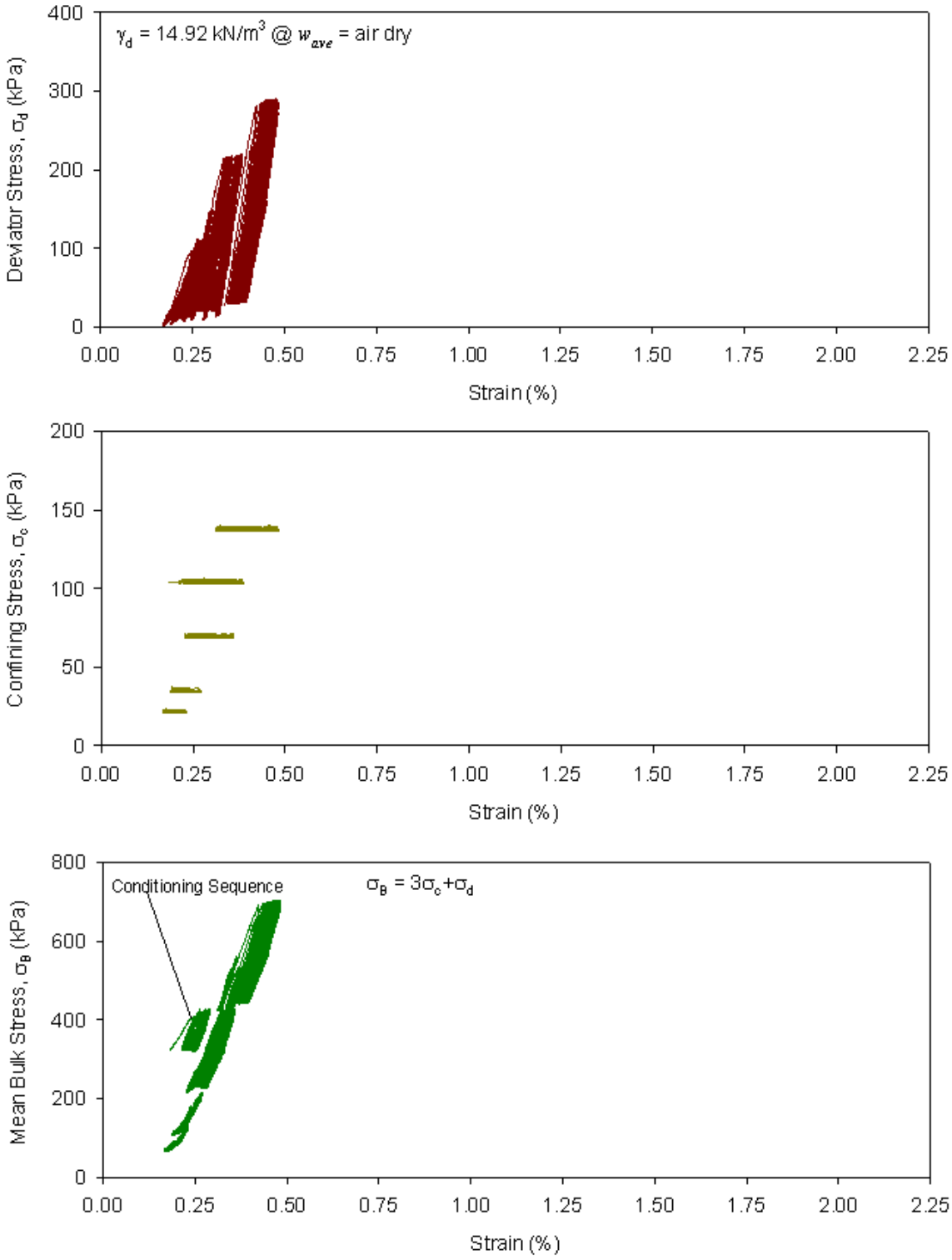

Figure 28. Cyclic stress-strain curves from M_r test for OGS+Foam sample

Figure 29 shows σ_B versus M_r for the three samples, the "universal model" prediction curves, and stress-strain curves from UU test.

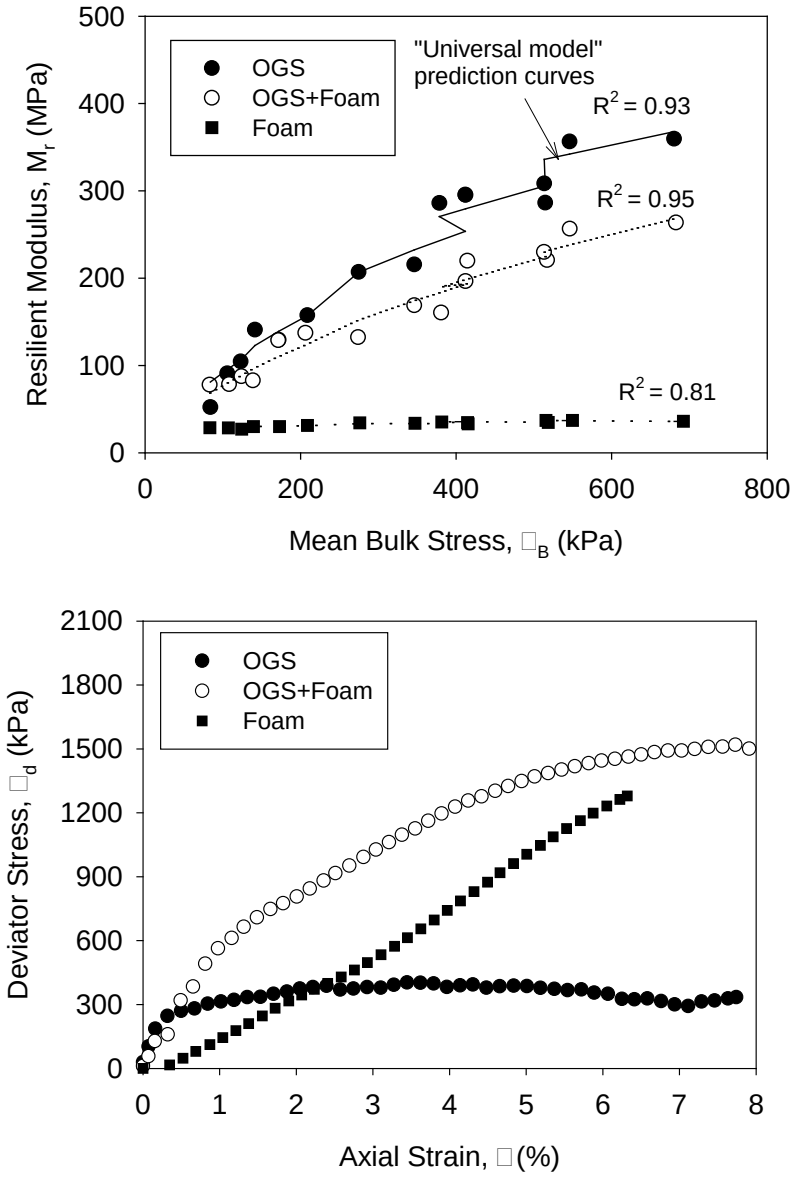

Figure 29. Bulk stress versus resilient modulus (top) and stress-strain curves from UU tests (bottom) for OGS, OGS+Foam, and foam samples

A bar chart plot comparing average M_r, s_u at failure or 5% strain, and s_u at 1% strain of the three samples is presented in Figure 30. Following are the key findings based on the M_r and UU test results and analysis:

- Compared to the OGS and OGS+Foam samples, the foam sample showed much higher permanent strain (ε_p), had a much lower M_r, and underwent much higher elastic deformation. The OGS+Foam sample showed lower (about 0.75 times on average) M_r

value than the OGS sample. However, it should be noted that the OGS sample had considerably higher γ_d than the OGS+Foam sample (OGS γ_d = 18.54 kN/m^3 and OGS+Foam γ_d = 14.92 kN/m^3).

- The UU stress-strain curve for the foam sample showed a near linear increase in deviator stress up to 6% axial strain. The OGS+Foam sample resulted in about 3.4 time higher s_u at failure than the OGS sample.

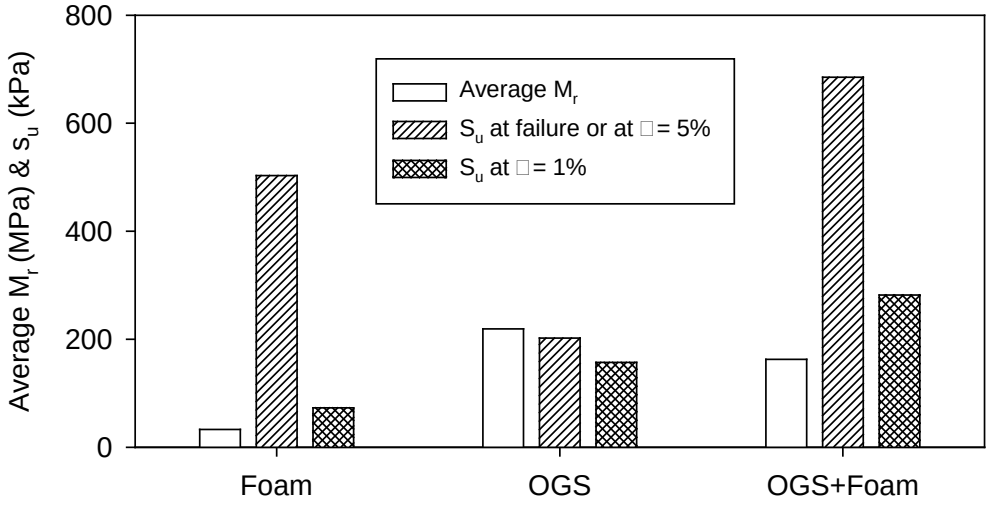

Figure 30. M_r and UU test results of foam, OGS, and OGS+Foam samples

CHAPTER 6. FIELD PERFORMANCE TEST RESULTS

This chapter presents results of field performance testing conducted by Penn DOT in terms of monitoring IRI and in situ testing conducted by ISU research team on several test sections for detailed analysis and performance assessment. A summary of the test sections is provided in Table 5 (Chapter 4). Two test sections (TS1 and TS2) involved four patching areas to evaluate the extent of spatial propagation of injected foam and measuring $E_{LWD\text{-}Z2}$, DCP-CBR, and K_{sat} properties of the subbase layer. Two test sections (TS6 and TS7) involved monitoring surface elevations shortly before and after foam stabilization. Five test sections (TS3, TS4, TS5, TS7, and TS8) involved obtaining performance test measurements before and after stabilization. One of these test sections (TS5) was treated with cementitious grout and the remaining with HDP foam. The cementitious grout section (TS5) and one of the foam treated section (TS7 and TS8) were tested shortly before and after treatment, and six to nine months after stabilization.

The results from Penn DOT IRI measurements and results from the different test sections are described in the following.

Penn DOT IRI Measurements

Penn DOT conducted IRI testing annually after the rehabilitation process between 2010 and 2014. The results are presented in Figure 31 as box plots of IRI measurements post-rehabilitation in comparison with measurements obtained pre-rehabilitation. Results indicated that the average IRI increased from 1.7 m/km before stabilization to about 1.9 m/km immediately after stabilization in July 2010, which suggest poor ability to control variations in the pavement surface elevation to minimize IRI. On average, the IRI measurements remained at about 1.9 m/km in 2014.

TS1/TS2: Evaluation of Spatial Propagation of Injected Foam and Properties of Stabilized and Unstabilized Subbase Layer in Patching Areas

The PCC surface layer was cut in the patching areas approximately mid-panel (where the crack was located) and was removed to expose the subbase layer. Pictures of patch removal and the bottom of patch are shown in Figure 32 and Figure 33.

Four patching areas were evaluated, of which one had one injection point (patch no. 1), one had three injection points (patch no. 2), and two had no injection points (patches nos. 3 and 4). Each patch area was approximately 3.7 m wide by 1.8 m long. The pavement corners, injection point locations, and the cracks were mapped by obtaining RTK-GPS spatial co-ordinates. The OGS+Foam mixture boundaries in the patching areas were also mapped using GPS measurements. In patch no. 2, OGS+Foam mixture was removed during pavement extraction (Figure 34).

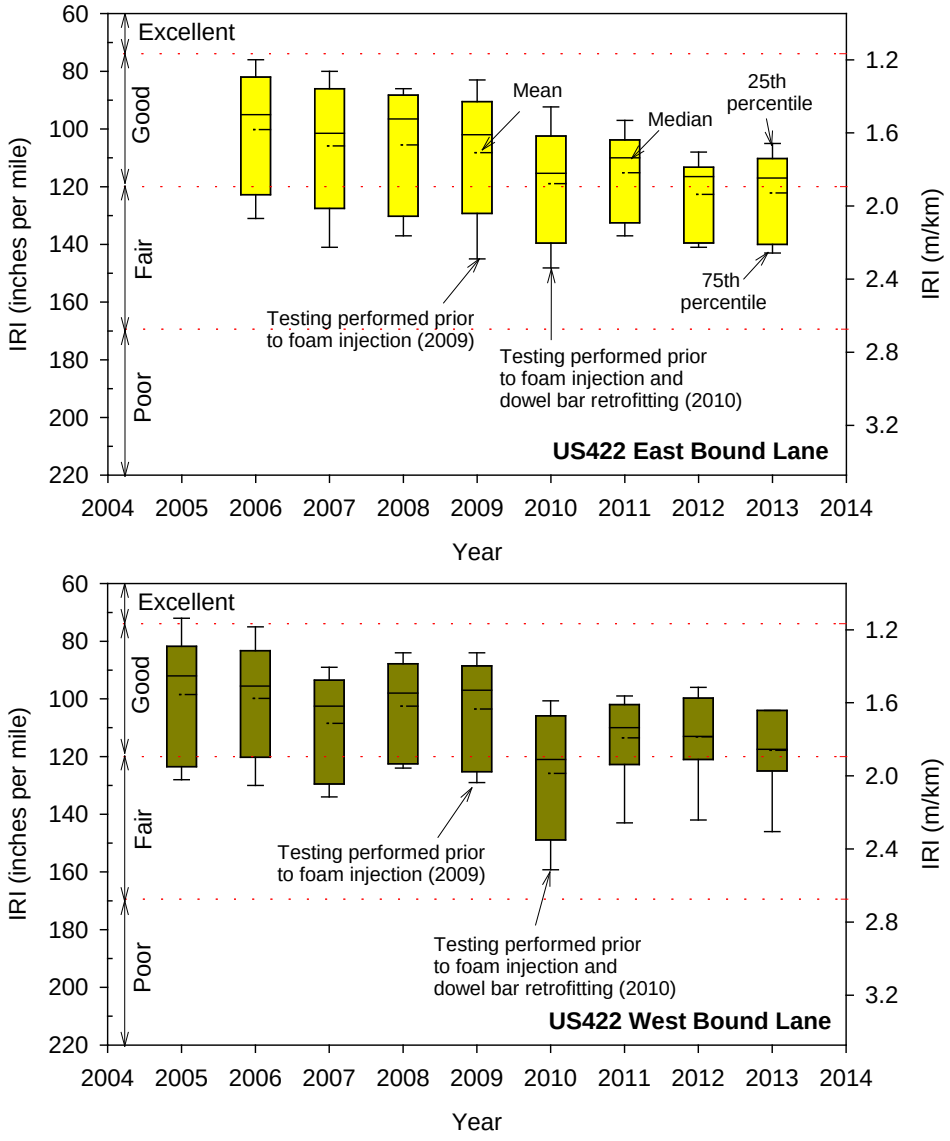

Figure 31. Box plots of IRI measurements on US 422 EB (top) and WB (bottom) lanes from 2005 to 2010

Figure 32. TS1: Crane lifting the PCC surface layer of a patch area

Figure 33. TS1: Bottom of the PCC surface layer in the patch area with treated subbase layer

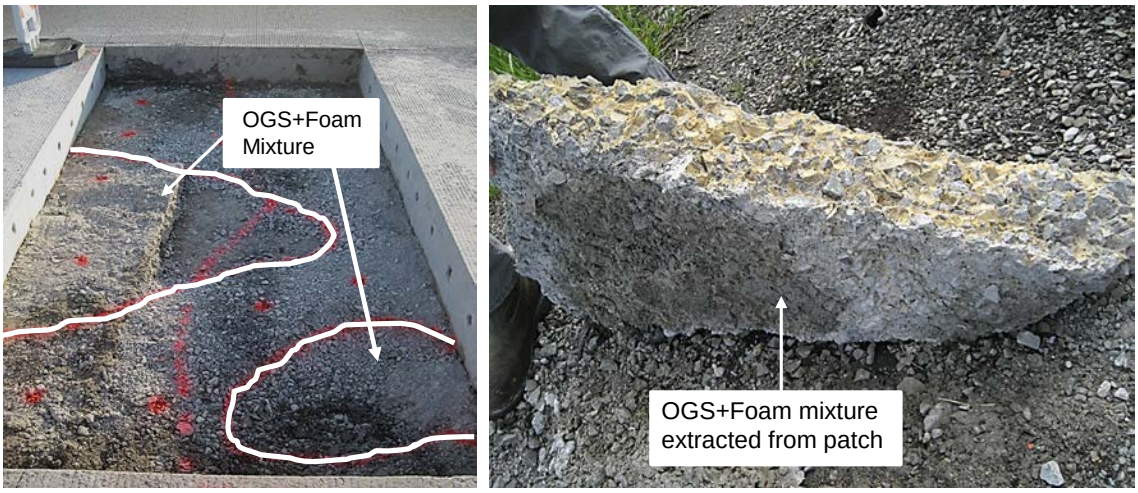

Figure 34. TS1: Picture of patch no. 2 showing OGS+Foam mixture boundary (left), close-up view of OGS+Foam mixture sample extracted from patch no. 2 (right)

Figure 35 and Figure 36 shows the locations of cracks, injection points, pavement panel boundaries, and OGS+Foam mixture boundaries in the patch areas. Patch no. 4 did not have an injection point but included areas with OGS+Foam because of injection points located close to the patch boundary. Measurements indicated that the spatial extent of foam propagation in the subbase layer ranged between 0.3 and 1.0 m from the injection point.

In-situ test measurements ($E_{LWD\text{-}Z2}$, K_{sat}, and DCP-CBR_{OGS}) were obtained from 13 to 15 test locations in patches nos. 2, 3, and 4. In-situ test locations are shown in Figure 35 and Figure 36. A summary of in-situ test measurement statistics (n, μ, σ, and COV) on OGS and OGS+Foam mixture are presented in Table 7. To visualize the spatial variation of $E_{LWD\text{-}Z2}$ and K_{sat} in the patch areas, Kriged contour maps of these measurements were generated as shown in Figure 35 and Figure 36, respectively. The contour maps were generated using semi-variogram analysis and fitting spherical semivariogram models to the data (Clark and Harper, 2002).

The test results indicate that the foam did not fully penetrate the full width and depth of the OGS layer, thus creating non-uniform support conditions. $E_{LWD\text{-}Z2}$ and K_{sat} values are higher at test locations with untreated subbase than at locations with OGS+Foam mixture. The average $E_{LWD\text{-}Z2}$ was about two times greater and the average K_{sat} was about two orders of magnitude greater at locations with untreated subbase than at locations with OGS+Foam mixture. Further, the average DCP-CBR_{OGS} value was higher at locations with OGS+Foam mixture than at locations with untreated subbase. Two of the three DCP tests (see Figure 37) on the OGS+Foam material indicated refusal near the surface (with < 1 mm per blow penetration). The K_{sat} contour maps highlight the spatially concentrated low permeability zones in areas with OGS+Foam material.

Low permeability of the OGS+Foam material was expected as the foam has a closed cell structure and is virtually impermeable. Low modulus but high shear strength (i.e., DCP-CBR_{OGS}) in the OGS+Foam mixture is an important determination in terms of selecting pavement design

input values for this material. The field results are confirmed by resilient modulus laboratory test results reported in Chapter 5, which showed that the OGS+Foam sample had a 3.4 times higher undrained shear strength and 1.5 times lower resilient modulus, when compared to an unstabilized OGS sample.

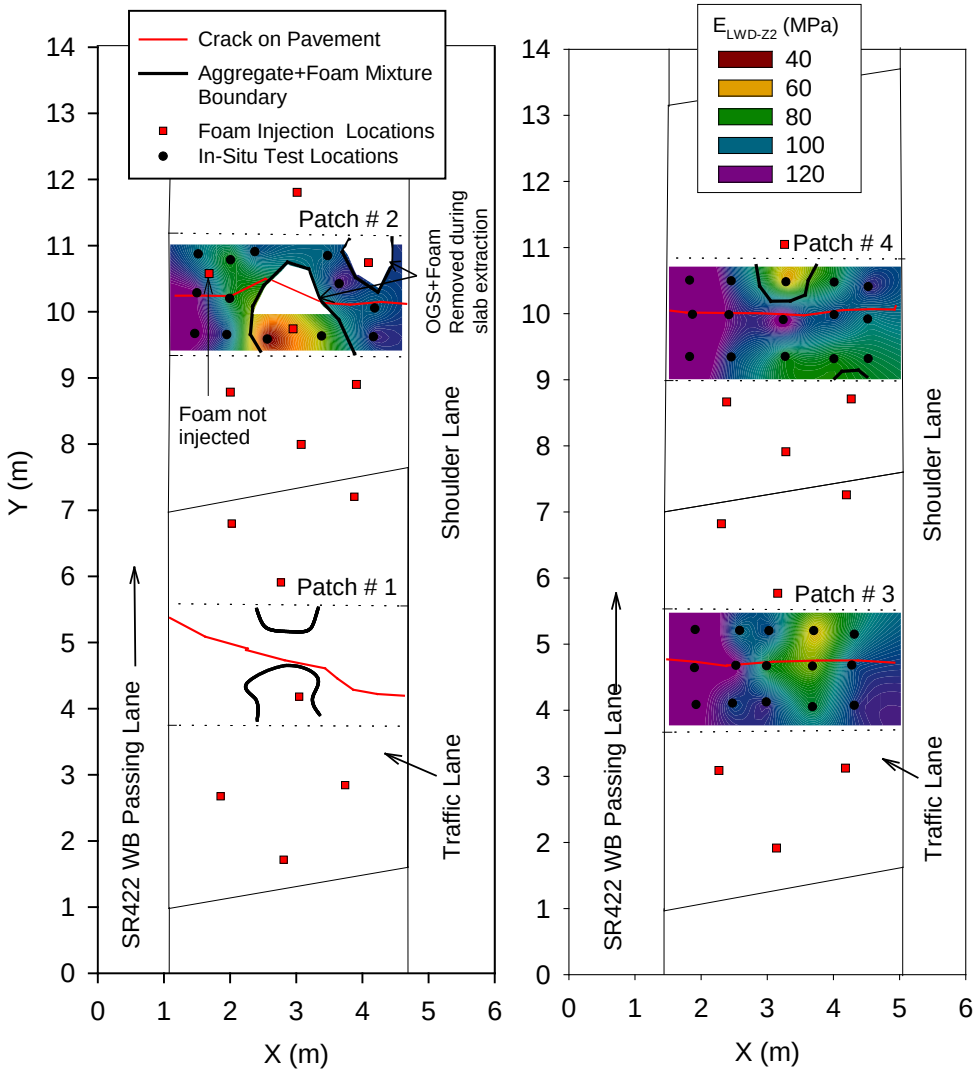

Figure 35. TS1/TS2: Location of cracks, OGS+Foam mixture boundaries, foam injection locations, and in-situ test locations on four patching areas overlaid with spatial contours of E_{LWD-Z2}

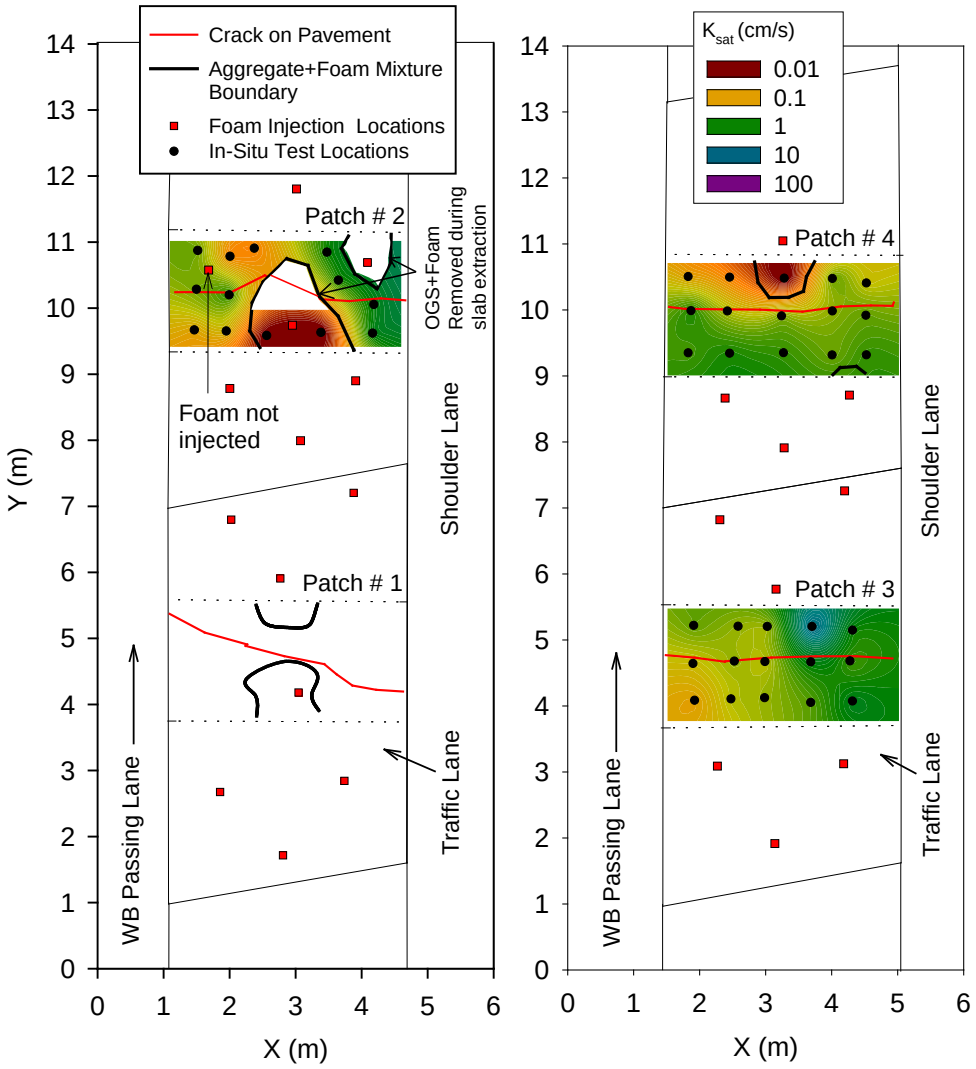

Figure 36. TS1/TS2: Location of cracks, OGS+Foam mixture boundaries, foam injection locations, and in-situ test locations on four patching areas overlaid with spatial contours of K_{Sat}

Table 9. TS1/TS2: Summary statistics of in situ measurements from test patches 2, 3, and 4

Material	Measurement	N	μ	σ	COV (%)
TS1: OGS	$E_{LWD\text{-}Z2}$, MPa	40	106	21	20
	K_{sat}, cm/s	40	7.3E-01	1.5E+00	210
	$DCP\text{-}CBR_{OGS}$ (%)	12	20	4	20
TS2: OGS + Foam	$E_{LWD\text{-}Z2}$, MPa	3	53	17	32
	K_{sat}, cm/s	3	5.4E-03	7.0E-04	13
	$DCP\text{-}CBR_{OGS}$ (%)	1	23	—*	—*
		2	DCP refusal at surface (< 1mm/blow [0.04 in./blow] at surface)		

*only one measurement

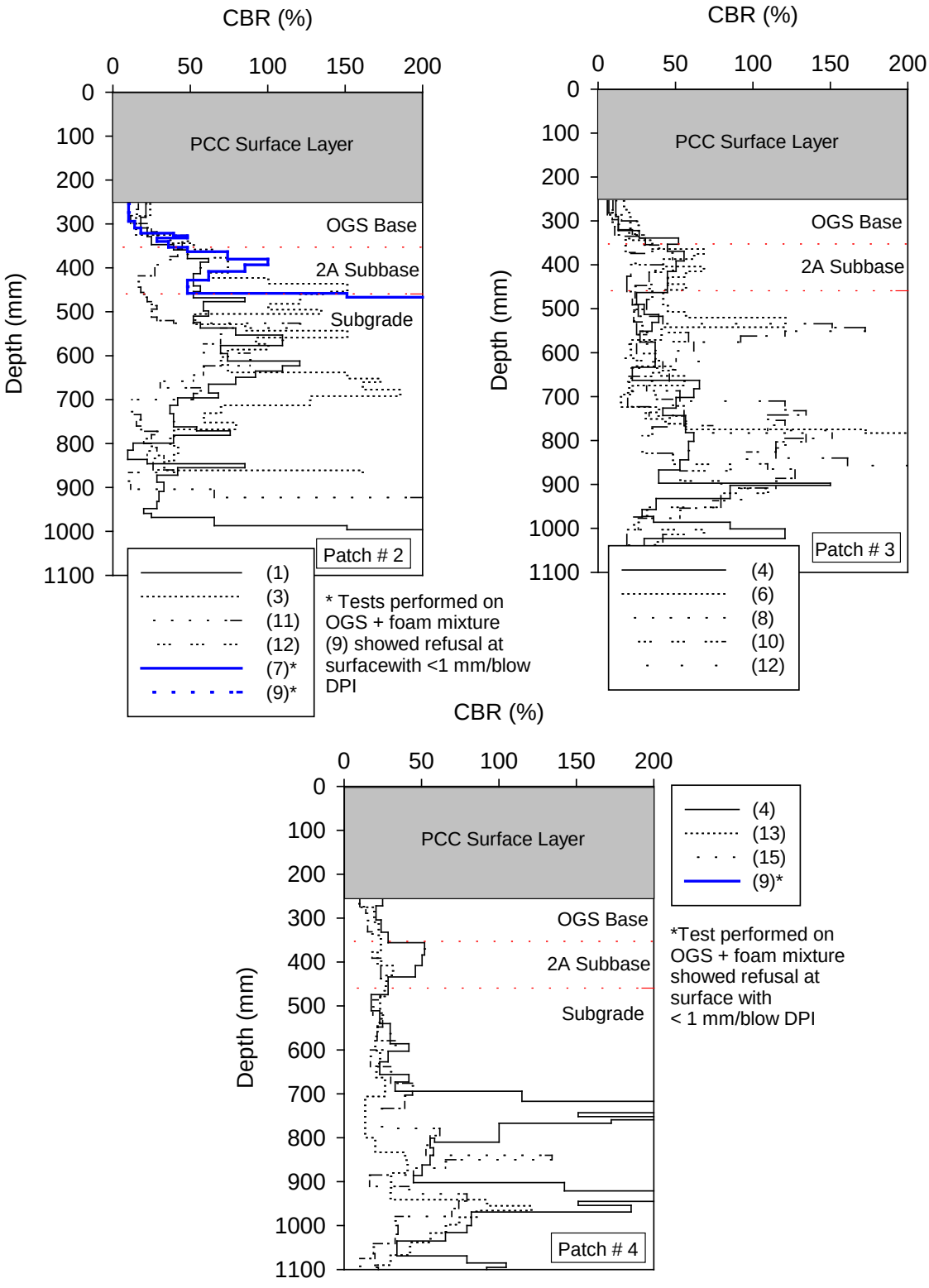

Figure 37. DCP-CBR profiles from patches areas 2, 3, and 4

TS6/TS7: Pavement Surface Elevation Changes Due to Foam Injection

Pavement surface elevations were monitored by obtaining RTS measurements shortly before and after foam stabilization on a 60 m long test section in TS6 (Figure 6) and on a 45 m long test section in TS7. Results from both test sections are separately presented in the following.

TS6 US422 EB

The test section consisted on nine PCC panels. Four of the nine panels did not have cracks before stabilization. The other five panels had mid-panel cracks. RTS pavement elevation profiles were obtained along three lines over the width of the driving lane (Figure 38): (a) line A-A located next to the passing lane, (b) line B-B located in the center of the driving lane, and (c) line C-C located next to the shoulder. Test points were located on either side of each crack and joint, and if no crack was present, measurement was obtained at the middle of the panel. The difference in elevation (ΔElevation) was calculated as the elevation after stabilization – elevation before stabilization. The ΔElevation results are compared to the specified maximum allowed upward movement of 1.3 mm (Penn DOT 2011). The ΔElevation profiles along the A-A, B-B, and C-C lines are presented in Figure 39.

The elevation monitoring results indicated that the pavement panels were raised after stabilization by an average of about 6 mm (σ = 3 mm) across the test section. The upward movement measured at all locations was greater than the 1.3 mm maximum limit per the project specification. This suggests that improved injection control systems may be needed to limit panel heave. However, no faulting was observed at the cracks, shortly after stabilization.

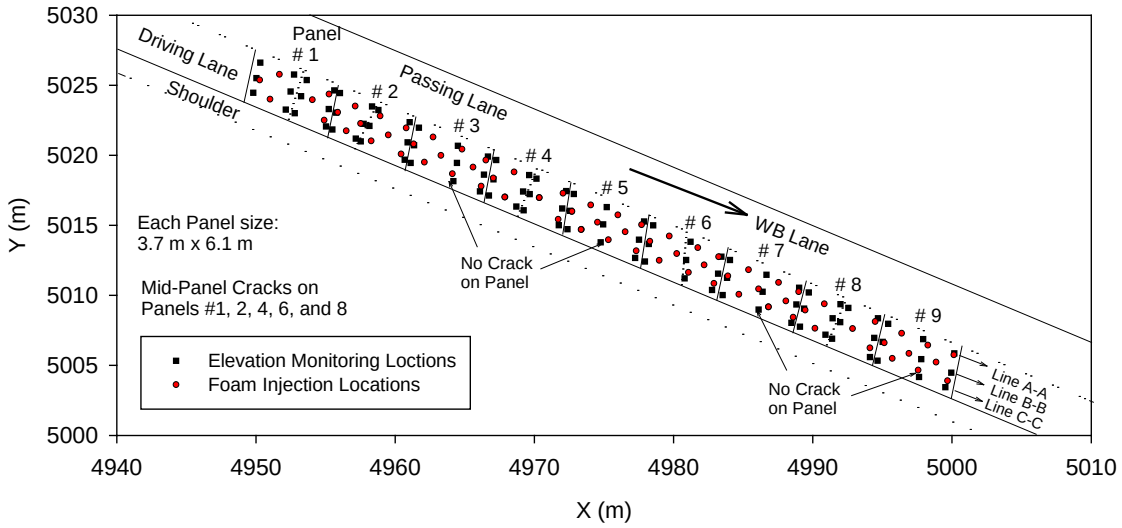

Figure 38. TS6: Plan view of elevation monitoring locations, foam injection locations, and A-A, B-B, and C-C survey lines

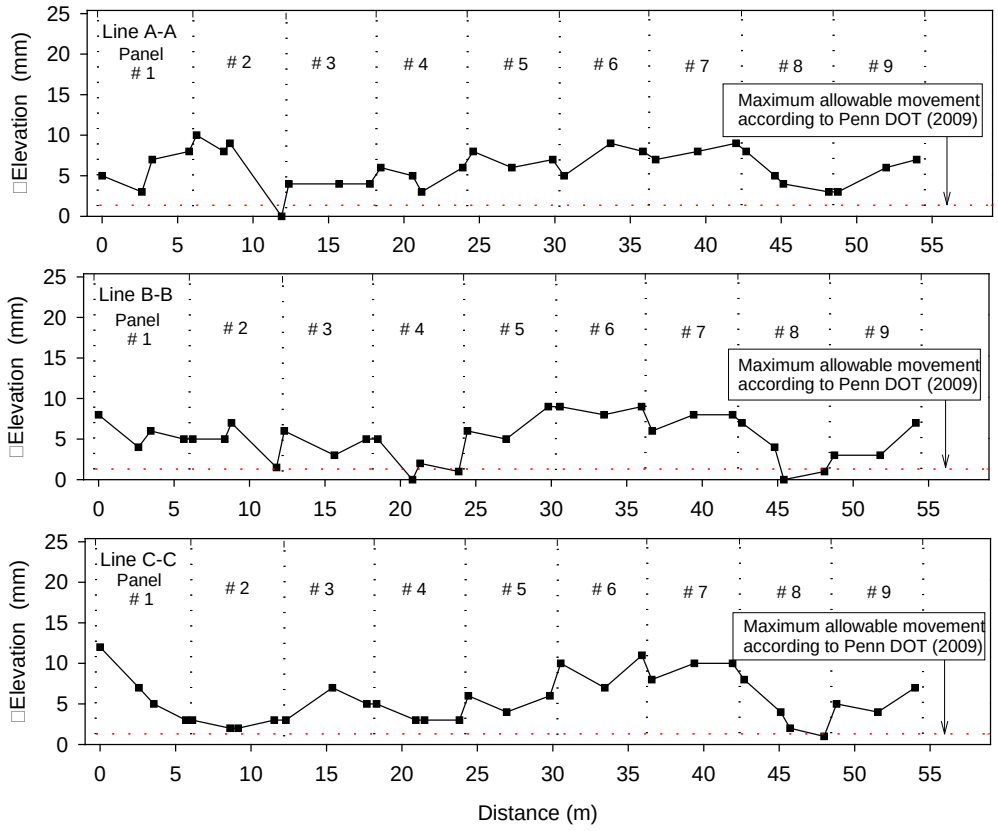

Figure 39. TS6: Results of elevation monitoring near joints and cracks on nine panels along A-A, B-B, and C-C lines

TS7 US422 WB

The test section consisted on five PCC panels (Figure 40). Two of the five panels did not have cracks before stabilization. The other three panels had mid-panel cracks. The panels are labeled as slabs 1 to 5 in Figure 40. RTS pavement elevation profiles were obtained on the pavement surface before and after the initial stabilization along three survey lines A, B, and C, over the width of the traffic lane. To assess the effects of more than one HDP injection, slabs 2 and 3 were treated a second time (i.e., secondary injection), by drilling new injection points (Figure 40). Note that the main purpose of secondary injection was to assess FWD deflections, which are presented in a later section.

RTS ΔElevation profiles after the initial and secondary HDP injection along the survey lines A, B, and C presented in Figure 41. The results indicate that the pavement slabs were raised by an average of about 13 mm (0.5 in.) with a standard deviation of about 8 mm (0.3 in.) across the test section after initial injection, and by about 21 mm (0.8 in.) with a standard deviation of about 8 mm (0.3 in.) across slabs 2 and 3 after secondary injection. Similar to the results in TS6, the upward movement measured at all locations was greater than the 1.3 mm maximum limit per the project specification.

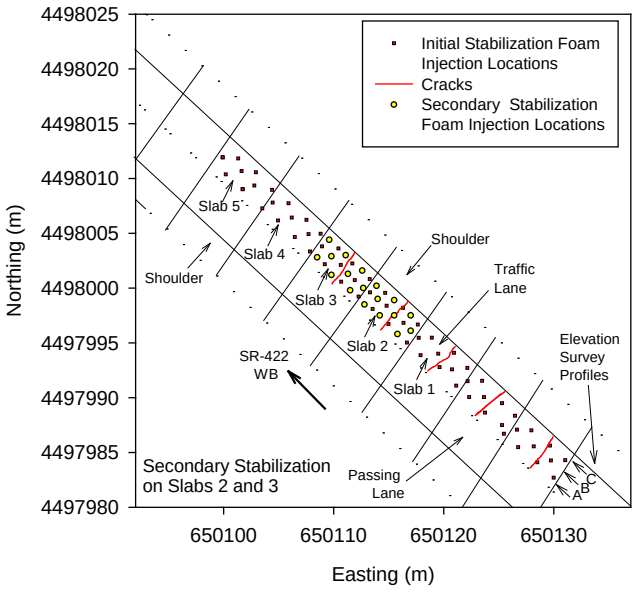

Figure 40. TS7: Plan layout showing cracks, initial and secondary foam injection locations, and elevation survey profile lines

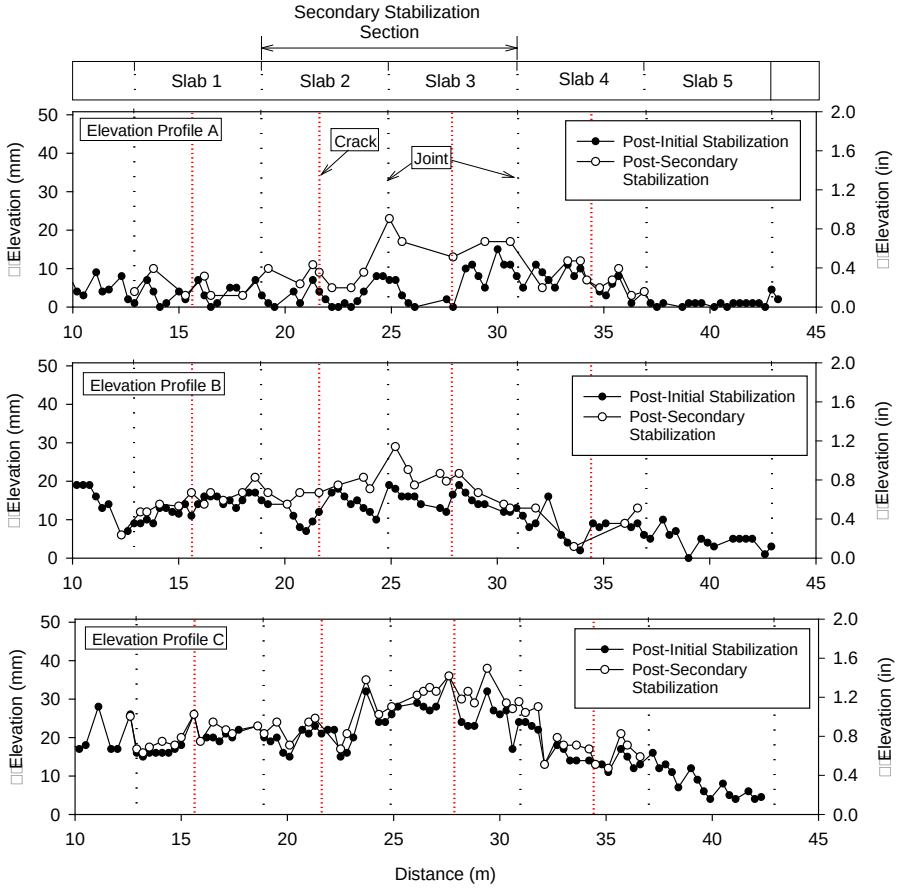

Figure 41. TS7: ΔElevation profiles from RTS measurements

TS5/TS8: Comparison between Cementitious Grout Stabilized and HDP Foam Stabilized Sections

The cementitious grout stabilized test section (TS5) was about 150 m long with twenty three pavement panels, and was located on US422 WB (Figure 42). Tests were conducted on driving lane. Ten panels were selected for testing, of which four showed mid-panel cracks. All cracked panels were repaired with dowel-bar retrofitting in May 2010. Tests were conducted in October 2009 before stabilization and in July 2010 after stabilization and dowel-bar retrofitting. Figure 42 shows the FWD test locations, crack locations, and fault measurements on TS5.

The HDP foam stabilized test section (TS8) was about 220 m long with thirty five pavement panels, and was located on US422 EB (Figure 43). Tests were conducted on both driving and passing lanes, but only tests on driving lane were used herein for comparison with TS5. Nine panels were selected for testing, of which seven showed mid-panel cracks. After foam stabilization, two cracked panels were repaired with full-depth patching while the remaining five panels were repaired with dowel bar retrofitting. Full depth patching and dowel-bar retrofitting repair work was done in May 2010. In situ tests were conducted in October 2009 shortly before and after stabilization, in November 2009, and in July 2010. Figure 43 shows the FWD test locations, crack locations, and fault measurements on TS8.

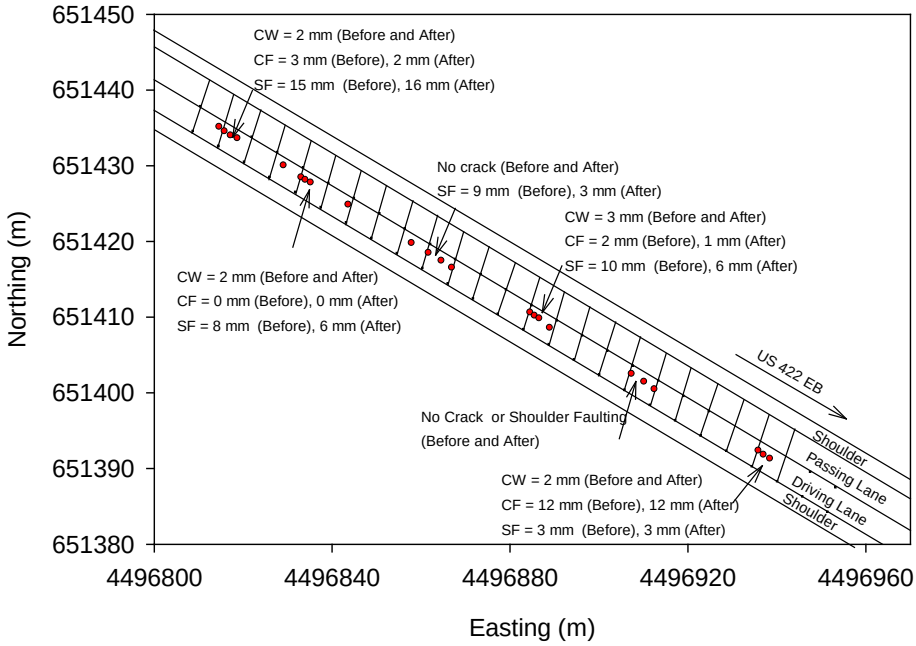

Figure 42. TS5: Plan view showing FWD test and crack locations, and fault measurements on cracked panels

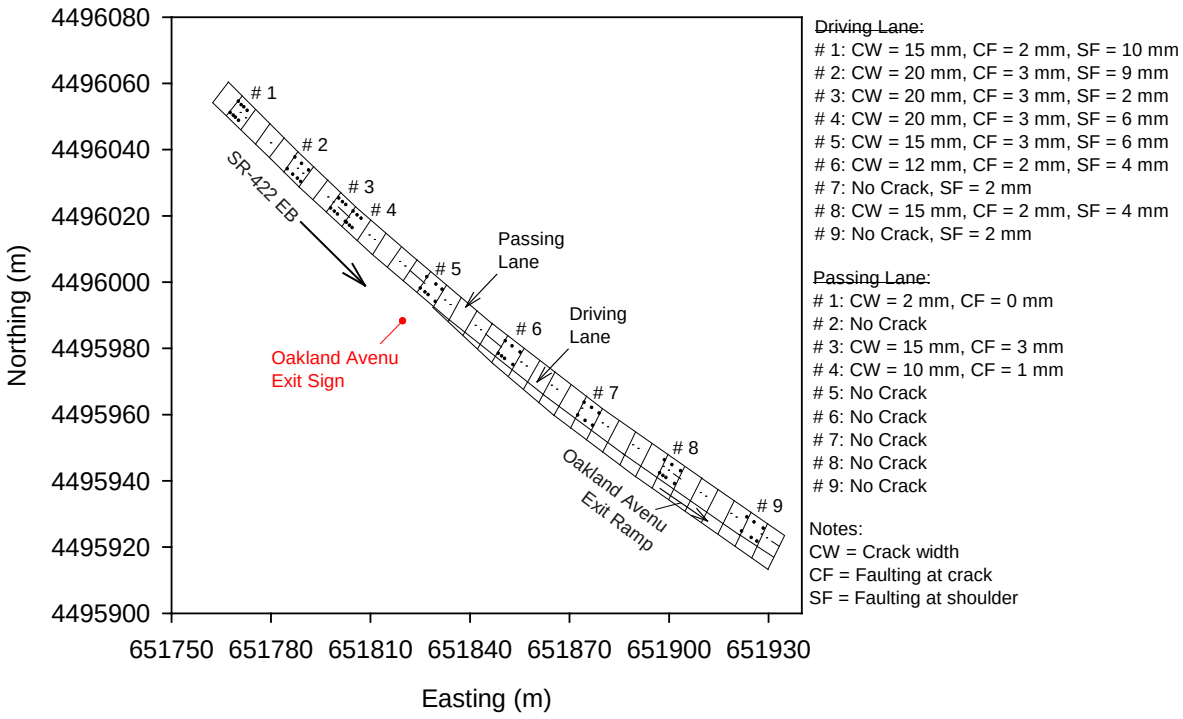

Figure 43. TS8: Plan view showing FWD test and crack locations, and fault measurements on cracked panels

In situ testing in TS5 and TS8 included FWD testing, and fault measurements (CF and SF) measurements before and after stabilization. FWD tests were conducted at mid-panel, near crack, and near joint.

The CF and SF results and FWD test results are presented as box plots in Figure 44 to Figure 48. The results are presented separately for measurements near cracks, joints, and mid-way between joint and crack. Statistical analysis results comparing before and after stabilization test results for the two methods are provided in Table 8, and comparing results between the grout and HDP test sections are provided in Table 9. The *t*-values that are greater than the minimum *t*-value are highlighted in the tables. The comparisons have been separated for measurements obtained near joints, cracks, and at mid-panel.

Faulting measurements (Figure 44) indicated that slabs were raised after HDP foam stabilization while less slab movement was measured after cementitious grout stabilization. On average, faulting reduced by about 2.5 mm near cracks and by about 4.6 mm near shoulder pavement, after HDP foam injection. Within the cementitious grout section, faulting was reduced on average by about 0.5 mm near cracks and by about 2.2 mm near the shoulder pavement. Per Penn DOT (2011), a maximum slab movement of 1.3 mm is allowed during slab stabilization.

Statistical *t*-test results on FWD measurements before stabilization indicated no statistically significant differences between the two test sections, with the exception of D_0 and I

measurements at the mid-panel (Table 4). It is important to have the two sections with similar conditions so that the comparison after stabilization is not biased.

Analysis of FWD measurements revealed differences between the two stabilization methods. In the HDP stabilized section, all FWD measurement parameters indicated statistically significant improvement near cracks. Near joints, SCI, BDI, BCI, AF, and LTE measurements showed improvement, but D_0 and I measurements did not. In the cementitious grout stabilized section, however, D_0 and I measurements did not show improvement near cracks but showed improvement near joints. All the remaining FWD measurement parameters showed improvement near joints and cracks (except BCI near cracks). No statistically significant improvement was determined in measurements obtained at the mid-panel, for both stabilization methods.

In both sections the BCI parameter showed improvement. As explained earlier, BCI represents strength/stiffness properties of the subgrade layer (at 600 mm to 900 mm depth below surface), which was not expected here as stabilization occurred at the PCC and subbase layer interface and top portions of the subbase layer.

Analysis results presented in Table 9 indicate that statistically significant differences between the two stabilization methods were observed only near cracks in terms of D_0, I, and BCI. This means that FWD measurements in the HDP foam stabilized section showed better improvement at cracks compared to the cementitious grout section.

LTE was a critical parameter in selecting locations for stabilization. Results indicated that LTE improved near cracks and joints in both cementitious grout and HDP foam stabilized sections. LTE measurements at cracks, although improved after HDP stabilization, did not increase to > 65% until after dowel bar retrofitting. Other critical parameters in selecting locations for stabilization were D_0 and I. These values showed improvement only near cracks in the HDP foam section and only near joints in the cementitious grout section.

Although FWD measurements indicated improvements with deflections under loading and LTE, faulting measurements indicated that slabs were lifted greater than the allowed 1.3 mm during HDP stabilization. This suggests a need for better process control in vertical movement control during stabilization, particularly with the HDP stabilization method.

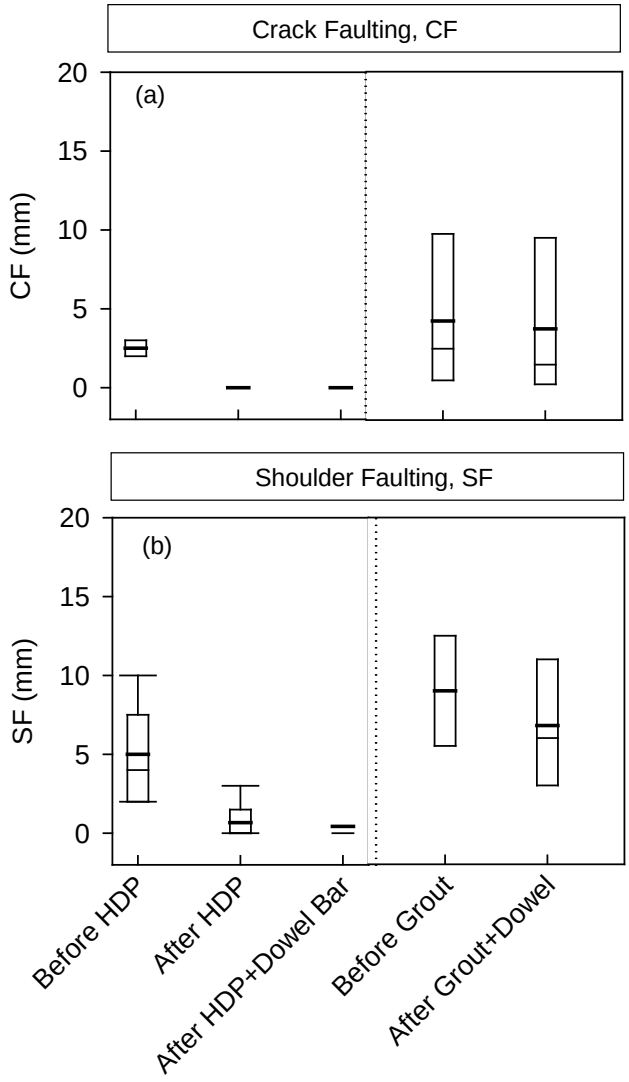

Figure 44. TS5/TS8: Box plots of (a) crack faulting and (b) shoulder faulting, before and after HDP/grout stabilization and dowel bar retrofitting at cracks

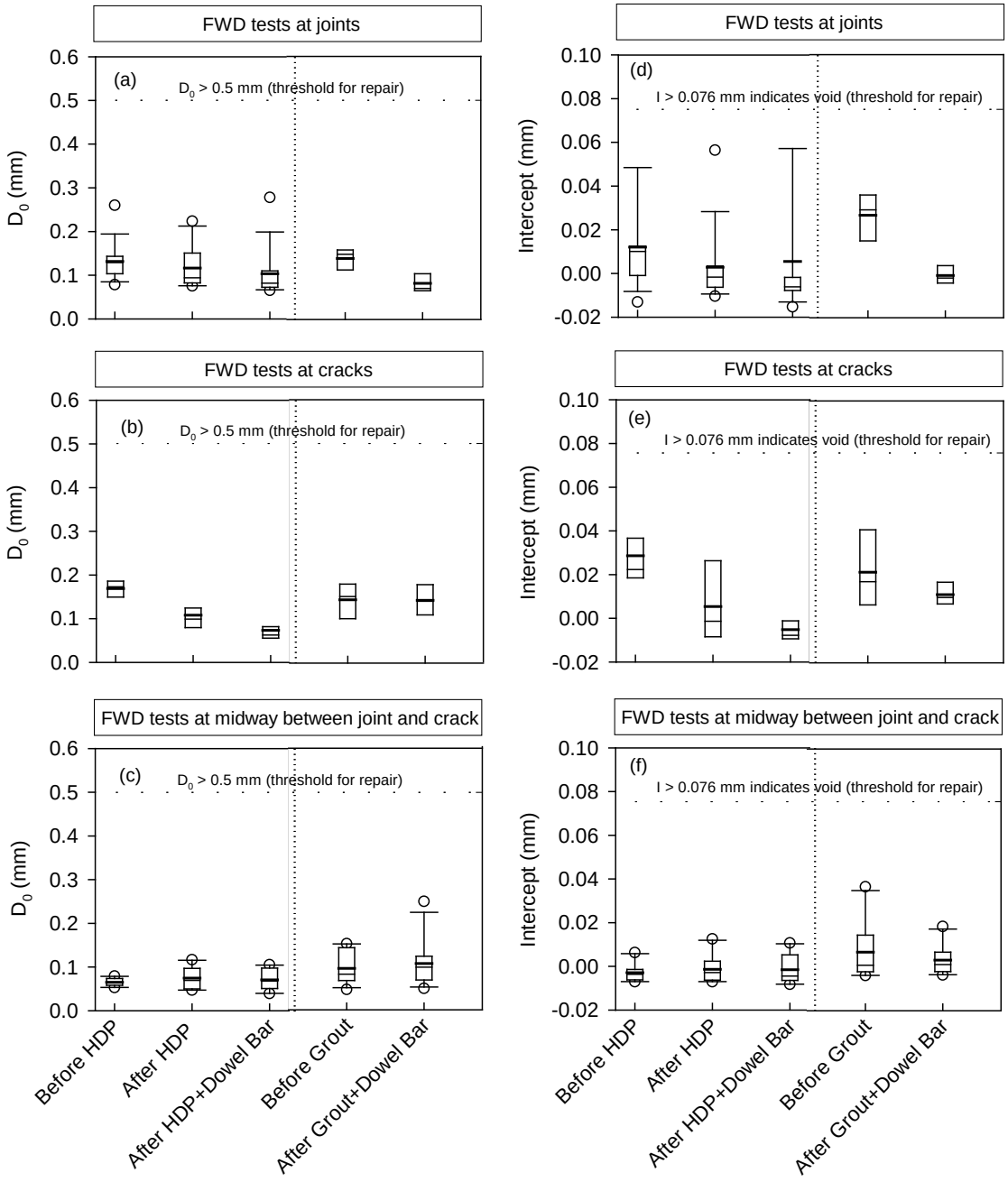

Figure 45. TS5/TS8: Box plots of (a) D_0 at joints; (b) D_0 at cracks; (c) D_0 at midway between joint and crack; (d) intercept at joints; (e) intercept at cracks; (f) intercept at midway of joint and crack, before and after HDP/grout stabilization and dowel bar retrofitting at cracks

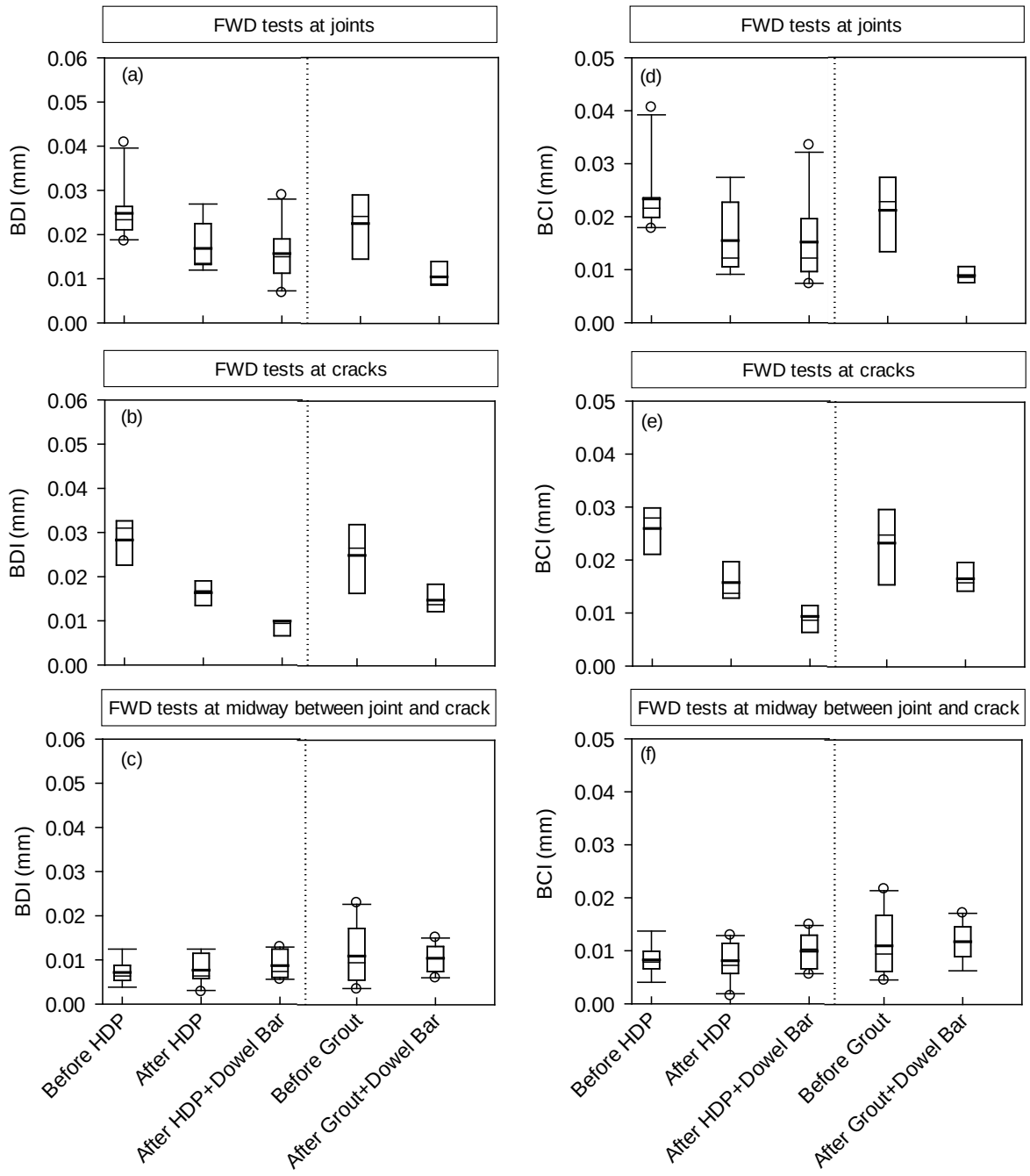

Figure 46. TS5/TS8: Box plots of (a) BDI at joints; (b) BDI at cracks; (c) BDI at midway between joint and crack; (d) BCI at joints; (e) BCI at cracks; (f) BCI at midway of joint and crack, before and after HDP/grout stabilization and dowel bar retrofitting at cracks

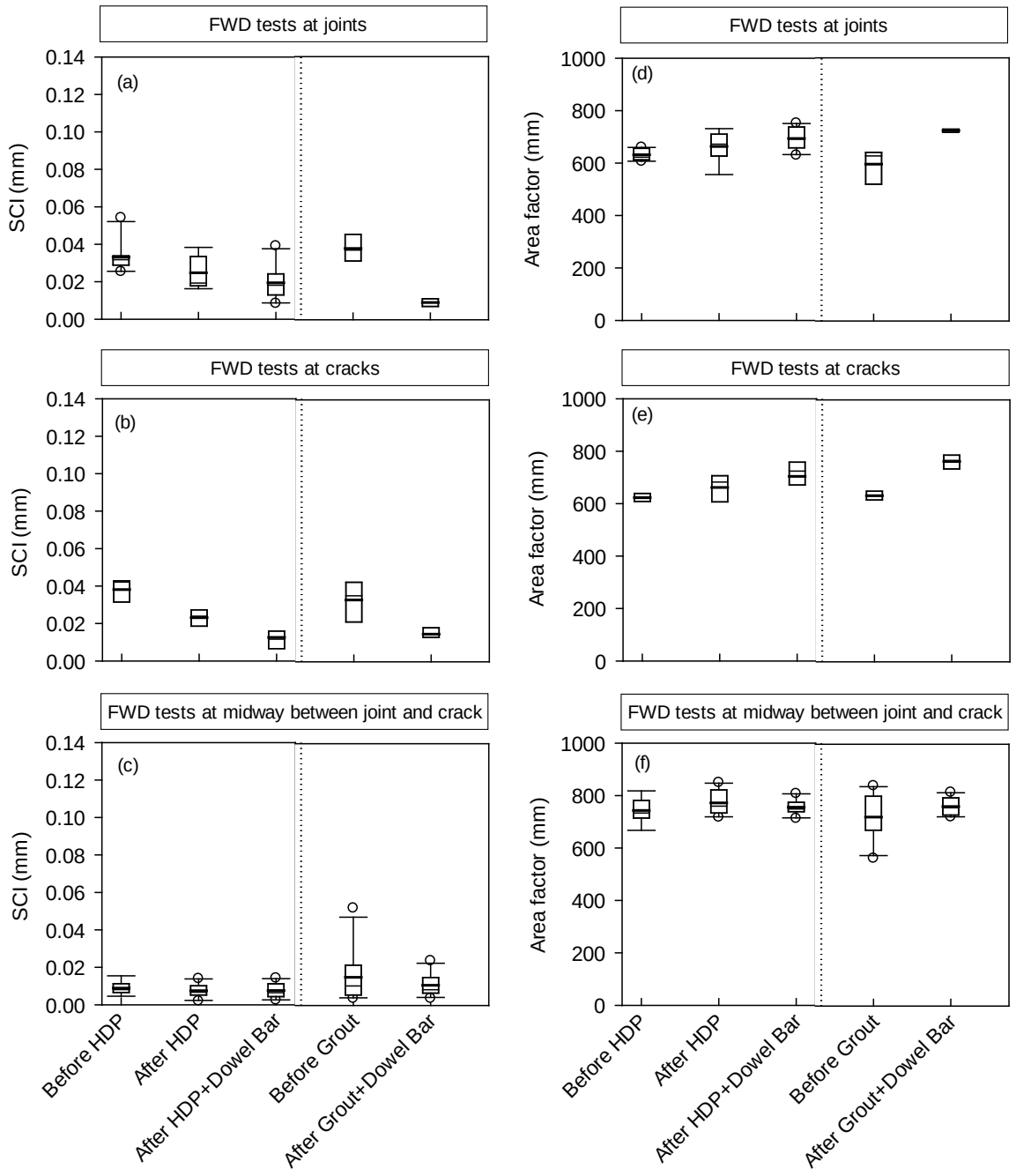

Figure 47. TS5/TS8: Box plots of (a) SCI at joints; (b) SCI at cracks; (c) SCI at midway between joint and crack; (d) area factor at joints; (e) area factor at cracks; (f) area factor at midway of joint and crack, before and after HDP/grout stabilization and dowel bar retrofitting at cracks

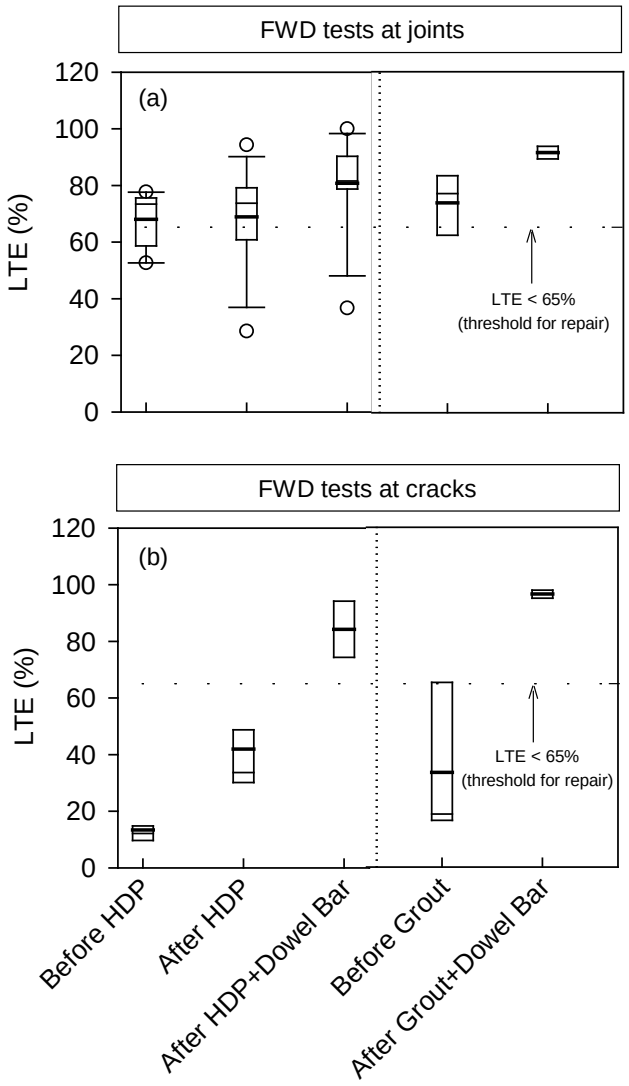

Figure 48. TS5/TS8: Box plots of (a) LTE at joints and (b) LTE at cracks, before and after HDP/grout stabilization and dowel bar retrofitting at cracks

Table 10. TS5/TS8: Results of statistical analysis comparing before and after stabilization test results

Parameter and Location		Before or after stabilization[1]	HDP				Cementitious Grout			
			Mean	COV (%)	*t*-value	P_r	Mean	COV (%)	*t*-value	P_r
D_0 (µm)	Joints	Before	132	31	1.64	0.111	139	17	5.02	<0.001
		After	104	56			82	25		
	Cracks	Before	169	18	5.97	<0.001	142	30	0.046	0.965
		After	73	39			140	26		
	Midway	Before	65	13	-0.72	0.483	89	38	-0.20	0.846
		After	71	34			91	29		
I (µm)	Joints	Before	12	213	0.56	0.580	27	47	5.86	<0.001
		After	6	709			-1	-516		
	Cracks	Before	27	66	4.50	<0.001	22	86	1.06	0.329
		After	-5	-125			11	48		
	Midway	Before	-3	-142	<0.01	0.997	7	189	0.803	0.433
		After	-3	-434			3	209		
SCI (µm)	Joints	Before	33	24	3.65	0.002	38	19	6.71	0.003
		After	19	46			9	22		
	Cracks	Before	38	17	6.70	<0.001	33	34	3.11	0.021
		After	13	53			15	23		
	Midway	Before	9	37	1.34	0.198	16	93	1.33	0.202
		After	7	50			10	45		
BDI (µm)	Joints	Before	25	25	3.30	0.004	23	33	2.62	0.059
		After	16	39			10	29		
	Cracks	Before	28	19	6.60	<0.001	25	33	2.27	0.064
		After	10	42			15	23		
	Midway	Before	7	36	-1.21	0.243	11	61	0.218	0.830
		After	9	34			11	30		
BCI (µm)	Joints	Before	23	28	2.52	0.021	21	34	2.92	0.043
		After	15	52			9	17		
	Cracks	Before	26	19	6.72	<0.001	23	33	1.65	0.151
		After	9	40			17	18		
	Midway	Before	8	33	-1.20	0.248	11	54	-0.35	0.727
		After	10	33			12	32		
AF (µm)	Joints	Before	632	4	-4.11	<0.001	596	11	-3.31	0.030
		After	694	6			724	1		
	Cracks	Before	623	2	-3.04	0.012	634	3	-7.86	<0.001
		After	704	8			765	4		
	Midway	Before	743	6	-0.68	0.503	722	11	-1.44	0.167
		After	755	4			762	4		
LTE (%)	Joints	Before	68	14	-2.39	0.026	74	18	-3.65	0.003
		After	81	19			92	3		
	Cracks	Before	13	41	-15.25	<0.001	33	94	-3.99	0.007
		After	84	13			97	2		

Notes: Highlighted cells indicate values that are statistically significant; number of tests on HDP stabilized sections: at joints = 16, at cracks = 7, at midway = 10; number of tests of cementitious grout stabilized sections: at joints = 8, at cracks = 4, at midway = 10. [1] *Before* indicates before construction and *after* indicates after dowel bar retrofitting.

Table 11. TS5/TS8: Results of statistical analysis comparing HDP and grout stabilization methods

Parameter and Location		Stabilization method	Before stabilization				After stabilization			
			Mean	COV (%)	*t*-value	P_r	Mean	COV (%)	*t*-value	P_r
D_0 (µm)	Joints	HDP	132	31	-0.48	0.636	104	17	1.04	0.308
		Grout	139	56			82	25		
	Cracks	HDP	169	18	1.25	0.245	73	30	-3.41	0.008
		Grout	142	39			140	26		
	Midway	HDP	65	13	-2.18	0.043	71	38	-1.83	0.083
		Grout	87	34			91	29		
I (µm)	Joints	HDP	12	213	-1.51	0.145	6	47	0.45	0.659
		Grout	27	709			-1	-516		
	Cracks	HDP	27	66	0.60	0.561	-5	86	-4.23	0.002
		Grout	22	-125			11	48		
	Midway	HDP	-3	-142	-2.27	0.036	-2	189	-1.58	0.131
		Grout	7	-434			3	209		
SCI (µm)	Joints	HDP	33	24	-0.94	0.366	19	19	1.94	0.079
		Grout	38	46			9	22		
	Cracks	HDP	38	17	0.87	0.413	13	34	-0.60	0.563
		Grout	33	53			15	23		
	Midway	HDP	9	37	-1.40	0.181	8	93	-1.07	0.299
		Grout	16	50			10	45		
BDI (µm)	Joints	HDP	25	25	0.54	0.599	16	33	1.39	0.193
		Grout	23	39			10	29		
	Cracks	HDP	28	19	0.72	0.498	10	33	-1.99	0.078
		Grout	25	42			15	23		
	Midway	HDP	7	36	-1.63	0.122	9	61	-1.36	0.193
		Grout	11	34			11	30		
BCI (µm)	Joints	HDP	21	28	0.07	0.949	15	34	1.33	0.210
		Grout	21	52			9	17		
	Cracks	HDP	26	19	0.62	0.553	9	33	-3.34	0.009
		Grout	23	40			17	18		
	Midway	HDP	8	33	-1.29	0.213	10	54	-1.23	0.234
		Grout	11	33			12	32		
AF (µm)	Joints	HDP	632	4	1.58	0.142	694	11	-1.21	0.253
		Grout	596	6			724	1		
	Cracks	HDP	623	2	-1.01	0.345	704	3	-1.95	0.083
		Grout	634	8			765	4		
	Midway	HDP	743	6	0.69	0.500	755	11	-0.47	0.647
		Grout	722	4			762	4		
LTE (%)	Joints	HDP	68	14	-1.12	0.277	81	19	-1.91	0.073
		Grout	74	24			92	3		
	Cracks	HDP	13	41	-1.71	0.121	84	13	-2.27	0.058
		Grout	33	47			97	2		

Notes: Highlighted cells indicate values that are statistically significant; number of tests on HDP stabilized sections: at joints = 16, at cracks = 7, at midway = 10; number of tests of cementitious grout stabilized sections: at joints = 8, at cracks = 4, at midway = 10. [1] *Before* indicates before construction and *after* indicates after dowel bar retrofitting.

TS3/TS4: Effects of HDP Foam Stabilization Shortly Before and Shortly After Stabilization near Mid-Panel

TS3/TS4 is located on the US 422 WB driving lane near Warren Road Bridge. TS3 results are from testing before HDP stabilization for comparison with TS4 results obtained after stabilization. The test section was stabilized with HDP foam on October 1, 2009. Pre-stabilization tests were conducted at 22 locations on the pavement surface on October 1, 2009, and post-stabilization tests were conducted on October 13, 2009. FWD tests were conducted by placing the FWD plate about mid-way between the crack and the joint of pavement slabs. Pre-stabilization DCP tests were conducted by drilling a hole through the pavement at three randomly selected test locations (at test points #3, #7, and #10). DCP tests were not conducted after stabilization due to time constraints. A plan layout of the test locations is shown in Figure 49.

D_0, E_{FWD-K3}, SCI, BDI, BCI, and area factor values calculated from FWD tests for four loading conditions before and after HDP stabilization are presented in Figure 50 to Figure 54. DCP-CBR profiles at three test locations before stabilization are presented in Figure 55. FWD intercept (I) values before and after stabilization are presented in Figure 56. Bar charts of average values of these measurement values with 1 x σ error bars for different loading conditions before and after stabilization are presented in Figure 57. Temperature measurements in the pavement indicated negative gradients at both times of testing (T_L = -0.04 ^oC/cm on October 1, 2010 and T_L = -0.08 ^oC/cm on October 13, 2010).

Following are the key changes observed from the FWD measurements after stabilization, which are presented as the range of the average and standard deviation values for the four applied loads:

- The average D_0 decreased by about 0.014 to 0.019 mm (7 to 16%) and the D_0 standard deviation decreased by about 0.015 to 0.021 mm (31 to 50%)
- The average E_{FWD-K3} increased by about 110 to 240 MPa (6 to 12%) and the E_{FWD-K3} standard deviation decreased by about 157 to 205 MPa (25 to 33%)
- The average SCI decreased by about 0.006 to 0.015 mm (43 to 48%) and the SCI standard deviation decreased by about 0.016 to 0.042 mm (85 to 89%)
- The average BDI reduced by about 0.001 to 0.002 mm (4 to 11%) and the BDI standard deviation decreased by about 0.004 to 0.008 mm (50 to 62%)
- The average BCI reduced by about 0 to 0.001 mm (0 to 6%) and the BCI standard deviation decreased by about 0.003 to 0.007 mm (44 to 50%)
- The average area factor increased by about 30 mm (4%) and the area factor standard deviation decreased by about 103 mm (72%)
- The average I value reduced by about 0.011 mm (220%) and the I value standard deviation decreased by about 0.007 mm (58%)

The changes in the FWD measurements suggest that the foundation layer support conditions were improved after HDP stabilization as reflected through a considerable decrease in the average SCI (by 50 to 62%) and I value measurements (by 200%). Other measurements did not

show considerable differences between pre- and post-stabilization measurements. However, the post-treatment variability (as measured by standard deviation) was lower than pre-stabilization variability.

the

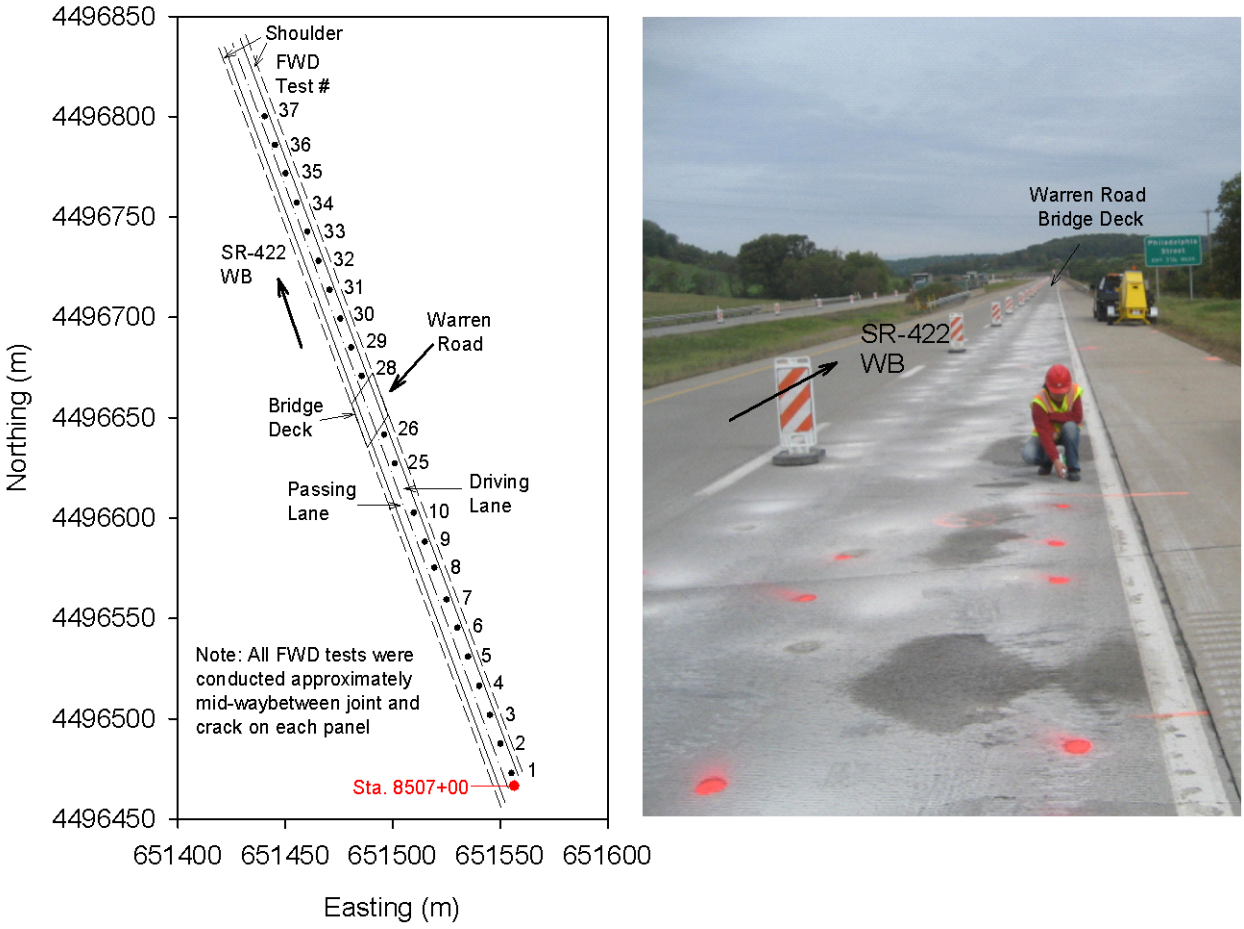

Figure 49. TS3/TS4: Plan layout of FWD test locations (left) and photograph of TS3/TS4 (right)

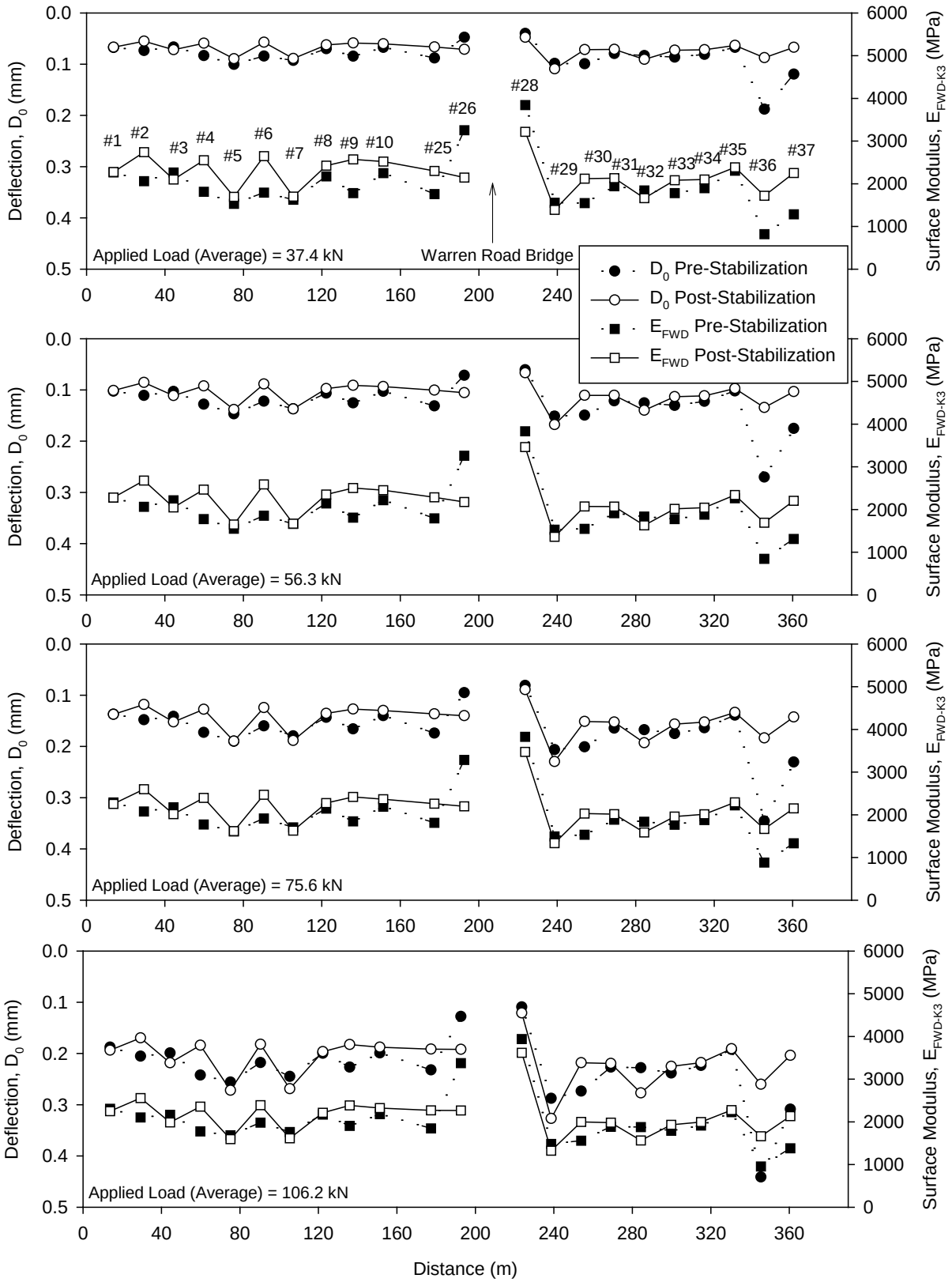

Figure 50. TS3/TS4: Pre- and post-stabilization E_{FWD-K3} and D_0 deflection measurements

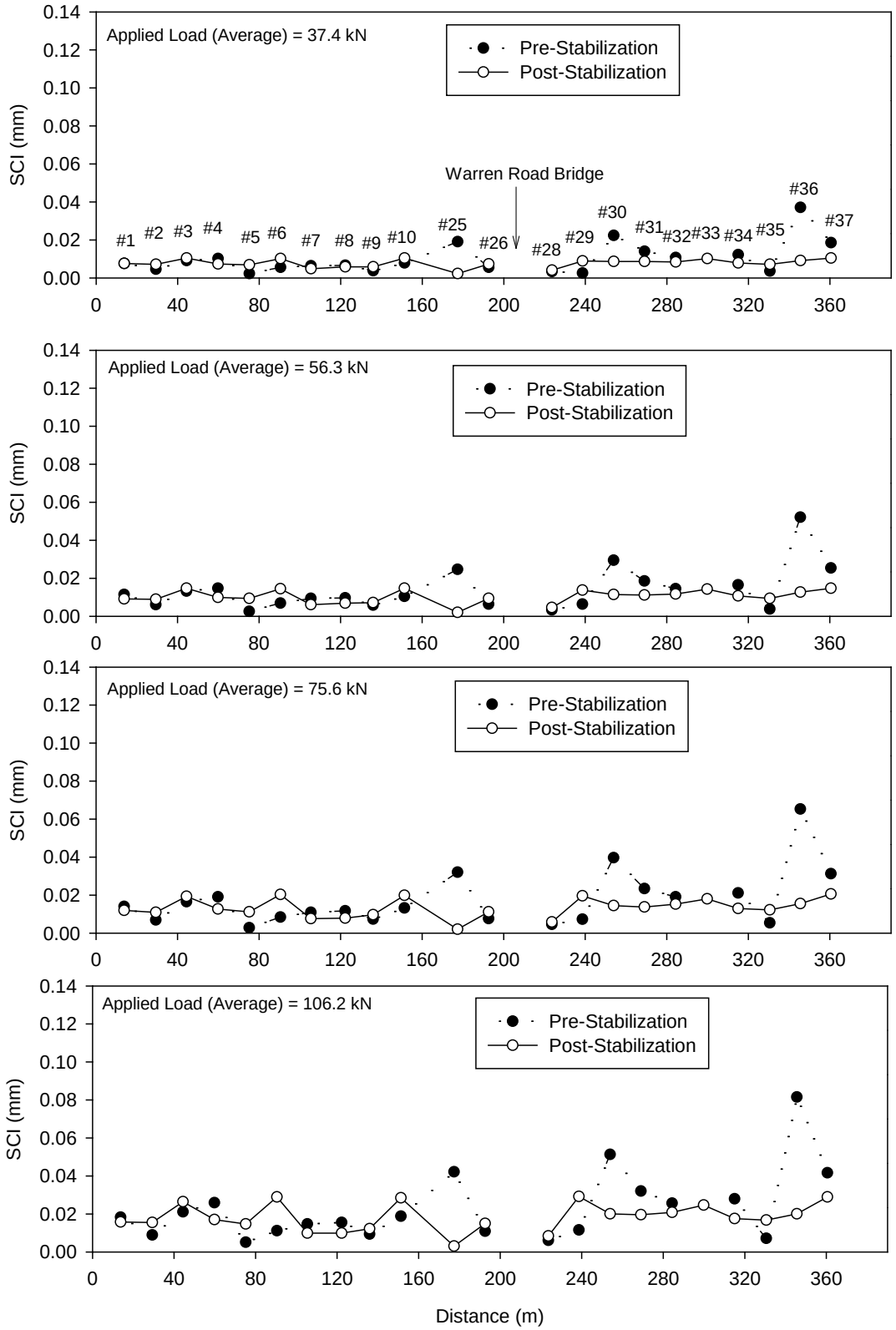

Figure 51. TS3/TS4: Pre- and post-stabilization SCI measurements

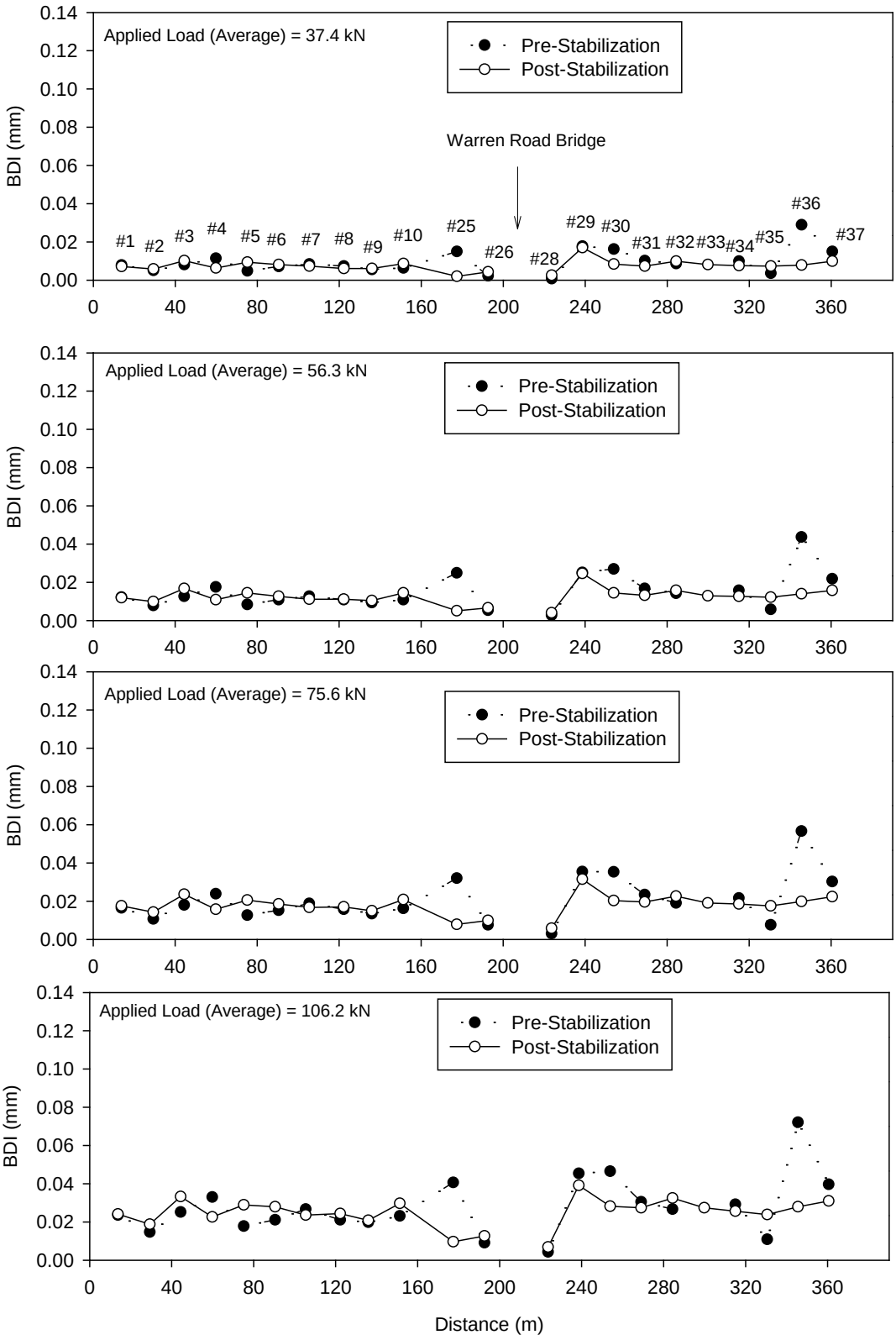

Figure 52. TS3/TS4: Pre- and post-stabilization BDI measurements

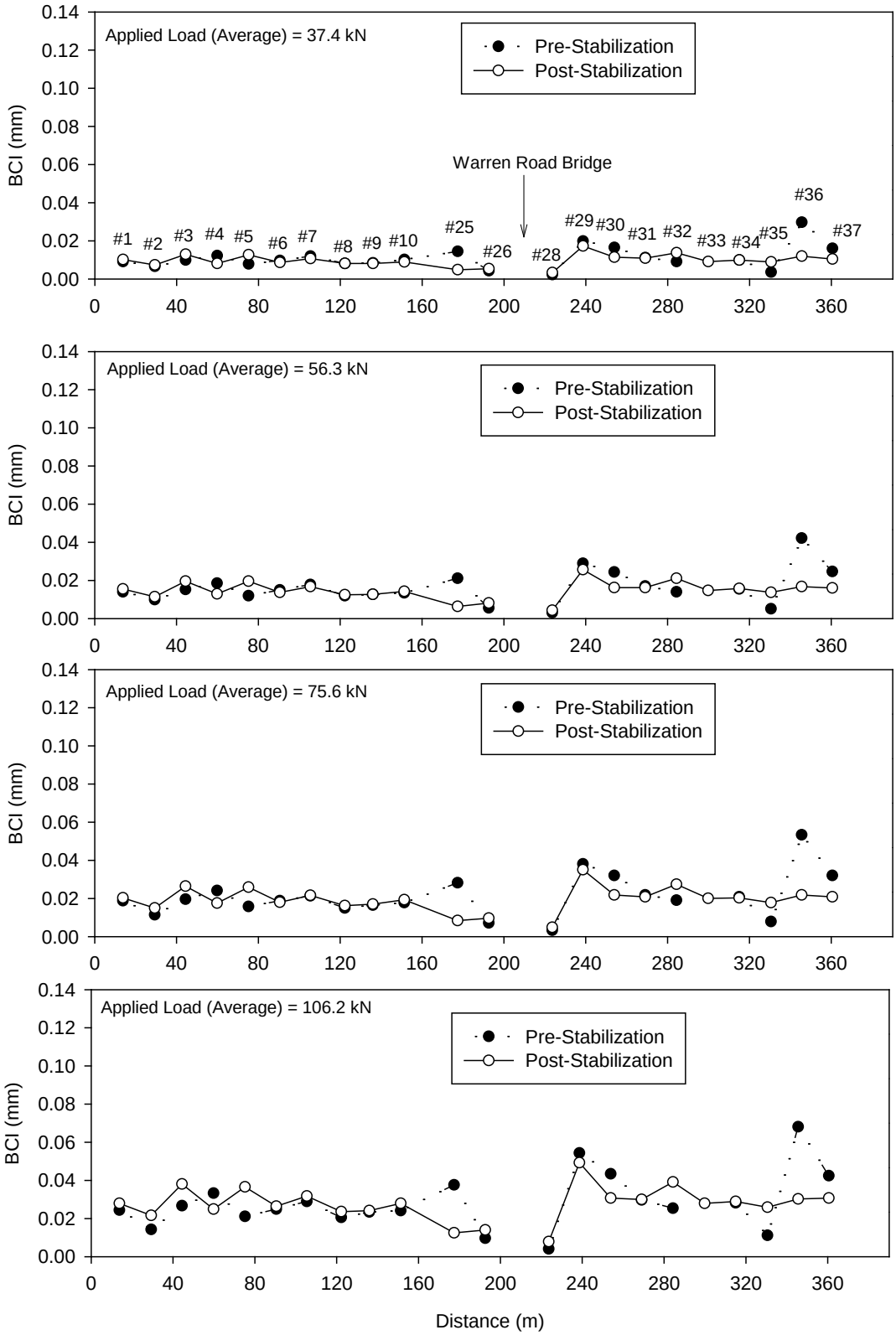

Figure 53. TS3/TS4: Pre- and post-stabilization BCI measurements

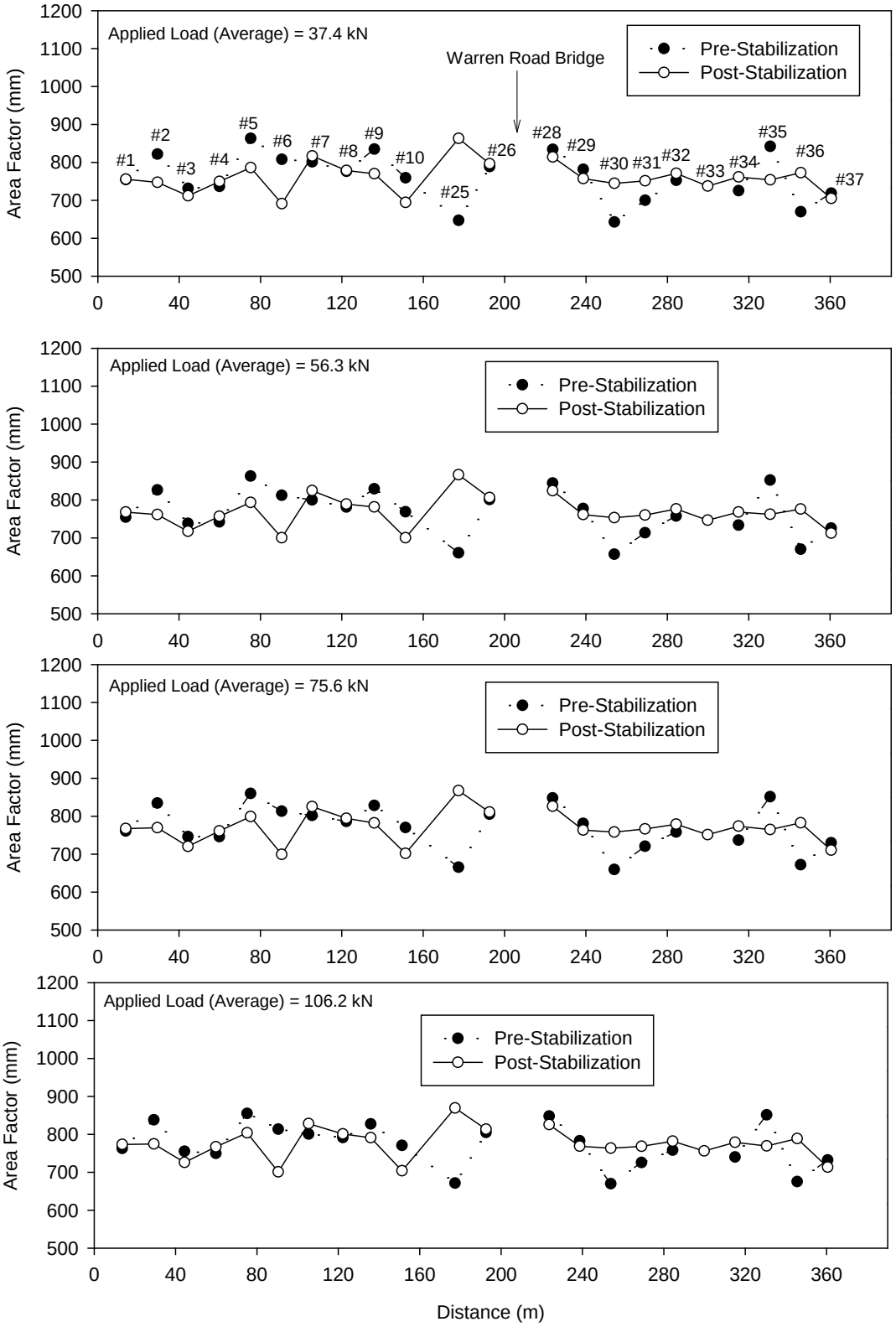

Figure 54. TS3/TS4: Pre- and post-stabilization FWD area factor measurements

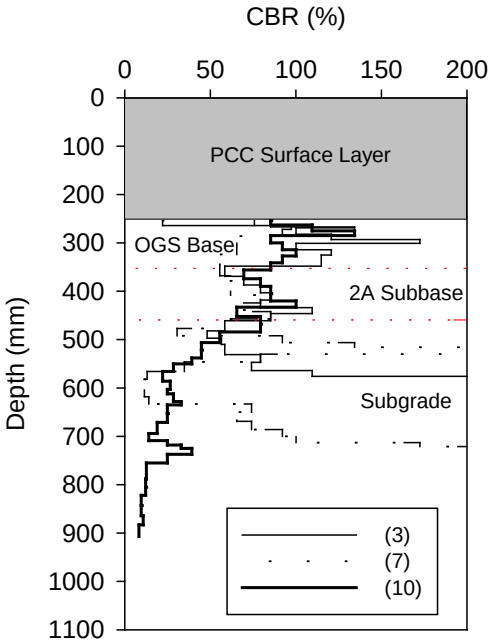

Figure 55. TS3-3, TS3-7 and TS3-10: Pre-stabilization DCP-CBR profiles

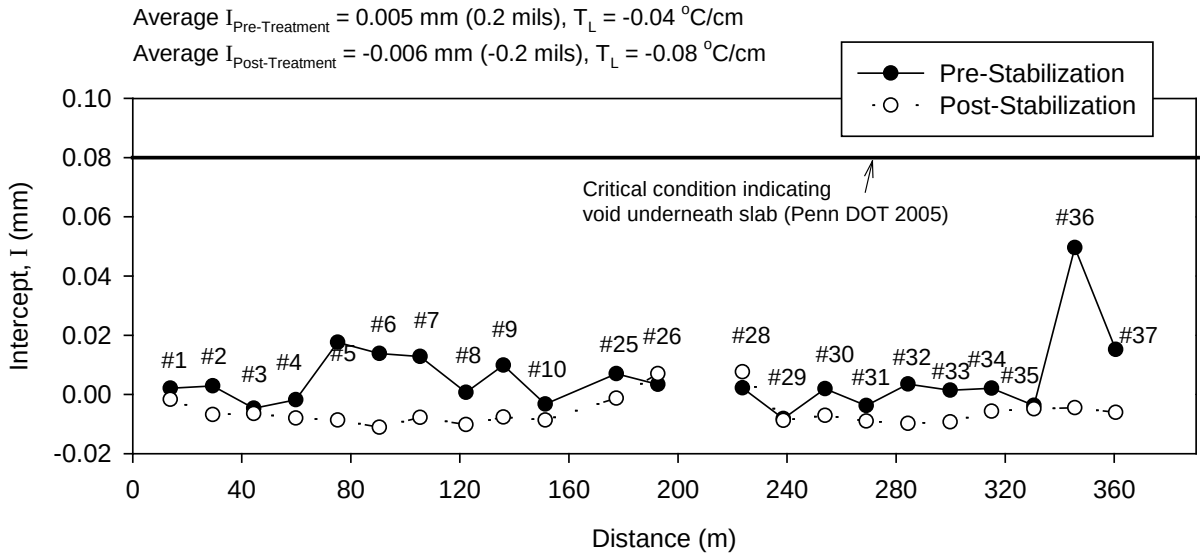

Figure 56. TS3/TS4: Pre- and post-stabilization FWD zero load intercept (I) measurements

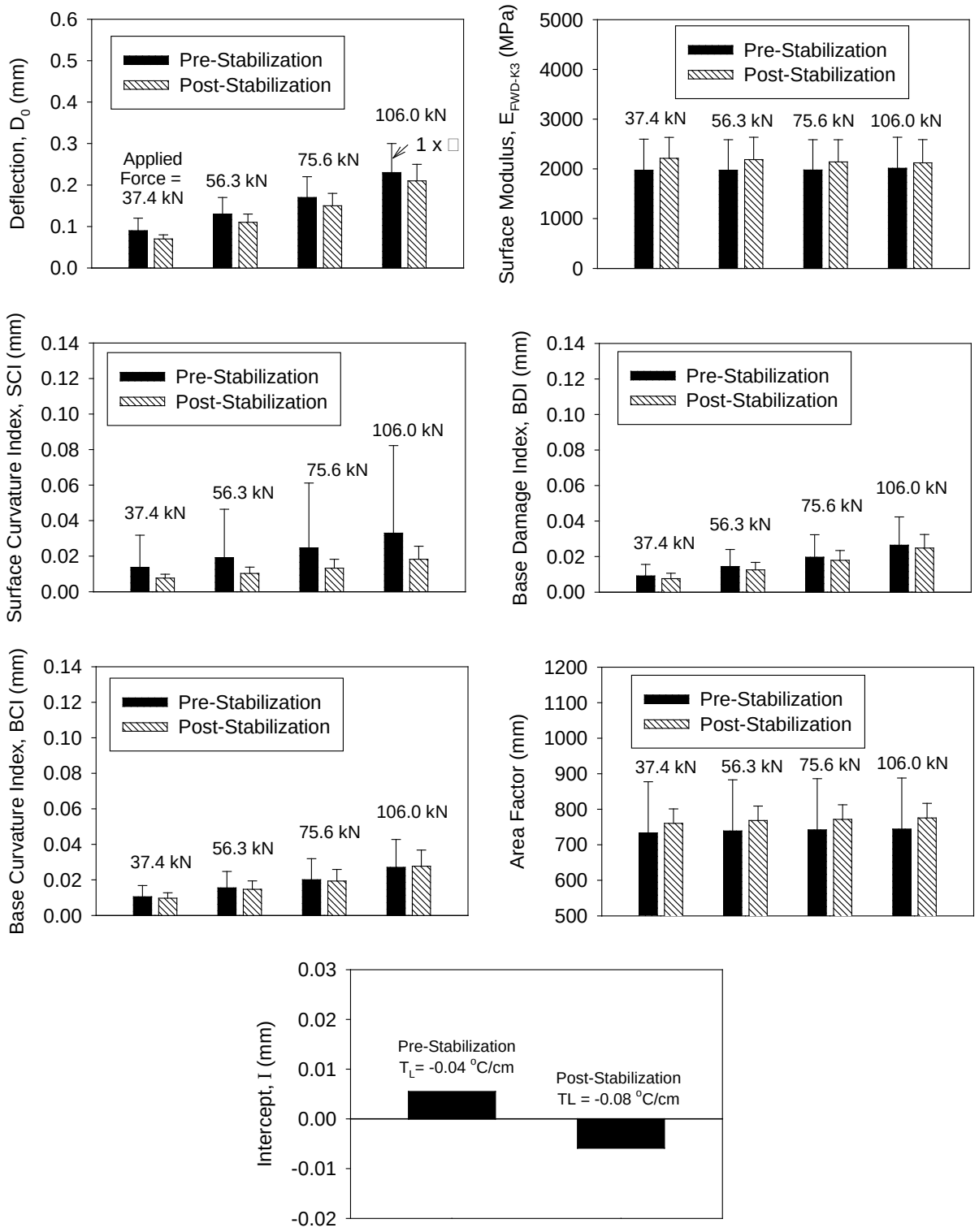

Figure 57. TS3/TS4: Pre- and post-stabilization D_0, E_{LWD-K3}, SCI, BDI, BCI, Area Factor, and I measurements with 1 x σ error bars

TS7: Effects of Initial and Secondary Foam Injection on FWD Measurements

TS7 consists of five pavement slabs located on the US 422 west bound driving (right) lane just east of the Pennsylvania Avenue Bridge. Initial HDP foam injection was performed on October 13, 2009. FWD test measurements (Figure 58) were obtained on the pavement surface before and after the initial injection. These tests were conducted along the lane center by placing the loading plate on both sides of joints and cracks and midway between cracks and joints. TS7 plan layout with locations of HDP foam injection points, pavement joint and crack locations, and fault measurements on each pavement slab are presented earlier in Figure 40.

To assess the effects of more than one HDP injection, two pavement slabs (slabs 2 and 3) as indicated in Figure 58. TS7: Photograph showing FWD testing along the center lane (Figure 58) were treated a second time (i.e., secondary injection) on November 3, 2009, by drilling new injection points. FWD tests were conducted after secondary injection on November 3, 2009. FWD measurements were obtained along the lane center and along the lane edge (close to the shoulder).

Summary statistics of D_0, I, and LTE along lane center and along lane edge near joints, cracks, and mid-panel are presented in Table 10. The t-test results are also provided in Table 10, comparing measurement values before and after initial stabilization and before and after secondary stabilization.

Figure 58. TS7: Photograph showing FWD testing along the center lane

Table 12. TS7: Summary statistics of FWD test measurements and t-test results

Time of Measurement	n	μ	σ	Observed t-value	Min. t-value (α = 0.05)	Statistically significant?
D_0 (μm) at Joints along Lane Center						
Before injection	10	96.0	15.3	—	—	—
After initial injection	14	76.8	32.4	1.731*	1.717	Yes
After secondary injection	8	76.1	17.0	0.056**	1.725	No
D_0 (μm) at Cracks along Lane Center						
Before injection	8	101.2	30.5	—	—	—
After initial injection	12	95.5	36.2	0.365*	1.734	No
After secondary injection	8	95.0	21.6	0.033**	1.734	No
D_0 (μm) at Mid-Panel along Lane Center						
Before injection	11	55.4	6.3	—	—	—
After initial injection	19	67.3	23.1	-1.662*	1.701	No
After secondary injection	12	107.4	66.2	-2.432**	1.699	Yes
I (μm) at Joints along Lane Center						
Before injection	10	3.9	5.7	—	—	—
After initial injection	14	-6.1	7.0	3.717*	1.717	Yes
After secondary injection	8	-12.7	4.0	2.419**	1.725	Yes
I (μm) at Cracks along Lane Center						
Before injection	8	3.3	8.4	—	—	—
After initial injection	12	-3.3	7.9	1.783*	1.734	Yes
After secondary injection	8	-13.3	10.0	2.481**	1.734	Yes
I (μm) at Mid-Panel along Lane Center						
Before injection	11	-3.4	2.0	—	—	—
After initial injection	19	-6.8	3.1	3.239*	1.701	Yes
After secondary injection	12	-1.1	9.4	-2.452**	1.699	Yes
LTE (%) at Joints along Lane Center						
Before injection	7	77.0	8.1	—	—	—
After initial injection	13	81.8	11.0	-1.010*	1.782	No
After secondary injection	8	78.2	5.8	0.845**	1.833	No
LTE (%) at Cracks along Lane Center						
Before injection	16	69.4	9.9	—	—	—
After initial injection	16	72.0	15.8	-4.529*	1.697	Yes
After secondary injection	14	77.6	13.5	0.984**	1.701	No
D_0 (μm) at Joints along Lane Edge						
After initial injection	4	114.5	14.5	—	—	—
After secondary injection	4	181.9	66.3	-1.984**	1.943	Yes
D_0 (μm) at Cracks along Lane Edge						
After initial injection	4	135.5	53.8	—	—	—
After secondary injection	4	270.3	53.1	-3.567**	1.943	Yes
I (μm) at Joints along Lane Edge						
After initial injection	4	0.0	3.6	—	—	—
After secondary injection	4	-12.9	15.5	1.628**	1.943	No

Time of Measurement	n	μ	σ	Observed t-value	Min. t-value (α = 0.05)	Statistically significant?
I (μm) at Cracks along Lane Edge						
After initial injection	4	-8.3	28.4	—	—	—
After secondary injection	4	11.5	30.9	-0.943**	1.943	No
LTE (%) at Joints along Lane Edge						
After initial injection	4	78.1	1.7	—	—	—
After secondary injection	4	78.0	9.2	0.024**	1.943	No
LTE (%) at Cracks along Lane Edge						
After initial injection	4	89.5	3.7	—	—	—
After secondary injection	4	78.8	24.6	0.862**	1.943	No

*t-value calculated when measurement values obtained before and after injection are compared
**t-value calculated when measurement values obtained after initial and secondary injection are compared.
Note: Negative observed t-values indicates higher values after stabilization while positive t-values indicate lower values after stabilization, compared to before stabilization.

Results indicated that the D_0 values near joints and cracks along the lane center showed a statistically significant decrease after the initial injection, but not after the secondary injection. A statistically significant decrease in D_0 values was observed after secondary injection near joints and cracks along the lane edge, however.

I-values showed statistically significant differences before and after initial and secondary injections, but were always less than the critical 0.0076 mm (7.6 μm). LTE values showed statistically significant improvement near cracks along the lane center after initial injection, but did not near joints. No statistically significant improvement was observed after secondary injection.

TS8: Performance Assessment of HDP Foam Injected Test Section

TS8 is located on the US 422 EB lanes just west of the Oakland Avenue intersection (Figure 59). The test section is about 220 m (720 ft) long and consists of passing and driving lanes in 35 pavement panels. All 35 panels in TS8 were injected with HDP foam on October 15, 2009. Nine selected panels were tested on driving and passing lanes as identified in Figure 59. Seven of those panels showed mid-panel cracks. After foam injection, two panels with cracks (#2 and #3) were repaired with full-depth patches, and five panels (#1, #4, #5, #6, and #8) were repaired with dowel bar retrofitting. Full-depth patch and dowel bar retrofitting work was done in June 2010. A picture of the test section is shown in Figure 60.

Field testing was conducted at joints and cracks, and at midway between cracks and joints before stabilization (on 10/13/2009). The same locations were tested seven days after foam stabilization (on 11/03/2009), about six months after foam stabilization (on 04/28/2010), and about nine months after foam stabilization (on 07/21/2010).

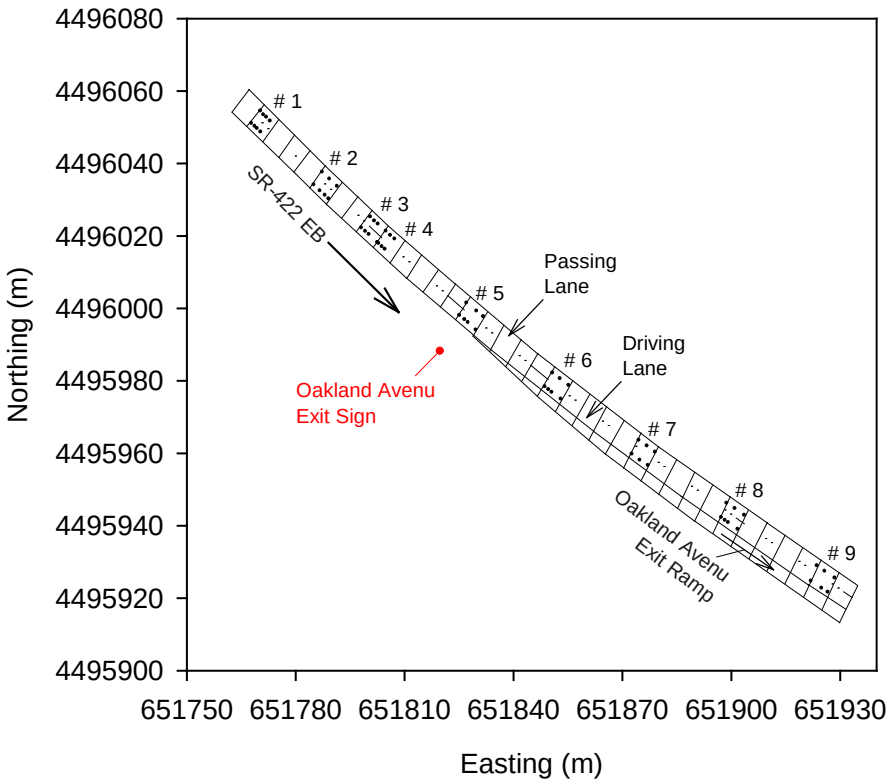

Figure 59. TS8: Plan view showing FWD test locations

Figure 60. TS8: Photograph showing test locations on driving and passing lanes

Bar charts of D_0 and I-values joints, cracks, and mid-panel from different testing times are presented in Figure 61(a) and Figure 61(b), respectively. Pavement surface temperatures and temperature gradient (TL) values for different testing dates are provided in Figure 61 (b). Bar charts of LTE values at joints and cracks from different testing times are presented in Figure 61 (c). Bar charts of $k_{dynamic}$ values at mid-panel from different testing times are presented in Figure 62. The FWD test results are summarized in Table 22, along with statistical t-test results. Positive t-values indicate that the measurements decreased after stabilization, while negative t-values indicate the opposite.

Statistical analysis of D_0 measurements indicated that improvement at joints and at mid-panel (i.e., a reduction in D_0) was not statistically significant after stabilization. However, the improvement at cracks was statistically significant after stabilization. The D_0 values decreased further during testing after 9 months, due to dowel bar retrofitting performed at 5 out of 7 crack locations and patching performed at 2 crack locations.

I-values at crack locations were higher than at joint or mid-panel locations before stabilization. These values decreased after stabilization with a statistically significant difference. However, the measurements at all locations and at all testing times were lower than the critical value (0.076 mm). Pavement temperatures shortly before and after stabilization and six months after stabilization indicated negative gradients (-0.02^{o}C/cm to -0.08oC/cm) in the panel, while at nine months after stabilization showed a positive gradient (+0.21^{o}C/cm). Based on data provided in Vandenbossche (2005), the influence of such small gradients on I-values is considered negligible.

LTE measurements at cracks showed statistically significant improvement after stabilization. On average, LTE at cracks increased from about 15% before stabilization to 45% shortly after stabilization and 86% after dowel bar retrofitting. LTE at joints did not show statistically significant improvement seven days after treatment, the values obtained 6 months and 9 months after stabilization showed statistically significant improvement. No statistically significant difference was noted in the $k_{dynamic}$ measurements obtained before and at all times after stabilization.

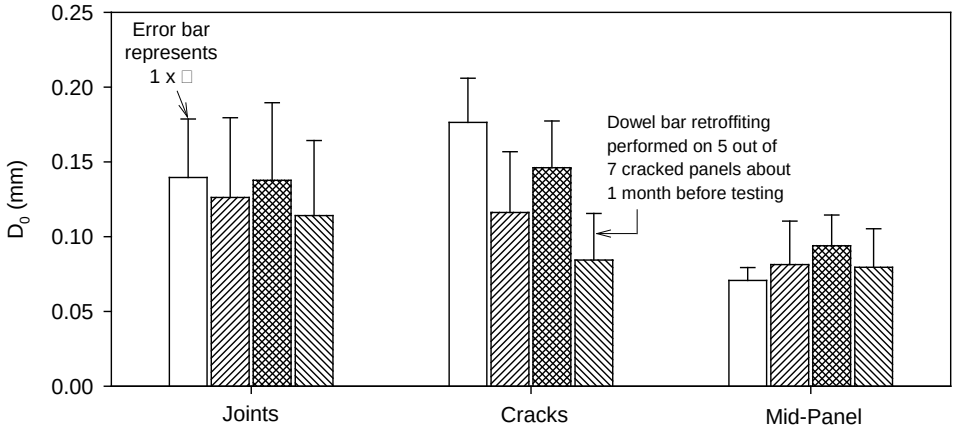

(a)

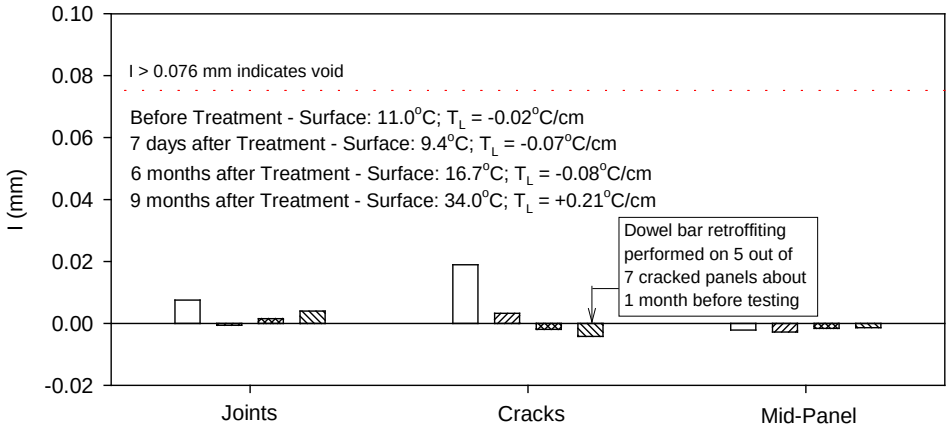

(b)

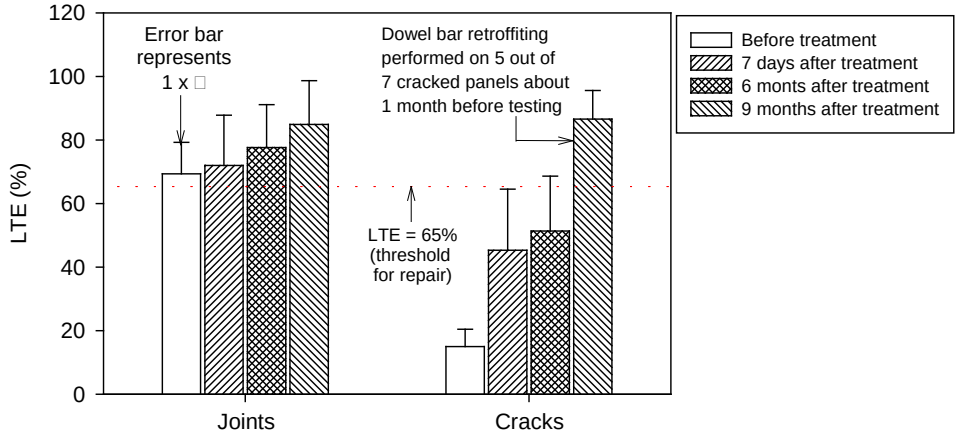

(c)

Figure 61. TS8: Results from FWD testing (at 40 kN applied load) shortly before and after stabilization, and 6 months and 9 months after stabilization: (a) D_0 values at joints, cracks, and mid-panel; (b) I-values at joints, cracks, and mid-panel; and (b) LTE values at joints and cracks.

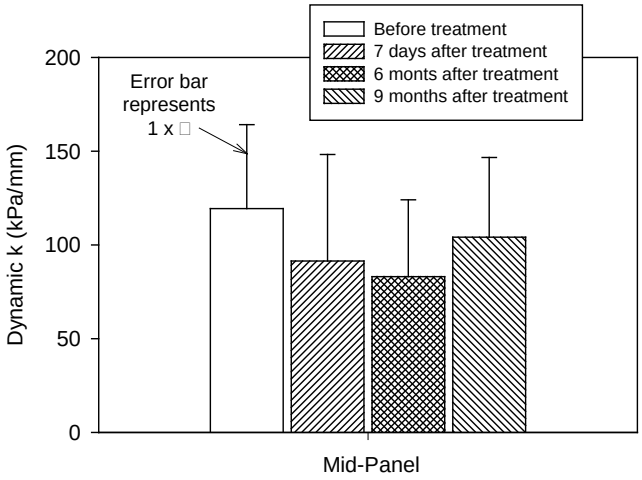

Figure 62. TS8: Results for $k_{dynamic}$ values from FWD testing (at 40 kN applied load) at mid-panel shortly before and after stabilization, and 6 months and 9 months after stabilization

Table 13. TS8: Summary statistics of FWD test measurements and results of t-tests

Time of Measurement	n	μ	σ	Observed t-value	Min. t-value (α = 0.05)	Statistically significant?
D_0 (mm) at Joints						
Before stabilization	16	0.140	0.039	—	—	—
7 days after stabilization	16	0.126	0.053	0.812	1.697	No
6 months after stabilization	14	0.138	0.052	0.121	1.701	No
9 months after stabilization*	16	0.114	0.050	1.564	1.697	No
D_0 (mm) at Cracks						
Before stabilization	7	0.176	0.030	—	—	—
7 days after stabilization	7	0.116	0.041	3.170	1.782	Yes
6 months after stabilization	5	0.146	0.031	1.578	1.812	No
9 months after stabilization*	7	0.084	0.031	3.077	1.782	Yes
D_0 (mm) at Mid-Panel						
Before stabilization	10	0.071	0.009	—	—	—
7 days after stabilization	10	0.081	0.029	-1.105	1.734	No
6 months after stabilization	8	0.094	0.021	-2.593	1.746	Yes
9 months after stabilization*	10	0.079	0.026	-1.020	1.734	No
I (mm) at Joints						
Before stabilization	16	0.008	0.018	—	—	—
7 days after stabilization	16	-0.001	0.013	1.485	1.697	No

Time of Measurement	n	μ	σ	Observed t-value	Min. t-value (α = 0.05)	Statistically significant?
6 months after stabilization	14	0.002	0.017	0.943	1.701	No
9 months after stabilization*	16	0.004	0.026	0.455	1.697	No
I (mm) at Cracks						
Before stabilization	7	0.019	0.013	—	—	—
7 days after stabilization	7	0.003	0.011	2.460	1.782	Yes
6 months after stabilization	6	-0.002	0.005	2.574	1.812	Yes
9 months after stabilization*	7	-0.004	0.005	2.852	1.782	Yes
I (mm) at Mid-Panel						
Before stabilization	10	-0.002	0.003	—	—	—
7 days after stabilization	10	-0.003	0.006	0.285	1.734	No
6 months after stabilization	8	-0.002	0.004	-0.350	1.746	No
9 months after stabilization*	10	-0.001	0.004	-0.503	1.734	No
LTE (%) at Joints						
Before stabilization	16	69.4	9.9	—	—	—
7 days after stabilization	16	72.0	15.8	-0.559	1.697	No
6 months after stabilization	14	77.6	13.5	-1.851	1.701	Yes
9 months after stabilization*	16	84.9	13.8	-3.094	1.697	Yes
LTE (%) at Cracks						
Before stabilization	7	15.0	5.5	—	—	—
7 days after stabilization	7	45.3	19.3	-4.005	1.782	Yes
6 months after stabilization	5	51.3	17.3	-2.848	1.812	Yes
9 months after stabilization*	6	85.6	9.5	-3.398	1.796	Yes
$k_{dynamic}$ *(kPa/mm) at Mid-Panel*						
Before stabilization	16	436.7	163.9	—	—	—
7 days after stabilization	16	334.4	207.9	1.181	1.730	No
6 months after stabilization	14	304.0	149.9	1.575	1.750	No
9 months after stabilization*	16	380.9	155.7	0.770	1.730	No

*About 1 month after dowel-bar retrofitting at 5 out of 7 crack locations and patching at 2 crack locations. Note: Negative observed t-values indicates higher values after stabilization while positive t-values indicate lower values after stabilization, compared to before stabilization.

TS9: Temperature Monitoring in Stabilized and Unstabilized Sections

The pavement base, subbase, and subgrade layers were instrumented with temperature sensors (I-buttons) down to a depth of about 1.5 m beneath the pavement surface. This main purpose of this monitoring was to investigate any insulation effects of foam stabilization that had been presumed in previous investigations (e.g., Oplan and Barnhart 1995). I-buttons were installed at two locations on the project: a control section (referred to as control) where no stabilization was performed; an HDP foam stabilized section (referred to as foam); and a cementitious grout treated section (referred to as grout).

I-button temperature measurements that were obtained every two hours from October 14, 2009 to April 28, 2010 are shown in Figure 63. Subsurface temperatures obtained in the first four months of 2010, at four ambient air temperatures ranging from 19ºC (-2ºF) to +28ºC (82ºF) yielded temperature profiles of the control and foam sections that do not show significant differences (Figure 64). Most of the I-buttons failed by April 29, 2010, so it was not possible to report changes in temperature profiles over the long term. Further, grout was injected on May 4, 2010, after the temperature sensors had failed, so no temperature profiles of the grout section are included here.

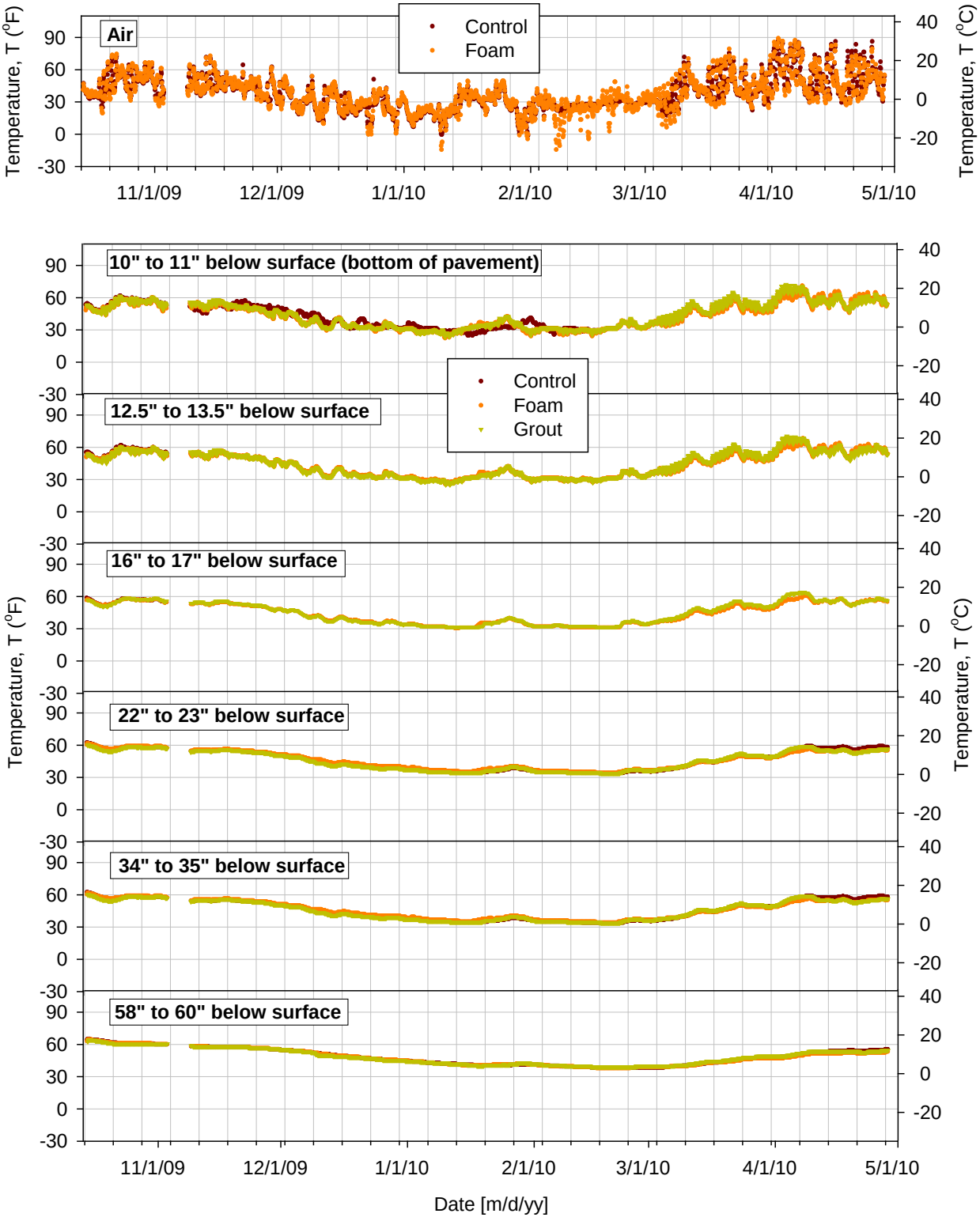

Figure 63. TS9: Temperatures in ambient air and at six depths below the pavement surface in control, foam, and grout sections

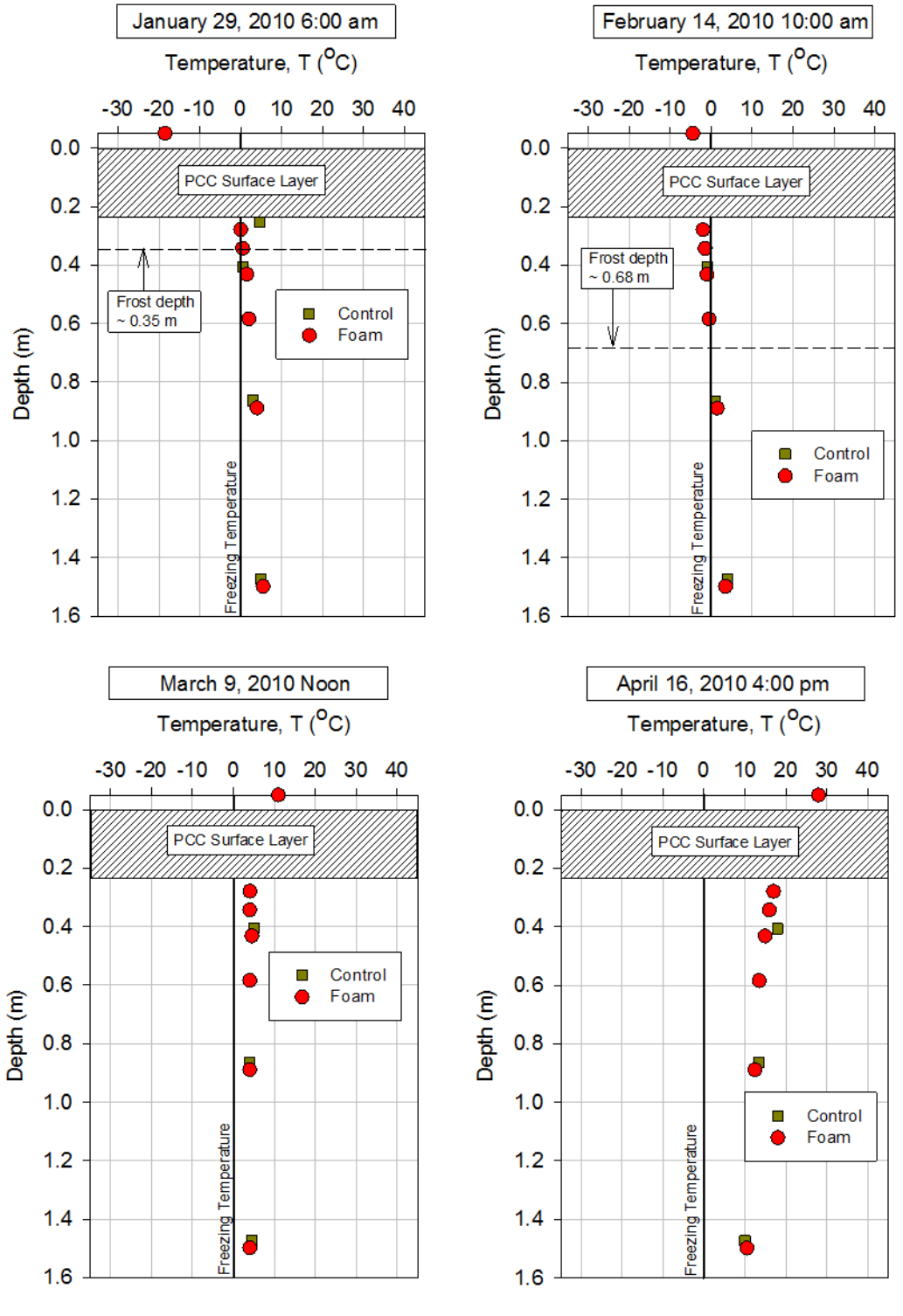

Figure 64. TS9: Temperature measurements with depth in control and foam sections during the freezing period (top two figures) and during the thawing period (bottom two figures)

CHAPTER 7. SUMMARY AND CONCLUSIONS

Laboratory Testing

- Particle size distribution curves of OGS materials indicate that 6 of the 11 samples collected were outside the specification limits for material passing the 38.1 mm (3/8 in.), No. 20, No. 40, No. 100, and No. 200 sieves. Percent fines content tests conducted on OGS materials indicated that 31 of the 41 samples contained percent fines content greater than the maximum 5% specification limit.
- Particle size distribution curves of 2A materials indicate that four of the 11 samples collected were outside the specification limits for material passing the 38.1 mm (3/8 in.), No. 4, and No. 100 sieves. Six of the 11 samples contained percent fines content greater than the maximum 10% specification limit.
- Compared to the OGS and OGS+Foam samples, the foam sample produced much higher permanent strain (ε_p), produced much lower M_r, and underwent much higher elastic deformation. The OGS+Foam sample showed a lower (about 0.75 times on average) M_r value than the OGS sample. However, it should be noted that the OGS sample had considerably higher γ_d than the OGS+Foam sample (OGS γ_d = 18.54 kN/m^3, OGS+Foam γ_d = 14.92 kN/m^3).
- The UU stress-strain curve for the foam sample showed a near linear increase in deviator stress up to 6% axial strain. The OGS+Foam sample resulted in about 3.4 time higher shear strength at failure than the OGS sample.

Penn DOT's IRI Testing History (2005 to 2014)

- The results from annual IRI testing from 2005 to 2010 indicate that the pavement sections were mostly within "fair" to "good" rating range. On average, the IRI increased slightly from 2005 (1.6 m/km or 99 in./mile) to 2009 (1.7 m/km or 106 in./mile).
- In 2010, after HDP foam stabilization and dowel bar retrofitting, the average IRI further increased to about 1.9 m/km (122 in./mile), which suggest poor ability to control variations in the pavement surface elevation to minimize IRI. On average, the IRI measurements remained at about 1.9 m/km in 2014.

In Situ Testing in Patching Areas with and without HDP Foam Stabilization

- Field observations indicate that the foam did not fully penetrate the full width and depth of the OGS layer, thus creating non-uniform support conditions.
- $E_{LWD\text{-}Z2}$ and K_{sat} values are higher at test locations with untreated subbase than at locations with OGS+Foam mixture. The average $E_{LWD\text{-}Z2}$ was about two times greater and the average K_{sat} was about two orders of magnitude greater at locations with untreated subbase than at locations with OGS+Foam mixture. Further, the average DCP-CBR_{OGS} value was higher at locations with OGS+Foam mixture than at locations with untreated subbase. Two of the three DCP tests (on the OGS+Foam material indicated refusal near the surface (with < 1 mm per blow penetration). The K_{sat} contour maps

highlighted the spatially concentrated low permeability zones in areas with OGS+Foam material.

- Low permeability of the OGS+Foam material was expected as the foam has a closed cell structure and is virtually impermeable. Low modulus but high shear strength (i.e., DCP-CBROGS) in the OGS+Foam mixture is an important determination in terms of selecting pavement design input values for this material. The field results are confirmed by resilient modulus laboratory test results =, which showed that the OGS+Foam sample had a 3.4 times higher undrained shear strength and 1.5 times lower resilient modulus, when compared to an unstabilized OGS sample.

Pavement Surface Elevation Monitoring in HDP Foam Treated Sections

- Pavement surface elevation monitoring on one test section (TS6) indicated that the panels were raised by an average of about 6 mm during the injection process. The upward movement in all panels was greater than the 1.3 mm maximum limit per the project specification. However, this process minimized the faulting at the cracks.
- Results on another test section (TS7) indicated that the pavement slabs were raised by an average of about 13 mm with a standard deviation of about 8 mm across the test section after initial injection, and by about 21 mm with a standard deviation of about 8 mm across slabs 2 and 3 after secondary injection. Similar to the results in TS6, the upward movement measured at all locations was greater than the 1.3 mm maximum limit per the project specification.

Comparison between Cementitious Grout and HDP Foam Stabilization Sections

- LTE showed statistically significant improvement near cracks and joints in both cementitious grout and HDP foam stabilized sections. LTE measurements at cracks, although improved after HDP stabilization, did not meet the targeted criteria (> 65%) until after dowel bar retrofitting.
- D_0 and I values showed statistically significant improvement only near cracks (and not near joints) in the HDP foam section and only near joints (and not near cracks) in the cementitious grout section.
- No statistically significant improvement was determined in any of the FWD measurements obtained at the mid-panel, for both stabilization methods.
- Faulting reduced by about 2.5 mm near cracks and by about 4.6 mm near shoulder after HDP foam injection. On cementitious grout section, faulting was reduced on average by about 0.5 mm near cracks and by about 2.2 mm near shoulder. These measurements indicate that slab movements were sometimes greater than the allowable 1.3 mm (per project specifications) and better process control measures are needed to control vertical movements, particularly with the HDP stabilization method.

Long-Term Performance of HDP Foam Stabilization Sections

- Statistical analysis of D_0 measurements indicated that improvement at joints and at mid-panel (i.e., a reduction in D_0) was not statistically significant after stabilization. However, the improvement at cracks was statistically significant after stabilization. The D_0 values decreased further during testing after 9 months, due to dowel bar retrofitting performed at 5 out of 7 crack locations and patching performed at 2 crack locations.
- I-values at crack locations were higher than at joint or mid-panel locations before stabilization. These values decreased after stabilization with a statistically significant difference. However, the measurements at all locations and at all testing times were lower than the critical value (0.076 mm).
- LTE measurements at cracks showed statistically significant improvement after stabilization. LTE at joints, however, did not show any statistically significant improvement. But, the values obtained 6 months and 9 months after stabilization showed statistically significant improvement.
- No statistically significant difference was noted in the $k_{dynamic}$ measurements obtained before and at all times after stabilization.

Recommendations for Future Work

The findings of this paper improve the understanding of the benefits and limitations of using injected foam technology to rehabilitate concrete pavements. Additional field studies that characterize the long-term durability of foam treated materials and life-cycle cost analysis of the rehabilitation method are needed to fully evaluate the use of this technology. Based on the lack of control for setting the final panel elevation, improved control systems may be needed to garner the full potential of injected foam technology.

REFERENCES

AASHTO. (1999). “Standard method of test for determining resilient modulus of soils and aggregate materials.” AASHTO T-307, American Association of State Highway and Transportation Officials, Washington, D.C.

AASHTO. (1993). *AASHTO design guide for design of pavement structures*. American Association of State Highway and Transportation Officials, Washington D.C.

Abu al-Eis, K., and LaBarca, I. (2007). “Evaluation of the URETEK method of pavement lifting.” Wisconsin Department of Transportation. Madison, Wisconsin.

ACPA. (1994). “Slab stabilization guidelines for concrete pavements.” Technical Bulletin TB018P. American Concrete Pavement Association, Skokie, IL.

ALDOT. (2012a). “Section 452–Slabjacking of portland cement concrete pavement.” Standard Specifications for Highway Construction. Alabama Department of Transportation, Montgomery, AL.

ALDOT. (2012b). “Section 453–Pressure grouting and repair of portland cement concrete pavement.” Standard Specifications for Highway Construction. Alabama Department of Transportation, Montgomery, AL.

ASTM D4694-09 (2009). “Standard test method for deflections with a falling-weight-type impulse load device.” American Standards for Testing Methods (ASTM), West Conshohocken, PA.

Andrei, D., M. W. Witczak, C. W. Schwartz, and J. Uzan. (2004). “Harmonized resilient modulus test method for unbound pavement materials.” *Transportation Research Record No. 1874*. Transportation Research Board, Washington, D. C., 29-37.

ASTM C117-04. (2010). “Standard test method for materials finer than 75μm (No. 200) sieve in mineral aggregates by washing.” American Standards for Testing Methods (ASTM), West Conshohocken, PA.

ASTM C136-06. (2010). “Standard test method for sieve analysis of fine and coarse aggregates.” American Standards for Testing Methods (ASTM), West Conshohocken, PA.

ASTM D2487-10. (2010). “Standard test method for classification of soil for engineering purposes (unified soil classification system).” American Standards for Testing Methods (ASTM), West Conshohocken, PA.

ASTM D3282-09. (2010). “Standard test method for classification of soils and soil-aggregate mixtures for highway construction purposes.” American Standards for Testing Methods (ASTM), West Conshohocken, PA.

ASTM D6951-03. (2010). “Standard test method for use of the dynamic cone penetrometer in shallow pavement applications.” American Standards for Testing Methods (ASTM), West Conshohocken, PA.

ASTM D6938-10. “Standard test method for in-place density and water content of soil and soil-aggregate by nuclear methods (shallow depth).” American Standards for Testing Methods (ASTM), West Conshohocken, PA.

Barron, B. (2004). “50-50 Change: Kansas DOT decides to go with polyurethane to correct 50 miles of Highway 50.” *Road and Bridges*, 42(12), 24–26.

Beckemeyer, C. A., Khazanovich, L., and Yu, H. T. (2002). “Determining amount of built-in curling in jointed plain concrete pavement.” *Transportation Research Record No. 1089*, Transportation Research Board, Washington, D.C., 85–92.

Brewer, W. B., Hayes, C. J., and Sawyer, S. (1994). "Uretek construction report." Report No. OK 94(03), Oklahoma Department of Transportation, Oklahoma City, OK, June.
Caltrans. (2010a). "Section 41-2–Pavement subsealing." Standard Specifications. California Department of Transportation, Sacramento, CA.
Caltrans (2010b). "Section 41-3–Pavement jacking." Standard Specifications. California Department of Transportation, Sacramento, CA.
Chen, D. H., and Scullion, T. (2007). "Using nondestructive testing technologies to assist in selecting the optimal pavement rehabilitation strategy." *Journal of Testing and Evaluation*, 35(2), 211–219.
Chen, D-H., and Won, M. (2008). "Field performance monitoring of repair treatments on jointed concrete pavements." *Journal of Testing and Evaluation*, 36(2), 119–127.
Chen, D-H., Won, M., and Hong, F. (2009). "Investigation of settlement of a jointed concrete pavement." *Journal of Performance of Constructed Facilities*, 23(6), 440–446.
Crawley, A. B., Albritton, G. E., and Gatlin, G. R. (1996). "Evaluation of the Uretek method for pavement undersealing and faulting correction." FHWA/MS-DOT-RD-96-113, Interim Report, Mississippi Department of Transportation, Jackson, MS.
Del Val, J. (1981). "Pressure grouting of concrete pavements." *Transportation Research Record: Journal of the Transportation Research Board*, 800, 38-40.
FHWA (2005). "Concrete pavement rehabilitation and preservation treatments." Tech Brief. Federal Highway Administration, Washington, D.C.
Gaspard, K., and Morvant, M. (2004). "Assessment of the Uretek process on continuously reinforced concrete pavement, jointed concrete pavement, and bridge approach slabs." LTRC Project No. 05-1 TA, Louisiana Department of Transportation and Development, Louisiana Transportation Research Center, Baton Rouge, LA.
Gaspard, K., and Zhang, Z. (2010). "Mitigating transverse joint faulting in jointed concrete pavement with polyurethane foam." *Transportation Research Record: Journal of the Transportation Research Board*, 2010, 3-11.
Horak, E. (1987). "Aspects of deflection basin parameters used in a mechanistic rehabilitation design procedure for flexible pavements in South Africa." University of Pretoria, South Africa.
Iowa DOT (2012). "Section 2539–Concrete pavement undersealing by pressure grouting." Standard Specifications for Highway and Bridge Construction. Iowa Department of Transportation, Ames, IA.
Janssen, D. J., and Snyder, M. B. (2000). "Temperature-moment concept for evaluating pavement temperature data." *Journal of Infrastructure Systems*, 6(2), 81–83.
Kilareski, W. P., and Anani, B. A. (1982). "Evaluation of in situ moduli and pavement life from deflection basins." *Presented at the 5th International Conference of Asphalt Pavements*, University of Michigan, Ann Arbor, MI.
KDOT. (2015). "Section 834–Undersealing." Standard Specifications for State Road & Bridge Construction. Kansas Department of Transportation, Topeka, KS.
Louisiana DOTD. (2006). "Section 602.14–Undersealing or slabjacking pavement." Standard Specifications for Roads and Bridges. Louisiana Department of Transportation and Development, Baton Rouge, LA.
MoDOT. (2009a). "Section 625.10–Slab undersealing." General Provisions and Supplemental Specifications to 2004 Missouri Standard Specifications for Highway Construction. Missouri Department of Transportation, Jefferson City, MO.

MoDOT. (2009b). “Section 625.20–Slab jacking.” General Provisions and Supplemental Specifications to 2004 Missouri Standard Specifications for Highway Construction. Missouri Department of Transportation, Jefferson City, MO.
NCDOT. (2008). “HDPF (High Density Polyurethane Foam) processes–General and slab leveling, undersealing and voidfilling.” Contract Proposal–Small Business Enterprise. North Carolina Department of Transportation, Greenville, NC.
Ni, J., and Cheng, W. (2011). “Quality control for grouting under rigid pavement.” *Proc., GeoHunan*, ASCE, 183-191.
NJDOT (2007a). “Section 451–Concrete slab stabilization.” Standard Specifications for Road and Bridge Construction, New Jersey Department of Transportation, Trenton, NJ.
NJDOT (2007b). “Section 903.08.03–Grout for undersealing of concrete pavement.” Standard Specifications for Road and Bridge Construction, New Jersey Department of Transportation, Trenton, NJ.
Ohio DOT. (2007). “Section 842–Correcting elevation of concrete approach slabs with high density polyurethane.” Supplemental Specifications, Ohio Department of Transportation, Columbus, OH.
OKDOT. (2009). “Section 426–Pressure grouting pavement.” Standard Specifications Book. Oklahoma Department of Transportation, Oklahoma City, OK.
Opland, W. H., and Barnhart, V. T. (1995). “Evaluation of the URETEK method for pavement undersealing.” Research Report, No. R-1340. Michigan Department of Transportation.
Ott, R. L., and Longnecker, M. (2001). *An introduction to statistical methods and data analysis*, Published by Duxbury, Thomson Learning Resource Center, Pacific Grove, CA.
Penn DOT. (2005). “Falling weight deflectometer.” Roadway Inventory and Testing Section. Commonwealth of Pennsylvania Department of Transportation, Harrisburg, PA. < www.dot.state.pa.us/Internet/Bureaus/pdBOMO.nsf/infoRMRIFWD> (Date Accessed: May 4, 2015).
Penn DOT. (2010). “Section ITEM 9000-0001–Slab stabilization.” Supplemental Specifications. Pennsylvania Department of Transportation, Harrisburg, PA.
Penn DOT. (2011). “Section 679–Slab stabilization.” Specifications. Pennsylvania Department of Transportation, Harrisburg, PA.
Penn DOT. (2015). High Speed Profiler. < http://www.dot.state.pa.us/Internet/Bureaus/pdBOMO.nsf/infoRMRIPROFILE > (Date accessed August 7, 2015).
Priddy, L. P., Jersey, S. R., and Reese, C. M. (2010). “Full-scale field testing for injected foam stabilization of portland cement concrete repairs.” *Transportation Research Record: Journal of the Transportation Research Board*, 2155, 24-33.
Priddy, L. P., and Newman, J. K. (2010). “Full-scale field testing for verification of mechanical properties of polyurethane foams for use as backfill in PCC repairs.” *Journal of Materials in Civil Engineering*, 22(3), 245-252.
Schmalzer, P. N. (2006). “LTPP Manual for Falling Weight Deflectometer Measurements – Version 4.1.” Report No. FHWA-HRT-06-132, Federal Highway Administration, McLean, VA.
SDDOT (2004a). “Section 391–Undersealing.” Standard Specifications for Roads & Bridges. South Dakota Department of Transportation, Pierre, SD.
SDDOT (2004b). “Section 392–Pavement jacking.” Standard Specifications for Roads & Bridges. South Dakota Department of Transportation, Pierre, SD.

Substad, R. N. (2002). “LTPP data analysis: Feasibility of using FWD deflection data to characterize pavement construction quality.” *NCHRP Web Document 52*, Project No. 20-50(9), National Cooperative Highway Research Program, Transportation Research Board of the National Academies, Washington, D.C.

Taha, R., Selim, A., Schaefer, V., Carlson, K., and Hasan, S. (1994). "Evaluation of undersealing of undoweled plain jointed PCC pavements in South Dakota." Final Report, South Dakota Department of Transportation. Pierre, SD.

Tayabji, S. D., Brown, J. L., Mack, J. W., Hearne, T. M., Anderson, J., Murrell, S., and Noureldin, A. S. (2000). “Pavement Rehabilitation.” *TRB Millennium Paper Series*, Washington, D.C.

Trimble Navigation Ltd. (2013). Trimble S3 Total Station Datasheet. Retrieved December 12, 2013, < http://trl.trimble.com/docushare/dsweb/Get/Document-469042/022543-492A_TrimbleS3_DS_0110_sec.pdf > (Date accessed 8/6/2015).

UDOT. (2012). "Section 02755–Concrete Slab Jacking." Standard Specifications for Road and Bridge Construction. Utah Department of Transportation, Salt Lake City, UT. Tartabini, S. (2008). “Urethane foam in highway construction and maintenance.” *Presented at the 84th Annual Northeast States Materials Engineers Association (NESMEA) Conference*, October 7-8, Atlantic City, NJ.
< www.nesmea.uconn.edu/pdf/nesmea08_Tartabini.pdf.pdf > (Data Accessed: June 20, 2010)

Vennapusa, P., and White, D. J. (2009). “Comparison of light weight deflectometer measurements for pavement foundation materials.” *Geotechnical Testing Journal*, 32(3), 239–251.

Vandenbossche, J. M. (2005). “Effects of slab temperature profiles on the use of falling weight deflectometer data to monitor joint performance and detect voids.” *Transportation Research Record*, 2005, Transportation Research Board, Washington, D.C., 75–85.

Witczak, M. W., and J. Uzan. (1988). “The universal airport design system–Report I of IV: Granular material characterization.” Department of Civil Engineering, University of Maryland, College Park. MD.

White, D., Vennapusa, P., and Zhao, L. (2014). “Verification and repeatability analysis of the in situ air permeameter test,” *Geotechnical Testing Journal*, 37(2), DOI: 10.1520/GTJ20130111.

White, D., Mekkawy, M., Sritharan, S., and Suleiman, M. (2007). “Underlying causes for settlement of bridge approach pavement systems,” *Journal of Performance of Constructed Facilities*, 21(4), 273–282.

Yu, L., Wang, R., and Skirrow, R. (2013). "The application of polyurethane grout in roadway settlements issues." GeoMontreal, Montreal, Canada.

Zorn, G. (2003). *Operating manual: Light drop-weight tester ZFG2000*, Zorn Stendal, Germany.

APPENDIX A: SLAB STABLIZATION (SECTION 679, PENNDOT 2011)

SECTION 679—SLAB STABILIZATION

679.1 DESCRIPTION—This work is the filling of voids beneath existing rigid base courses or pavements at locations as directed.

679.2 MATERIAL—

(a) Cement. Section 701

(b) Water. Section 720.1

(c) Admixtures. Section 711.3
A multiphase wetting agent and an expansive agent may be used. Use an accelerator if required.

(d) Pozzolan. Section 724.2

(e) Rapid Set Concrete Patching Materials. Supplied by a manufacturer listed in Bulletin 15. Use within the shelf life and temperature limitations set by the manufacturer.

(f) Mix Design. Submit a mix design to the District Executive for review and acceptance before starting work. Include with the submittal: independent laboratory testing showing 1, 3, and 7-day compressive strengths; flowability; shrinkage and expansion results; and the time of initial set. Proportion the mix as follows:

One part cement (by volume)
Three parts pozzolan (by volume)
Admixtures—if required and accepted
Water—an amount such that the time of efflux is within 10 seconds to 15 seconds (ASTM C 939)

Furnish mix with an expansion of 0% to 10% (ASTM C 940), an initial setting time of 1 hour to 6 hours (AASHTO T 131) and bleeds no more than 2.5% of the volume (ASTM C 940).

A 7-day compressive strength of 4.8 MPa (700 pounds per square inch) minimum is required, based on the average of five test cylinders (PTM No. 521).

Submit a new mix design if the source of any material is changed.

679.3 CONSTRUCTION—

(a) General. Do begin this work until it is satisfactorily shown that qualified personnel, with successful experience, are available at the job.

Do not perform work if daytime temperatures are below 2 °C (35F) or if the subgrade and/or base course material is frozen.

(b) Deflection Testing. If no preliminary testing was performed, test each joint and crack as directed, and as follows:

Do not perform testing if air temperature exceeds 21 °C (70F). Do not test during spring thaw conditions or if subgrade is frozen.

Furnish and maintain four gauges capable of detecting slab movement to within 0.03 mm (0.001 inch). Use approved gauge mounts. Furnish and maintain a vehicle having a dual-tire single axle with an 80 kN (18,000-pound) single axle load. Verify by measuring the force of gravity upon a certified scale.

Position two gauges as shown on the Standard Drawings. Zero both gauges to the pavement surface with no force on the slab on both sides of the joint or crack.

Slowly move the test vehicle into position and stop when the test axle is in the position shown on the Standard Drawings for the loaded approach slab condition. Read both gauges and record the results.

Move the test vehicle slowly across the joint and stop it in the position shown on the Standard Drawings for the loaded leave slab condition. Read both gauges and record the results.

Repeat this procedure at every transverse joint and crack.

Stabilize all joints or cracks that have a loaded slab corner deflection of 0.5 mm (0.020 inch) or more, and a joint efficiency at 65%* or more.

Patch and stabilize all joints or cracks that have a loaded slab corner deflection of 0.5 mm (0.020 inch) or more, and a joint efficiency of less than 65%.

Joint efficiency (JE) is defined as follows:

$$JE = \frac{\text{Unloaded Slab Corner Deflection}}{\text{Loaded Slab Corner Deflection}} \times 100$$

* Use the highest Loaded Slab Corner Deflection and the lowest joint efficiency at each joint or crack.

(c) Equipment.

1. Grout Plant. Provide a satisfactory positive displacement cement injection pump and a satisfactory mixing machine, capable of operating at a minimum speed of 800 rpm and a maximum speed of 2000 rpm.

2. Water Tanker. Supply water from a water truck with adequate capacity and pressure for delivery to the grout machine.

3. Drill. Provide generator, core drill, and diamond-tip core barrels, or other satisfactory equipment capable of drilling the grout injection holes through the pavement and base material; and equipment in satisfactory condition and operated to produce holes that are smooth, vertical, and do not break out the bottom of the slab.

4. Vertical Movement Testing. Supply satisfactory equipment to measure slab lift, capable of detecting simultaneously the lift of the pavement edge, or of any two outside slab corners adjacent to a joint and the adjoining shoulder. Use equipment with a capability of making these measurements to within 0.03 mm (0.001 inch).

5. Miscellaneous. Provide necessary hoses, valving, and valve manifolds with positive cutoff and bypass provisions to control pressure and volume, pressure gauges with gauge protectors, expanding packers or hose for positive seal during grout injection, hole washing tools, drill steel, bits, and any other miscellaneous tools required.

(d) Procedure.

1. Drilling Holes. Drill grout injection holes in the pattern shown on the Standard Drawings, or as directed. Drill holes not larger than 38 mm (1 1/2 inches) in diameter, vertical and round, and to a depth sufficient to penetrate any stabilized base.

2. Mixing. Accurately measure the dry materials by mass, if in bulk, or provide them packaged in uniform volume sacks. Batch with water through a meter or scale that totals the day's consumption.

Do not hold mixed material in the mixer or injection pump sump for more than one hour after mixing. Dispose of material held for longer times.

Make flowability measurements at least two times during each work shift.

3. Void Filling. During the filling operation, use a positive means of monitoring lift as specified in Section 679.3(c)4. Upward movement of the pavement greater than 1.3 mm (0.05 inch) will not be allowed. Lower an expanding rubber packer or hose, connected to the discharge from the pump, into the hole. Do not extend the discharge end of the packer or hose below the lower surface of the concrete pavement. Pump each hole until maximum pressure is built up or material is observed flowing from hole to hole. Do not exceed a maximum pressure of 1.4 MPa (200 pounds per square inch), unless otherwise directed. Monitor the pressure in the grout line. Protect the gauge from the grout slurry. Allow the water, displaced from the void structure by the grout, to flow out freely. Excessive loss of the grout through the cracks, joints, or from back pressure in the hose or in the shoulder area will not be allowed.

4. Correcting Panel Displacement. Grind pavement, raised in excess of the 1.3 mm (0.05-inch) allowable tolerance, to the correct grade. Grind as specified in Section 514.3, except grind into the high slab.

5. Radial Cracks. Radial cracks spreading outward from the grout injection holes indicate poor quality or improper methods. Stop work until the cause is determined and corrected.

6. Transverse Cracks. If transverse cracks develop between adjacent grout injection holes, replace the entire slab at no cost to the Department.

7. Hole Patching. Upon completion of the work, patch drill holes full depth with a rapid set, non-shrink concrete patching material. Strike patches flush with the surface of the surrounding pavement.

(e) Retesting. Twenty-four hours after grouting and before acceptance, retest each stabilized joint or crack as specified in Section 679.3(b). Regrout slabs that deflect 0.5 mm (0.020 inch) or more and retest. The Representative may accept any slab that continues to show movement, in excess of that specified, after two properly performed groutings; or direct the removal and replacement, with a full depth concrete patch, as specified in Section 516 and paid for separately.

(f) Opening to Traffic. Do not open to traffic for a minimum of 12 hours after grouting operations have been completed.

679.4 MEASUREMENT AND PAYMENT—

(a) Deflection Test. Each

(b) Holes Drilled. Each
The price includes patching of the hole.

(c) Grout Material. Kilograms of Cement (Bags of Cement)
The unit price includes an accelerator, if required. For each 1.5 m (5 linear feet) of radial cracking, as specified in Section 679.3(d)5, the Department will reduce this pay item by 42.6 kg (one bag) of cement. The Department will not pay for any wasted grout material.

APPENDIX B: INTERNATIONAL ROUGHNESS INDEX RATING